12-2014

SCATTERING AMPLITUDES IN FLAT SPACE AND ANTI-DE SITTER SPACE

Savan Kharel
University of Tennessee - Knoxville, skharel@vols.utk.edu

To the Graduate Council:

I am submitting herewith a dissertation written by Savan Kharel entitled "SCATTERING AMPLITUDES IN FLAT SPACE AND ANTI-DE SITTER SPACE." I have examined the final electronic copy of this dissertation for form and content and recommend that it be accepted in partial fulfillment of the requirements for the degree of Doctor of Philosophy, with a major in Physics.

George Siopsis, Major Professor

We have read this dissertation and recommend its acceptance:

Christine Nattrass, Mike Guidry, Fernando Schwartz, Yuri Efremenko

Accepted for the Council:
Carolyn R. Hodges

Vice Provost and Dean of the Graduate School

(Original signatures are on file with official student records.)

12-2014

SCATTERING AMPLITUDES IN FLAT SPACE AND ANTI-DE SITTER SPACE

Savan Kharel
University of Tennessee - Knoxville, skharel@vols.utk.edu

To the Graduate Council:

I am submitting herewith a dissertation written by Savan Kharel entitled "SCATTERING AMPLITUDES IN FLAT SPACE AND ANTI-DE SITTER SPACE." I have examined the final electronic copy of this dissertation for form and content and recommend that it be accepted in partial fulfillment of the requirements for the degree of Doctor of Philosophy, with a major in Physics.

George Siopsis, Major Professor

We have read this dissertation and recommend its acceptance:

Christine Nattrass, Mike Guidry, Fernando Schwartz, Yuri Efremenko

Accepted for the Council:
Carolyn R. Hodges

Vice Provost and Dean of the Graduate School

(Original signatures are on file with official student records.)

Scattering Amplitudes in Flat Space and Anti-de Sitter Space

A Dissertation Presented for the

Doctor of Philosophy

Degree

The University of Tennessee, Knoxville

Savan Kharel

December 2014

To my parents, grandparents, and my brother

Acknowledgements

Thanks to my advisor Professor George Siopsis for his help and support. I am grateful for his readiness to guide me through projects of my interest. I am indebted to all my teachers and in particular I would like to thank Professors Monika Lynker and Rolf Schimmrigk for giving me an opportunity to do research in string theory as an undergraduate. Finally, I would like to thank Professors Yuri Efremenko, Mike Guidry, Christine Nattrass, and Fernando Schwartz for their support.

I am eternally grateful to my parents whose never-failing patience, courage, and generosity has been a great source of inspiration in my life. Thanks to my brother, Samik, for his support. Also, I would like to acknowledge my special intellectual debt to my beloved grandfather.

During the course of graduate school I was fortunate to have a friend in James Alsup who I thank for all his thoughtful advices. My warm thanks go to Slade Trammell for his kindheartedness when I needed it the most. I would like to thank Andrew Ratkiewicz for his continued friendship and insightful conversation over the last ten years. Similarly, I would like to thank my colleague Kubra Yeter, Suman Ganguli, and Eleftherios Moschandreu. Thanks to the folks at Golden Roast coffee shop where I spent countless hours thinking about physics, and occasionally playing chess.

Many people have given me intriguing and fun company during my journey as

a graduate student. I would like to thank Adrian Mertens, Anindya Dey, Xian Camanho, Michel Buck, Matt Young, Qinlong Luo, Kay Kolos, Yannen Jagannethen, Riei Ishizeki, and Jakub Sikorowski.

Finally, I would like to thank Jay Norrell for helping me edit parts of this dissertation.

To follow knowledge like a sinking star, Beyond the utmost bound of human thought.

Abstract

We calculate gauge theory one-loop amplitudes with the aid of the complex shift used in the Britto- Cachazo-Feng-Witten (BCFW) recursion relations of tree amplitudes. We apply the shift to the integrand and show that the contribution from the limit of infinite shift vanishes after integrating over the loop momentum, with a judicious choice of basis for polarization vectors. This enables us to write the one-loop amplitude in terms of on-shell tree and lower-point one-loop amplitudes. Some of the tree amplitudes are forward amplitudes. We show that their potential singularities do not contribute and the BCFW recursion relations can be applied in such a way as to avoid these singularities altogether. We calculate in detail n-point one-loop amplitudes for n = 2, 3, 4, and outline the generalization of our method to $n > 4$. In addition to scattering amplitudes in flat space, we studied amplitudes in Anti-de Sitter (AdS) space, which is equivalent to conformal correlators in the boundary of the Anti-de Sitter space. We discuss the use of the embedding formalism and Mellin transform in the calculation of tree-level correlators of scalar and vector fields in AdS/CFT. We present an iterative procedure that builds amplitudes by sewing together lower-point off-shell diagrams. Both scalar and vector correlators are shown to be given in terms of Mellin amplitudes. We apply the procedure to the explicit calculation of three-, four- and five-point correlators.

Table of Contents

List of Tables

List of Figures

Chapter 1

Introduction

Quantum field theory is the framework that describes our present understanding of high-energy particle physics. Scattering amplitudes are crucial objects in quantum field theory and they are essential in connecting theories and experiments. Using scattering amplitudes one can construct cross-sections that will determine the probabilities for scattering processes to occur at collider experiments. At high-energies the theory that are most interesting are the Yang-Mills theory and its close cousin Quantum Chromodynamics (QCD). These theories are necessary frameworks for describing interactions between elementary particles such as quarks and gluons. To compute scattering amplitudes in a quantum field theory, we customarily take a local Lagrangian from which we extract the corresponding Feynman rules for gauge fields, fermions, and scalars. We can use the same prescription, which is derived from the Einstein-Hilbert Largrangian, to calculate graviton amplitudes. At tree level, we add up all the diagrams constructed out of the Feynman rules to obtain the amplitude. Similarly, to calculate the loop contribution, we add up all the possible diagrams and finally integrate over the internal momenta. With the loop amplitudes, we may find that the integrals are divergent, which can be handled by the method known as regularization. Moreover, ultraviolet divergences that occur at high-energies lead to renormalization. While the steps outlined above are elaborate, the prescription for

calculating observables in quantum field theory is very well understood and extremely fruitful in our study of fundamental interactions.

But over the years, physicists have discovered that amplitudes in gauge theories and gravity have remarkable features and striking simplicity that cannot be found by merely looking at the symmetries of the Lagrangian or the corresponding Feynman rules. This is specially true for scattering amplitudes involving quarks, gluons, and gravitons. Parke and Taylor had the first glimpse of this simplicity and conjectured a general form for tree-level scattering amplitudes of gluons [1]. In a similar spirit, Dewitt calculated gravitational amplitudes, which also had striking simplicity [2]. While it is indisputable that the Feynman diagrammatic approach has traditionally been the most useful method, it is fair to ask why such an immensely cumbersome process produces such simple results. The following table illustrates the complexity of this method.

Table 1.1: Feynman diagrams needed to compute tree-level n-gluon scattering.

$n-point$	4	5	6	7	8	9	10
Feynman diagrams	4	25	220	2,485	34,300	559,405	10,525,900

It is clear from this table that the Feynman prescription is too convoluted to calculate amplitudes of any but the few simple cases. As external particles increase, the number of Feynman diagrams contributing to gluon amplitude grows faster than the factorial rate. Even more surprisingly, in many cases the answers obtained after such cumbersome calculations tend to be strikingly simple, and can even be written in a closed form. Such simplicity suggests that Feynman diagrams hide interesting structures. One of the earliest calculations to exploit this powerful structure was provided by the Berends-Giele recursion relation [3]. In addition, it became evident through the unitarity-based method that scattering amplitudes at loop level have interesting factorization properties [48]. In 2003, Witten made an important conceptual development in the study of scattering amplitudes. He observed

that the structure of scattering amplitudes of massless gauge theories are very simple in twistor space. For instance, a tree-level n-point amplitude with $q-$negative helicity gluons is zero unless it lies on a curve of degree $= q - 1$. Witten constructed twistor string theory, where the calculation of amplitudes involved curves in twistor space, which manifested these geometric properties [9].

It is instructive to reflect on why the the Feynman diagrammatic method is so inefficient. Each of the Feynman diagrams are dependent on the choice of the gauge. The scattering amplitude, on the other hand, which is the physical observable of the theory, is gauge invariant. It is interesting to wonder whether there could be an on-shell method which avoids this unphysical degree of freedom. Moreover, besides the inherent gauge variance of individual Feynman diagrams, scattering amplitudes have hidden symmetries such as color kinematic duality, dual conformal symmetry, and Yangian symmetry, just to name a few (see for instance [5, 6]). These symmetries are not evident from merely studying the Lagrangian of the theory. Such interesting symmetries form part of the motivation to study scattering amplitudes and their striking properties.

One of the successful methods in this direction has been the use of an on-shell method known as the Britto-Cachazo-Feng-Witten (BCFW) recursion relation. This method provides an on-shell recursion relation for calculating the scattering amplitudes of gauge theory and gravity. The BCFW method complexifies the momenta, which allows the study of the analytic structure of the function. Finally, we can reconstruct the physical amplitudes through the analysis of the singularities that appear after we complexify the momentum. Recently this procedure divulged a recursive structure not only for Yang-Mills tree-level amplitudes but also for tree-level amplitudes in general relativity. There has been much progress in theories with supersymmetry. For instance, scattering amplitudes in the gauge theory with the largest possible supersymmetry—known as $\mathcal{N} = 4$ super Yang-Mills theory— admit a dual description as a supersymmetric Wilson loop (see [7, 8]). As a consequence, supersymmetric amplitudes manifest other symmetries mentioned earlier, namely

dual (super) conformal and Yangian symmetries. Such symmetries of the theory again are not manifest in the standard Feynman diagrammatic method. With detailed studies of the properties of $\mathcal{N} = 4$ super Yang-Mills theory, we now know that it is characterized by loop amplitudes which have BCFW-like recursive structure. It has also been found that recursive structures of the theory are connected to a structure in algebraic geometry known as the positive Grassmannian. We now know that the BCFW-construction of the theory provides an on-shell representation of supersymmetric theory [10, 11, 12, 13, 14, 15, 16, 17]. Part of the goal of the present work is to go beyond the supersymmetric case and generalize the recursive structure to pure Yang-Mills theory.

We might be tempted to think that a sufficiently powerful computer would make these calculations trivial. While it would be unwise to understate the role of computers in physics, in calculating amplitudes we often encounter poles that cancel between diagrams, and numerical errors are common. With computers it is extremely difficult to obtain the simple, compact answers given by the modern methods. Besides their theoretical value, the most obvious use for these amplitudes is to develop efficient and accurate ways of understanding the standard model processes that occur in high-energy accelerators such as the Large Hadron Collider (LHC). For instance, background to new physics such as supersymmetry is very large because of strong dependence on renormalization and factorization scales. It is therefore useful to understand leading order and next-to leading order QCD backgrounds to expose any hidden physics, such as supersymmetry, that could emerge in high-energy particle colliders.

Concurrently, we investigate whether the success of scattering amplitudes in flat space can be extended to the study observables in a theory of quantum gravity. The so-called Anti-de Sitter /Conformal Field Theory (AdS/CFT) is a concrete example of the holographic principle of quantum gravity [35, 36]. It defines quantum gravity for certain classes of geometries characterized by asymptotic conditions, such as asymptotically flat or Anti-de Sitter spacetimes. The correspondence concerns type

IIB string theory in an asymptotically $AdS_5 \times S_5$ spacetime, often referred to as the bulk, with $\mathcal{N} = 4$ super Yang-Mills theory. More explicitly, the theory includes gravity and is non-perturbatively defined by a dual conformal field theory without gravity, namely 3+1 dimensional supersymmetric Yang-Mills theory with gauge group $SU(N)$. The S-matrix happens to make sense in the asymptotic geometries, and we can compute its matrix elements, which are the conformal correlators at the boundary. After significant interest and progress in scattering amplitudes, it is natural to wonder BCFW recursion could be used study AdS amplitudes. In AdS we need to integrate over the different points where this interaction can occur. While some progress has been made in writing down higher-point AdS amplitudes in terms of lower-point AdS amplitudes, it is important to find efficient ways of computing these amplitudes. The correlators calculated using the BCFW-like recursion relation are not useful in exploiting powerful conformal symmetry. The goal of the present work is to explore the proper basis of calculating these AdS scattering amplitudes.

The outline for the thesis is as follows. In chapter 2, we briefly review non-Abelian gauge theory and perturbation theory. We also review the BCFW recursion relation at tree-level. Furthermore, we will give a heuristic derivation of Anti-de Sitter space and Conformal Field using the stacked D3 brane which is a source for gravitational backreaction.

In chapter 3 we present a computational step taken to generalize the BCFW recursion relation to one loop amplitudes. We demonstrate that after integrating over the loop momenta, the contribution of the pole vanishes at large complex shift. This requires choosing an appropriate basis for the polarization vectors. Finally, we are able to express one-loop amplitudes in terms of tree amplitudes and lower-point one-loop amplitudes. In general, the tree amplitudes obtained from the loop include forward amplitudes that are plagued by divergences. We show that these potential divergences do not contribute, and discuss how the BCFW recursion relations can be applied so as to avoid the divergences, reducing the one-loop amplitudes to three-point tree amplitudes.

In chapter 4, we discuss how we have used a new tool to study scattering amplitudes in AdS space. While we have made dramatic progress in S-Matrix theory in a flat space by using hidden symmetries, recursion relations, and well-chosen bases, we need a new formalism with which to study amplitudes in AdS. This new formalism is of interest for formal reasons, for what it teaches us about both quantum gravity in asymptotically Anti-de Sitter spaces and about conformal field theories with gravity duals. We argue that the Mellin representation is a natural framework for gauge and scalar theory AdS amplitudes, or equivalently, correlation functions in conformal field theory; and that the Mellin represntation is structurally similar to the momentum representation used to calculate flat-space S-matrix elements.

Chapter 2

Preliminaries

In a textbook example of quantum field theory, we write a Lagrangian and using Feynman path integral, and we consequently quantize the theory. Moreover, by perturbatively expanding the path integral we obtain Feynman rules and the corresponding Feynman diagrams. The classical Yang-Mills Lagrangian is given by the following [21],

$$\begin{aligned}\mathcal{L} &= \bar{\Psi}(i\partial\!\!\!/ - m)\Psi - \frac{1}{4}(\partial_\mu A^a_\nu - \partial_\nu A^a_\mu)^2 + g A^a_\mu \bar{\Psi}\gamma^\mu t^a \Psi \\ &\quad -g f^{abc}(\partial_\mu A^a_\nu)A^{\mu b}A^{\nu c} - \frac{1}{4}g^2(f^{eab}A^a_\mu A^b_\nu)(f^{ecd}A^{\mu c}A^{\nu d}) \end{aligned} \tag{2.1}$$

where A is the gauge field, ψ is a fermion field, and g is the coupling constant. Similarly, terms such as f^{abc} are the structure constants and t^a are the generators. In this convention Greek letters are spacetime indices and Roman letters identify gauge indices. We can derive the Feynman rules using perturbation theory. While the actual derivation is technical (but straightforward), we can see how these interactions are sensible by simply looking at the Lagrangian. The first term in equation 2.1 corresponds to the fermion propagator, and the second term corresponds to the boson propagator. The term containing two fermion fields, Ψ and a gauge field A will correspond to a vertex where a gluon interacts with a fermion. Similarly, the fourth

and fifth term in the second line of the Lagrangian respectively correspond to three and four gluon vertices. The explicit rules are given in table 2.1.

Table 2.1: Feynman Rules for Yang Mills Theory in Feynman Gauge

Description	Diagram	Rules
Three Gluon Vertex	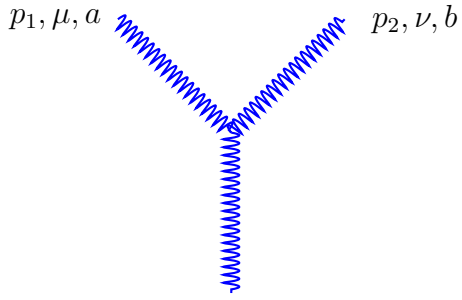	$= -gf^{abc}(g^{\mu\nu}(p_1 - p_2)^\rho + g^{\nu\rho}(p_2 - p_3)^\mu + g^{\rho\mu}(p_3 - p_1)^\nu)$
Quark Gluon Vertex	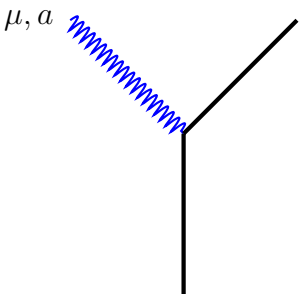	$= -ig\gamma^\mu t^a$
Gluon Propagator		$= \frac{ig_{\mu\nu}\delta_{ab}}{p^2 + i\epsilon}$
Fermion Propagator		$= \frac{i(\not{p} + m)\delta_i^{\bar{j}}}{p^2 - m^2 + i\epsilon}$
Four gluon vertex	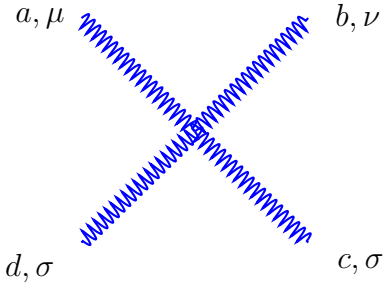	$= 2ig^2 \left(f^{abe}f^{ecd}g^{\mu[\rho}g^{\sigma]\nu} + f^{dae}f^{ebc}g^{\mu[\nu}g^{\sigma]\rho} + f^{cae}f^{ebd}g^{\mu[\nu}g^{\rho]\sigma}\right)$

2.1 Color Decomposition

In Yang Mills, fields of theory contain more than spacetime indices, but also indices relating their transformation under the gauge group. The gauge group of our interest is $SU(3)$, but let us work more generally with $SU(N)$. The color algebra for the group is generated by $N \times N$ traceless hermitian matrices t^a, where a is the adjoint color index that runs from 1 to $N^2 - 1$. Similarly, the quarks and the anti-quarks carry N and $\overline{N}$ indices, where i and $\bar{j}$ run from $1 \cdots N$. The generators are normalized by $Tr(t^a t^b) = \delta^{ab}$. Similarly, the structure constants f^{abc} are defined by,

$$[t^a, t^b] = i\sqrt{2} f^{abc} t_c \ , \tag{2.2}$$

where f^{abc} are the structure constant, and they satisfy the Jacobi identity:

$$f^{ade} f^{bcd} + f^{bde} f^{cad} + f^{cde} f^{abd} = 0. \tag{2.3}$$

One can use the normalization of the generators of $SU(3)$ in the following way:

$$\mathrm{Tr}\left(t^a t^b\right) = \frac{1}{2}\delta^{ab}. \tag{2.4}$$

Here, we will consider tree-level Feynman diagrams, pick a vertex, and replace the color structure function using,

$$f^{abc} = -\frac{i}{\sqrt{2}} \mathrm{Tr}\left(t^a t^b t^c - t^c t^b t^a\right) \ . \tag{2.5}$$

Now we can see how there are many strings of generators t^a which are traced in our expression for amplitudes, which are in the form $Tr(\cdots t^a \cdots) Tr(\cdots t^a \cdots)$. In addition, there are possibilities of external quarks, which means strings of t^a's terminate by fundamental indices and hence can be written as $(t^{a_1} \cdots t^{a_n})^{\bar{i}_1}_{i_2}$.The traces

in the f^{abc} at the vertices can be merged by the Fierz identity:

$$\sum_a (t^a)_i^{\bar{j}} (t^a)_k^{\bar{l}} = \delta_i^{\bar{l}} \delta_k^{\bar{j}} - \frac{1}{N_c} \delta_i^{\bar{j}} \delta_k^{\bar{l}} \ . \tag{2.6}$$

This will ensure that for gluon scattering amplitudes at tree level, all color factors combine to form a single-trace factor for each term, where $\frac{1}{N}$ cancel among themselves. Hence,

$$\mathcal{A}_n^{\text{tree}} = \sum_{\sigma \in (\mathcal{S}_n)/(\mathbb{Z}_n)} \text{Tr}\left(t^{a_{\sigma(1)}} \cdots t^{a_{\sigma(n)}}\right) A^{(tree)}(p_{\sigma(1)}, \epsilon_{\sigma(1)} \ldots p_{\sigma(n)}, \epsilon_{\sigma(n)}), \tag{2.7}$$

where $\mathcal{S}_n$ is the permutation group of n elements, and the sum runs over all permutations modulo cyclic permutations. We can also sum over all permutations and divide the result by n. The color-stripped amplitudes A^{tree} are cyclically symmetric. Also, these amplitudes are still gauge invariant. Furthermore, these amplitudes have the following property upon reflection:

$$A(1, 2, \ldots, n) = (-1)^n A(n, \ldots, 2, 1). \tag{2.8}$$

Here, we have denoted $A(\epsilon_1, p_2; \cdots; \epsilon_n, p_n) = A(1, 2 \cdots, n)$. The color ordered amplitudes obey dual Ward identity:

$$\begin{aligned} &A(1, 2, \ldots, n) + A(2, 1, 3, \ldots, n) + A(2, 3, 1, \ldots, n) + \\ &A(2, 3, \ldots, 1, n) = 0 \ . \end{aligned} \tag{2.9}$$

In chapter 3, we study color-ordered partial amplitudes for one loop. By using the completeness relation for the generators t^a and color-decomposition properties, we can decompose the one-loop amplitudes over a color basis of the maximum of two traces. The general form can be written as follows:

$$\begin{aligned}\mathcal{A}_n^{\text{1-loop}} &= \sum_{\sigma\in\mathcal{S}_n/\mathbb{Z}_n} N \;\; \text{Tr}\left(t^{a_{\sigma(1)}}\cdots t^{a_{\sigma(n)}}\right) A_{n;1}^{\text{1-loop}}(\sigma(1),\ldots,\sigma(n)) \\ &\quad + \sum_{c=2}^{\lfloor\frac{n}{2}\rfloor+1} \sum_{\sigma\in\mathcal{S}_n/\mathcal{S}_{n;c}} \text{Tr}\left(t^{a_{\sigma(1)}}\cdots t^{a_{\sigma(c-1)}}\right) \\ &\quad \text{Tr}\left(t^{a_{\sigma(c)}}\cdots t^{a_{\sigma(n)}}\right) A_{n;c}^{\text{1-loop}}(\sigma(1),\ldots,\sigma(n)) \end{aligned} \tag{2.10}$$

The leading contribution for $N\to\infty$ is the single trace contribution.

2.1.1 Warmup Example I: Tree level amplitudes involving gluons

In this example, we will see how color ordering works for four-point tree-level amplitudes. Often in our calculations we will encounter the product of structure constants such as $f^{a_1,a_2,b}f^{a_3,a_4,b}$. As mentioned before, we are interested in writing them as a string of generators. Using equation 2.5, we write down,

$$\begin{aligned} f^{a_1,a_2,b}f^{a_3,a_4,b} &= -\frac{i}{\sqrt{2}}\text{Tr}\left[t^{a_1}t^{a_2}t^b - t^{a_1}t^bt^{a_2}\right] f^{a_3,a_4,b} \\ &= -\frac{1}{2}\text{Tr}[t^{a_1}t^{a_2}t^{a_3}t^{a_4} - t^{a_1}t^{a_2}t^{a_4}t^{a_3} - t^{a_1}t^{a_3}t^{a_4}t^{a_2} + t^{a_1}t^{a_4}t^{a_3}t^{a_2}] \,. \end{aligned} \tag{2.11}$$

When we compute the four point amplitude, we realize that this amplitude contributes to four different color structures and four different color-ordered partial amplitudes. For simplicity, we will choose an amplitude with two negative polarization and two positive polarization. These amplitude are known as Maximal Helicity Violating (MHV) amplitudes. It is also interesting to note that amplitudes with one negative (positive) helicity and remaining positive (negative) helicities and amplitudes with all positive and all negative helicities are identically zero. Moreover, after this decomposition, each color stripped amplitude is still gauge invariant. Once we have

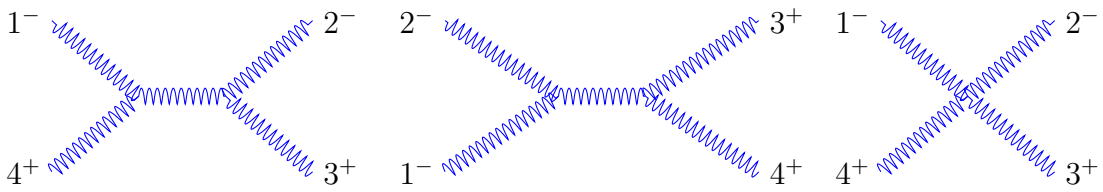

Figure 2.1: Feynman Diagrams in the four-point all gluon tree amplitudes

a representative amplitude we can construct the full amplitude by merely permuting the amplitude by permuting the generators. This is the first important simplification that we make to study scattering amplitudes. Many times, the calculation becomes quite simple if we choose a method known as spinor helicity (see A.1 for details). For simplicity we will chose the reference momenta to be $q_1 = q_2 = k_4$ and $q_3 = q_4 = k_1$. This will lead to significant degree of simplification. For the four-point scattering amplitudes, we can immediately write the full amplitude:

$$\begin{aligned}\mathcal{A}_4(\epsilon_1, k_1; \cdots; \epsilon_4, k_4) &= g^2 \left[t^{a_1}t^{a_2}t^{a_3}t^{a_4} - t^{a_1}t^{a_2}t^{a_4}t^{a_3} - t^{a_1}t^{a_3}t^{a_4}t^{a_2} + t^{a_1}t^{a_4}t^{a_3}t^{a_2}\right] \\ &\quad A_4(\epsilon_1, k_1; \cdots; \epsilon_4, k_4) \end{aligned} \tag{2.12}$$

Using Feynman rules from table (2.1), we calculate the four point amplitude with two negative helicities and two positive helicities:

$$\begin{aligned} A_4(\epsilon_1^-, k_1; \epsilon_2^-, k_2; \epsilon_3^+, k_3; \epsilon_4^+, k_4) &= \frac{i}{2}\big[\epsilon_1^- \cdot \epsilon_2^- (k_1 - k_2)^\mu + (\epsilon_2^-)^\mu \epsilon_1^- \cdot (2k_2 + k_1) + \\ &\quad (\epsilon_1^-)^\mu \epsilon_2^- \cdot (-2k_1 - k_2)\big] \frac{g^{\mu\nu}}{(k_1 + k_2)^2} \big[\epsilon_3^+ \cdot \epsilon_4^+ (k_3 - k_4)_\nu \\ &\quad + (\epsilon_4^+)_\mu \epsilon_3^+ \cdot (2k_4 + k_3) + (\epsilon_3^+)_\nu \epsilon_4^+ \cdot (-2k_3 - k_4)\big] \\ &= \frac{i}{2\langle 1\,2\rangle[2\,1]}\big[-4\epsilon_2^- \cdot \epsilon_3^+ k_2 \cdot \epsilon_1^- k_3 \cdot \epsilon_4^+\big] \\ &= \frac{\langle 1\,2\rangle^4}{\langle 1\,2\rangle\langle 2\,3\rangle\langle 3\,4\rangle\langle 4\,1\rangle} \end{aligned} \tag{2.13}$$

We have used simple spinor helicity identities to simplify the expressions in the last line (see A.1). Amplitudes with two negative (positive) polarization and other positive

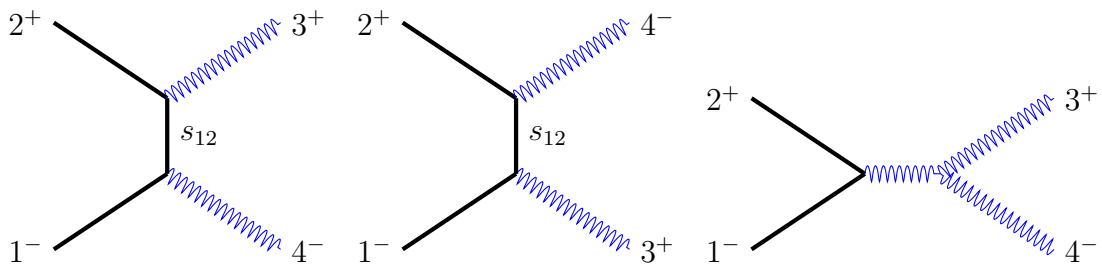

Figure 2.2: Feynman diagrams needed to compute four point quark-gluon interaction

(negative) polarization are known as Maximal Helicity Violating (MHV) amplitudes. One of the mysterious properties of the amplitudes is that using the right basis and the appropriate technique helps one to express scattering amplitudes in terms of simple expressions like the one above. The use of proper technique and the correct basis is a very important part of calculating scattering process in both flat space and Anti-de Sitter space, and it will be a recurrent theme of in our work.

2.1.2 Warmup Example II: Tree level amplitudes involving quarks and gluons

In this section we look at the process that involves quark-gluon interactions. Such a process is useful in the study of, for instance, J/ψ production in colliders. We start by looking at the four-point calculation, where the expression for the amplitude can be written using 2.1

$$A_4 = ig^2\epsilon_\mu\epsilon^*_\nu\bar{u}(p_1)\gamma^\mu\frac{-\not{k}_1 - \not{p}_1 + m}{-2p_1\cdot k_1}\gamma^\nu t^a t^b v(-p_2) \tag{2.14}$$

The analysis here is similar to one carried out in [20]. We can write down the amplitude for $gg \mapsto qq$

$$ig^2 A(1^-_{\bar{q}}, 2^+_q, 3^+, 4^-) = \left(\frac{ig}{\sqrt{2}}\right)^2 \frac{1}{i}[2|\not{\epsilon}_3\left(-\frac{\not{p}_5}{p_5^2}\right)\not{\epsilon}_4|1\rangle + \left(\frac{ig}{\sqrt{2}}\right)[2|\not{\epsilon}_5|1\rangle i \left(\epsilon_3^+ \cdot \epsilon_4^- \epsilon_5^+ \cdot k_3 + \epsilon_4^- \cdot \epsilon_5 \epsilon_3 \cdot k_4 + \epsilon_5 \cdot \epsilon_3^+ \epsilon_4^-\right)\Big|_{\epsilon_5^\nu \epsilon_5^\mu \mapsto \frac{ig^{\mu\nu}}{s_{12}}} \quad (2.15)$$

There are special ways to choose the polarization vectors [24, 20]

$$\not{\epsilon}_+(k;q) = \frac{\sqrt{2}}{\langle qk\rangle}\left(|k]\langle q| + |q\rangle[k|\right), \qquad \not{\epsilon}_+(k;q) = \frac{\sqrt{2}}{[qk]}\left(|k\rangle[q| + |q]\langle k|\right) \quad (2.16)$$

By using the reference vectors $q_3 = k_4$ and $q_4 = k_3$ we can completely get rid of the last term. Hence we write the partial amplitude as

$$ig^2 A(1^-_{\bar{q}}, 2^+_q, 3, 4) = \frac{\frac{1}{2}[2|\not{\epsilon}_{3^+}(\not{p}_1 + \not{k}_4)\not{\epsilon}_{4^-}|1\rangle}{-s_{14}} \quad (2.17)$$

We can use the identity $\not{p} = -|p\rangle[p| - |p]\langle p|$ This equation becomes:

$$A(1^-_{\bar{q}}, 2^+_q, 3, 4) = \frac{[23]\langle 41\rangle[13]\langle 41\rangle}{\langle 43\rangle[34]s_{14}} \ . \quad (2.18)$$

After massaging this expression a bit, we write down:

$$A(1^-_{\bar{q}}, 2^+_q, 3, 4) = \frac{\langle 21\rangle\langle 13\rangle^3}{\langle 12\rangle\langle 23\rangle\langle 34\rangle\langle 41\rangle} \ . \quad (2.19)$$

Hence, by choosing the right basis one can simplify amplitudes involving quarks and gluons to a compact and a simple form.

2.2 BCFW Recursion Relation

In this section, we review the so-called Britto-Cachazo-Feng-Witten (BCFW) recursion relation. It is also worth noting that even though the BCFW recursion relation

in the present work has been applied to gauge theories it is not specific to a particular theory and can be applied to a wide class of theories with some modification. The construction is based on shifting two arbitrary external momenta using complex on-shell momenta. Consider a color-ordered amplitude A as a function of momentum, i.e. $A = A(\epsilon_1, k_1; \epsilon_3, k_3; \cdots, \epsilon_n, k_n)$. In the BCFW prescription, we linearly shift two external momenta in a complex variable z. Hence, we pick two momenta,

$$k_1 \mapsto k_1(z) = k_1 + z\ q \quad , \qquad k_2(z) = k_2 - z\ q\ . \tag{2.20}$$

We also require the on-shell condition, i.e., $k_1(z)^2 = 0$ and $k_2(z)^2 = 0$, which means that the particles are still massless. This can be easily satisfied using conditions such as $q \cdot k_{1,2} = 0$. We may choose $q = \epsilon_{1,2}$ where $\epsilon_{1,2}$ are the polarization vectors associated with shifted momenta, k_1 and k_2. This setup transforms the scattering amplitude into the analytic function of z, so that $A \mapsto A(z)$. At tree level, $A(z)$ has an extremely simple analytic structure.* All the singularities come from the propagator of the following form:

$$\frac{1}{P(z)^2} = \frac{1}{P(0)^2 - 2\ z\ q \cdot P} \tag{2.21}$$

It turns out that all the singularities are located at $z_p = \frac{P(0)^2}{2q \cdot P}$. All singularities are simple poles. The remarkable thing is that for certain amplitudes in some theories, $A(z)$ vanishes for large z. Since meromorphic functions that vanish at infinity are completely characterized by their poles,

$$\frac{1}{2\pi i} \oint \frac{dz}{z} A(z) = A(0) + \text{Infinities}\ . \tag{2.22}$$

*While the idea behind using BCFW recursion relation is to avoid usage of Feynman diagrams, readers who know about Feynman diagrams are probably aware that singularities in Feynman diagrams come from its propagator, which, at tree level, leads to simple poles.

Now, if $A(z)$ vanishes in the limit $z \mapsto \infty$, then the sum of all residues is zero and the expression gives us the BCFW recursion relation:

$$A(0) = \sum_{z_p} Res_{z=z_p} \frac{A(z)}{z} = \sum \frac{A_L(z_p) A_R(z_p)}{P(0)^2} \tag{2.23}$$

where $A(0)$ is the original, unshifted amplitude, and A_L and A_R are the factorized left and the right amplitudes.

In chapter 3 we investigate the applicability of the complex shifts in the recursion relation in order to calculate loop level amplitudes.

2.2.1 Physical Interpretation of the BCFW relation

In this section we discuss the physical interpretation of BCFW. The discussion here will be at a heuristic level, and for more details we ask the reader to look at [39]. One might naively imagine that any individual Feynman diagrams at the level of tree diagrams in gauge and gravity amplitudes grow with energy because their associated interactions are coupled with derivatives. Hence in this naive analysis, it is surprising that summing these diagrams can yield an on-shell amplitude that actually vanishes at large momenta. However $z \mapsto \infty$ is crucial for the validity of the BCFW recursion. In [39], the authors provide a physical description of this remarkable vanishing behavior by considering gauge and gravity amplitudes at large complex momenta. They illustrate that the external legs which have been complex-deformed can be interpreted as a hard particle propagating through a background of the gas of soft particles corresponding to the remaining external legs. Thus, in the case of gauge theory, one can compute the large z structure of amplitudes using the background field method[†]. At this stage we would like to briefly digress and emphasize the difference between the old *S-matrix* program and its modern renaissance, which is propelled

[†]The background field method is a useful gauge invariant procedure to calculate the effective action where gauge potential is split into a background potential and a high momentum potential. One expands the potential around a "background" value and the Green's functions are evaluated as a function of the background. For the original paper, please refer to [58]

by BCFW and similar discoveries. While the spirit of the old S-matrix program was similar (i.e determining amplitudes directly from their singularities), the scattering was mostly restricted to $2 \mapsto 2$ scattering[‡]. In contrast to the BCFW, where the two external momenta are complexified, in the *old S-matrix program*, one complexified the Mandelstam variables. Hence, it was not clear how one could understand higher-point amplitudes. The BCFW recursion relations beautifully realizes the old S-matrix dream of computing scattering amplitudes using an on shell quantity without referring to the off-shell Lagrangian. As stated earlier, BCFW ideas do not rely on twistors or the spinor-helicity formalism. It is in fact a general property of quantum field theory in any number of dimensions. One of the interesting ideas about the BCFW recursion relation is that one would naively imagine that a simple theory leads to simpler perturbation. The increasing use and study of the BCFW recursion relation shows that while such a recursion relation can completely determine S-matrix for gauge theories, it is not easy to extend it to scalar theories. In fact the gravitational amplitudes exhibit the best UV behavior at infinite complex momentum.

2.3 AdS/CFT Correspondence

In this section, we will discuss the so-called AdS/CFT correspondence, which is also often referred to as the *gauge gravity duality*. The salient idea of the correspondence is that a UV complete theory of quantum gravity, i.e. string or M-theory in $d+1$ dimensions, is exactly equivalent to gauge theory in d dimensions [26]. First we will think about the idea heuristically, and more details can be found in [28]. An interesting question one can ask is whether it is possible to construct a massless spin-2 particle, i.e. a graviton, as a bound state of massless spin-1 gauge bosons. The naive answer to the question is that it would be impossible to make a graviton as a compositie particle of spin-1, which was demonstrated in the famous and beautiful

[‡]S-matrix theory had failed to explain pion to pion scattering. In the BCFW, we are mostly concerned with massless particles.

result of Weinberg and Witten [37]. However, we know that this no-go theorem has flaws. It turns out that the assumptions imposed in the Weinberg-Witten theorem violates one of the most crucial properties of any consistent theory of quantum gravity, the holographic principle. The hint for the holographic principle originates from the classic result of black hole thermodynamics [33, 34]. We know that the entropy of a black hole known as the Hawking-Bekenstein entropy is proportional to its area in Planck units, and this is the largest possible entropy for a system with given surface area.

$$S_{BH} = \frac{A}{4G} \ . \tag{2.24}$$

This is radical idea is in sharp distinction with generic non-gravitational systems, e.g. a bathtub full of water. The hidden assumption in the Weinberg-Witten theorem is that the gauge boson constituents live in the same spacetime as the graviton. Now we know that the graviton should actually live in one more spacetime dimension than where the gauge boson lives. This idea is a crucial insight for understanding the correspondence between gauge theory and the theory of gravity. The most studied and well-known example of this equivalence is the duality between conformal field theory and gravity on Anti-de Sitter space. In this thesis, we will study observables in the AdS/CFT duality. In the following, we will briefly outline the duality which will follow the usual treatment to introduce the subject. However, the outline here is not meant to be self contained. The reader interested in learning the AdS/CFT duality is referred to a beautiful review [28] full of conceptual details and physical insights. Other excellent reviews include [29, 32].

The original conjecture of the AdS/CFT correspondence can be summarized in the following:

$$\text{Type II B string theory in } AdS_5 \times S^5 \leftrightarrow \mathcal{N} = 4, D = 4 \text{ super YM theory} \ .$$

Since this is the most studied example, we will briefly outline the derivation. As in figure 2.3, we will consider a stack of N coincident parallel D3-branes in flat

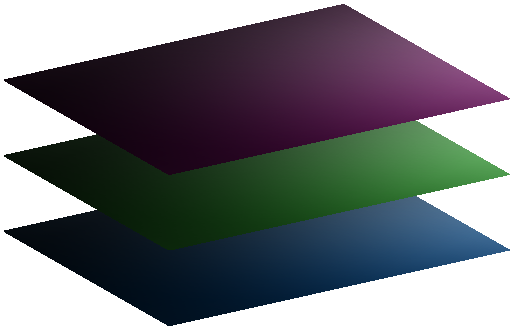

Figure 2.3: Stacked N D3 branes in flat Minkowski space and the string coupling g_s is weak

Minkowski space. At weak string coupling with fixed N such that $\lambda = g_s N << 1$, the gravitational backreaction of the D3 brane is small. In this background, the theory contains two types of excitation: open strings, which are the excitation of D3 branes, and closed strings, the excitation of ten-dimensional bulk spacetime. If we then take the string length to be small, there is a decoupling between the remaining massless open string modes on the stack of branes and the remaining massless closed string modes in the bulk.

2.3.1 The Near Horizon Limit

The massless modes on the brane are described by $d = 4$, $\mathcal{N} = 4$ super Yang-Mills theory. The D3 branes act as the source of the bulk fields. When $\lambda = g_s N >> 1$, the string theory is described by the black 3-brane in the supergravity background:

$$ds^2 = \frac{1}{\sqrt{h(r)}}\eta_{\mu\nu}dx^\mu dx^\nu + \sqrt{h(r)}dx^a dx^b \tag{2.25}$$

where,

$$\mu, \nu = 0, 1, \cdots 3 \quad a, b = 4, \cdots 9 \quad \text{and,} \quad h(r) = 1 + \frac{R^4}{r^4} = 1 + \frac{4\pi g N \alpha'^2}{r^4}. \tag{2.26}$$

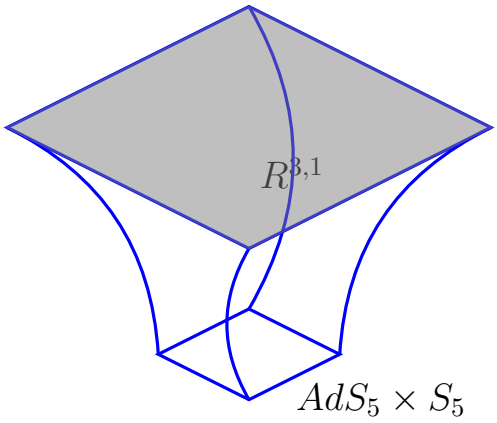

Figure 2.4: Near horizon geometry of AdS representing the throat area where $r << R$ and 10-dimensional flat Minkowski $r >> R$

Here, $x^a x^a = r^2$. If we take the limit where $\alpha' \mapsto 0$ fixing λ, we obtain the following metric:

$$ds^2 = \frac{r^2}{R^2}\eta_{\mu\nu}dx^\mu dx^\nu + \frac{R^2}{r^2}dx^a dx^b + R^2 d\Omega_5^2 \ , \tag{2.27}$$

which decouples from the asymptotically flat region. The first two terms are the Anti-de Sitter space and AdS_5 metric, and the last term is the metric for the five-sphere, S_5. Despite $R \mapsto 0$ and $\alpha' \mapsto 0$, the string sigma model in the near-horizon region retains a finite coupling set by the ratio $\frac{R}{\alpha'} = \lambda^{\frac{1}{4}}$. Finally, we are left with type IIB closed string theory in the AdS background, which is described by equation 2.27. The stunning observation of AdS/CFT is that for two decoupled theories, i.e $\mathcal{N} = 4$ super Yang-Mills theory and the type IIB super string theory on $AdS_5 \times S_5$, are equivalent for all values of couplings. The two couplings of the theories are related by:

$$g_s = \frac{g_{YM}^2}{4\pi} \ . \tag{2.28}$$

When the field theory is weakly coupled, the dual string theory geometry is strongly curved, which makes computations hard. On the other hand, when the string-theory geometry is weakly curved, and a supergravity approximation is justified, the dual gauge theory is strongly coupled. While we have presented a

specific case, it is important to emphasize that it is only one of many dualities between gravitational theories and gauge theories. The equality also means that the symmetries and the spectrum of the two sides of the theory are equivalent. In this thesis, we study the equality between correlation functions. So what are the reasons for the duality? The evidence of the duality are discussed in review such as [28].

- The correlation functions are the same in both sides.
- The symmetries on the gravity side and the gauge theory match.
- The predictions of the duality for strongly coupled gauge theories can be compared with numerical calculations as well as analytical calculations
- The predictions have helped us study many aspects of strongly coupled systems such as condensed matter systems and heavy ions (see [30, 31] references therein).

2.4 AdS Scattering Amplitudes

The AdS/CFT correspondence maps the bulk field and the gauge theory operators. The quantitative form of this matching can be written in the following way:

$$\left\langle e^{d^4x\phi_0(x)\mathcal{O}(x)} \right\rangle = \mathcal{Z}[\phi_i(x,u)|_{u=0} = u^{4-\Delta}\phi_i(x)] \ . \tag{2.29}$$

The left-hand side in the above equation corresponds to the expectation value taken in the gauge theory, where $\phi_i(x)$ is the source for an operator $\mathcal{O}$. This expectation can be computed by expanding the exponential and evaluating the off-shell correlation functions in the gauge theory. The right-hand side corresponds to string theory in $AdS_5 \times S_5$, which calculates the S-matrix elements for the AdS amplitudes.

2.4.1 Scalar Fields in Anti-de Sitter space

Here we will give a terse discussion on scalar fields on Anti-de Sitter space in the Poincare patch . For detail, we will refer readers to [19]. The wave equation is given by

$$\frac{z^2}{R^2}\left[{\partial_z}^2 - \frac{d}{z}\partial_z - {\partial_t}^2 + \partial\cdot\partial\right]\phi = m^2\phi \ . \tag{2.30}$$

One can take the Fourier transform of the scalar field,

$$\phi(z,x) = \int \frac{d^{p+1}q}{(2\pi)^{p+1}}\phi(z,q)e^{q\cdot x} \ . \tag{2.31}$$

Then we obtain:

$$\left[{\partial_z}^2 - \frac{d}{z}\partial_z - q^2 + \frac{m^2L^2}{z^2}\right]\phi(z,q) = 0 \ . \tag{2.32}$$

This gives us a solution in terms of the Bessel function:

$$\phi(z,q) \sim z^{d+1}Z_\nu(\sqrt{q^2}z) \ , \quad \text{where,} \quad \nu = \frac{1}{2}\sqrt{(d+1)^2 + 4m^2L^2}, \tag{2.33}$$

where Z_ν represents the two linearly independent solutions of the Bessel function. The solution scales as

$$\phi_\pm \sim z_\pm^\Delta \ , \Delta_\pm = \frac{1}{2}(d+1) \pm \nu \ . \tag{2.34}$$

2.4.2 Propagators in Anti De Sitter space

Now in AdS_{p+2} we can write down the propagator for for two bulk-to-bulk points

$$(\Box - m^2)G(z,x,x') = z^5\delta(z-z')\delta^4(x-x') \tag{2.35}$$

where we have used the Poincare coordinates. The explicit expression can be written as

$$G_\Delta(z,x;z',x') = \frac{\Gamma(\Delta)}{2^{\Delta+1}\pi^2\Gamma(\Delta-1)}\eta^{-\Delta}F\left(\frac{\Delta}{2},\frac{\Delta+1}{2};\Delta-1;\frac{1}{\eta^2}\right) \ , \tag{2.36}$$

where

$$\eta^2 = \frac{z^2 + z'^2 + (x - x')^2}{2zz'}. \tag{2.37}$$

As one of the two bulk points move to the boundary, the bulk-to-bulk propagator approaches the bulk to boundary propagator.

$$\lim_{z \mapsto 0} \eta^2 = \frac{z^\Delta}{2\Delta - 4} K_\Delta(x; z', x') \tag{2.38}$$

In chapter 4, we will develop a formalism to succinctly write down both the bulk to bulk propgator and bulk to boundary propagator in an embedding formalism for propagation of scalar as well as spin particles.

Chapter 3

Loop Amplitudes in Flat Space for Yang Mills Theory

3.1 Introduction

As we have discussed, there are several reasons to improve on our understanding of scattering amplitudes in gauge theories, ranging from the development of an efficient and accurate calculation of standard model processes that occur in high energy accelerators such as the Large Hadron Collider (LHC), to formal developments, such as understanding the properties of quantum field theory and quantum gravity.

In the last few years, there has been extraordinary progress in the study of scattering amplitudes. We learned that the scattering amplitudes of gravity and gauge theories have more structure and symmetries than are manifest in the Lagrangian. One of the first extraordinary properties of scattering amplitudes was discovered in the mid-eighties by Parke and Taylor who found an extremely simple and compact expression for Maximally-Helicity-Violating (MHV) amplitudes [1]. The modern renaissance in the study of scattering amplitudes was led by an important conceptual development due to Witten [9] who observed that the structure of gauge theory

scattering amplitudes is very simple in twistor space. For recent reviews of scattering amplitudes, see, e.g., [22, 23].

Witten's seminal work inspired an important contribution by Cachazo, Svrcek, and Witten [25] and its extension, the Britto-Cachazo-Feng-Witten (BCFW) recursion relations (for tree-level discussion see the discussion in 2.2). In the BCFW prescription, a pair of the external momenta in a tree amplitude are analytically continued into the complex plane, turning the amplitude into a meromorphic function. Thus, these amplitudes are shown to be determined by the residues of their poles. The BCFW technique exploits this property in order to recursively construct physical amplitudes from irreducible three-point amplitudes. However, in order to effectively use recursion relation, the residue of the pole at infinity must vanish. This is the case in gauge theories and gravity, but not in generic field theories [39]. In the last few years much progress has been realized in our understanding of scattering amplitudes based on the BCFW recursion relation. For example, the BCFW recursion relations have been applied to amplitudes involving gravitons [40, 41, 42, 43], string theory [44, 45, 46], and anti-de Sitter (AdS) space [68].

The extension of the BCFW recursion relations to loop amplitudes is not straightforward. Loop amplitudes receive, in general, a non-vanishing contribution from the pole at infinity. They also possess cuts, in addition to poles, which makes the application of Cauchy's theorem more cumbersome. In the mid-nineties, powerful on-shell unitarity methods were developed for the calculation of scattering amplitudes [48, 49] (for a review, see [50]). A generalization of the BCFW recursion relations and the unitarity method to loop amplitudes was then considered [51, 52, 53, 54]. An alternative approach, in which one applies the BCFW recursion relations to the *integrand* of the loop amplitude, was recently discussed [55]. In the case of $\mathcal{N} = 4$ super Yang-Mills gauge theory, all loop amplitudes were thus obtained in the planar limit [57].

In this work, we re-visit the application of BCFW recursion relations to the *integrand* of gauge-theory loop amplitudes. We concentrate on one-loop amplitudes,

although our results can be generalized to higher loop order. We show that the contribution of the pole at infinite complex shift can be made to vanish, after integrating over the loop momentum, by a judicious choice of basis for the polarization vectors. This enables us to express one-loop amplitudes in terms of tree amplitudes and lower-point one-loop amplitudes. The tree amplitudes include forward amplitudes which are plagued by divergences, in general. We show that these potential divergences do not contribute and discuss how the BCFW recursion relations can be applied so as to avoid the divergences, thus reducing the one-loop amplitudes to three-point tree amplitudes. This work was published in [56]. We perform the calculation in detail for two-point (section 3.2), three-point (section 3.3), and four-point (section 3.4) one-loop amplitudes. In section 3.5, we outline the generalization of our method to one-loop amplitudes with $n > 4$. In section 3.6, we summarize our conclusions. We work with color ordered amplitudes throughout, to simplify the discussion.

3.2 Two-point loop amplitude

In this section, we consider a two-point one-loop amplitude. Ignoring group theory factors, it can be written as an integral over the loop momentum,

$$A_2^{1-\text{loop}}(k_1, \epsilon_1; -k_1, \epsilon_2) = \int \frac{d^{2\omega} l}{(4\pi)^{2\omega}} \mathcal{A}_2^{1-\text{loop}}(k_1, \epsilon_1; -k_1, \epsilon_2) \ , \tag{3.1}$$

where ω is a dimensional regularization parameter, and the two polarization vectors are null, with $\epsilon_1 \cdot k_1 = \epsilon_2 \cdot k_1 = 0$. The momentum k_1 is off shell. To apply the BCFW recursion relations, we shift $k_1 \mapsto k_1 + z\epsilon_1$. Consequently, we shift the second polarization vector,

$$\epsilon_2 \mapsto \epsilon_2' \equiv \epsilon_2 - z \frac{\epsilon_2 \cdot \epsilon_1}{k_1^2} k_1 \ . \tag{3.2}$$

We will use the background gauge [58] in order to compute this amplitude. There is only one diagram that contributes to this amplitude (figure 3.1).

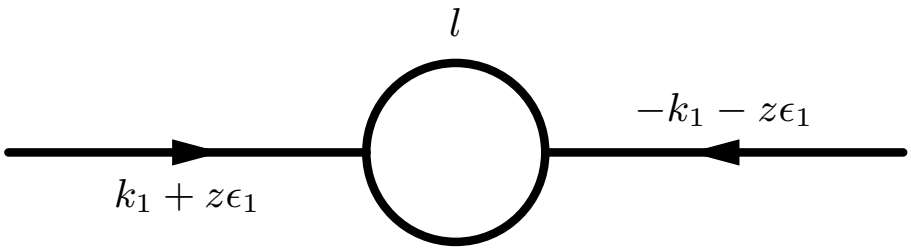

Figure 3.1: Diagram contributing to the two-point one-loop amplitude.

At large z, the *integrand* behaves as

$$\mathcal{A}_2^{1-\text{loop}} = \frac{1}{2}\frac{\epsilon_1 \cdot \epsilon_2}{l^2} + \frac{5}{2}\frac{\epsilon_1 \cdot \epsilon_2}{k_1^2}\,\frac{k_1 \cdot l}{l^2} + \mathcal{O}\left(\frac{1}{z}\right) \ . \tag{3.3}$$

Upon integration over the loop momentum, the leading $\mathcal{O}(1)$ term becomes a linear combination of tadpole tensor integrals,

$$I_{\mu_1\mu_2\ldots} = \int \frac{d^{2\omega}l}{(4\pi)^{2\omega}}\,\frac{l_{\mu_1} l_{\mu_2}\cdots}{l^2} \ , \tag{3.4}$$

which vanish. Therefore, we have no contribution from $z \to \infty$ and the entire contribution to the two-point diagram comes from the residue of the pole of the integrand at

$$z = z_1 = \frac{(l - k_1)^2}{2\epsilon_1 \cdot l} \tag{3.5}$$

From Cauchy's theorem, we obtain for the integrand

$$\mathcal{A}_2^{1-\text{loop}}\Big|_{z=0} = -\frac{1}{z_1}\text{Res}_{z\to z_1}\mathcal{A}_2^{1-\text{loop}} + \ldots \tag{3.6}$$

where the dots represent contributions that vanish upon integration over the loop momentum. Explicitly, for the *integral* we obtain

$$A_2^{1-\text{loop}} = +5\epsilon_1^\mu \epsilon_2^\nu I_{\mu\nu}(k_1) + \frac{5}{2}\epsilon_1 \cdot \epsilon_2 k_1^2 I(k_1) - \epsilon_1.\epsilon_2 k_1^\mu I_\mu(k_1) \tag{3.7}$$

in terms of the two-point tensor integrals,

$$I_{\mu_1\mu_2\ldots}(k_1) = \int \frac{d^{2\omega}l}{(4\pi)^{2\omega}} \frac{l_{\mu_1} l_{\mu_2} \cdots}{l^2(l-k_1)^2} \ , \tag{3.8}$$

which is in agreement with the result of a direct calculation of the loop integral. Evidently, the residue contributing to the loop amplitude is a four-point tree diagram contributing to the forward amplitude (see figure 3.2),

$$A_4^{\text{tree}}(k_1', \epsilon_1; -k_1', \epsilon_2'; l', \epsilon_3; -l', \epsilon_4) \tag{3.9}$$

where ϵ_2' is given by (3.2) with $z = z_1$ (defined in (3.5)), and we have defined

$$k_1' = k_1 + z_1\epsilon_1 \quad , \qquad l' = l - k_1 - z_1\epsilon_1 \ , \tag{3.10}$$

to simplify the notation. Two legs are on-shell, since $(l')^2 = 0$. For the two-point loop amplitude, we expect

$$A_2^{1-\text{loop}} = \int \frac{d^{2\omega}l}{(4\pi)^{2\omega}} \frac{1}{(l-k_1)^2} \sum_{\epsilon_3} A_4^{\text{tree}}\Big|_{\epsilon_4 = \epsilon_3^*} \ . \tag{3.11}$$

However, the forward amplitude is singular. To regulate it, introduce a small momentum p_μ orthogonal to the polarization vector ϵ_2',

$$p \cdot \epsilon_2' = 0 \tag{3.12}$$

and consider the amplitude

$$A_4^{\text{tree}}\left(k_1', \epsilon_1; -k_1' - p, \epsilon_2'; l' + p, \epsilon_3; -l', \epsilon_4\right) \tag{3.13}$$

in the limit $p_\mu \to 0$.

Since we are working with color-ordered amplitudes, to avoid ordering the legs carrying the loop momentum, we shall average over this amplitude and the one obtained by interchanging the two legs carrying the loop momentum.

The contribution of diagram *(a)* of figure 3.2 is regular. In the limit $p_\mu \to 0$, we obtain

$$\sum_{\epsilon_3} A_4^{\text{tree},(a)}\Big|_{\epsilon_4=\epsilon_3^*} = \frac{\epsilon_1 \cdot \epsilon_2'(\frac{5}{2}k_1^2 + k_1' \cdot l') + 5\epsilon_1 \cdot l'\epsilon_2' \cdot l' + \frac{5}{2}\epsilon_1.k_1'\epsilon_2'.l'}{l^2} \ . \tag{3.14}$$

The contribution of the diagram *(b)* of figure 3.2 is singular,

$$\sum_{\epsilon_3} A_4^{\text{tree},(b)}\Big|_{\epsilon_4=\epsilon_3^*} = \frac{\epsilon_1 \cdot \epsilon_2'(\frac{3}{2}p^2 + 3p \cdot k_1' - 3p \cdot l' - 6k_1' \cdot l') - 3\epsilon_1 \cdot l'\epsilon_2' \cdot p}{p^2} \tag{3.15}$$

Finally, the contribution of diagram *(c)* is regular,

$$\sum_{\epsilon_3} A_3^{\text{tree},(c)}\Big|_{\epsilon_4=\epsilon_3^*} = -\frac{3}{2}\epsilon_1 \cdot \epsilon_2' \ . \tag{3.16}$$

The singular contribution is easily seen to vanish after removing the color ordering on the legs carrying the loop momentum. This is done by averaging with the expression obtained by replacing $l' \to -l' + p$ (or, equivalently, replacing $l \mapsto \frac{1}{2}p$ in (3.15)). Then the numerator on the right-hand side of (3.15) vanishes after using (3.12).

We obtain the finite forward tree amplitude

$$\sum_{\epsilon_3} A_4^{\text{tree}}\Big|_{\epsilon_4=\epsilon_3^*} = \frac{-5\epsilon_1 \cdot \epsilon_2\epsilon_1 \cdot l\frac{k_1 \cdot l}{k_1^2}z_1 + \epsilon_1 \cdot \epsilon_2\epsilon_1 \cdot l z_1 + \frac{3}{2}\epsilon_1 \cdot \epsilon_2 k_1^2 + \epsilon_1 \cdot \epsilon_2 k_1 \cdot l + 5\epsilon_1 \cdot l\epsilon_2 \cdot l}{l^2} \tag{3.17}$$

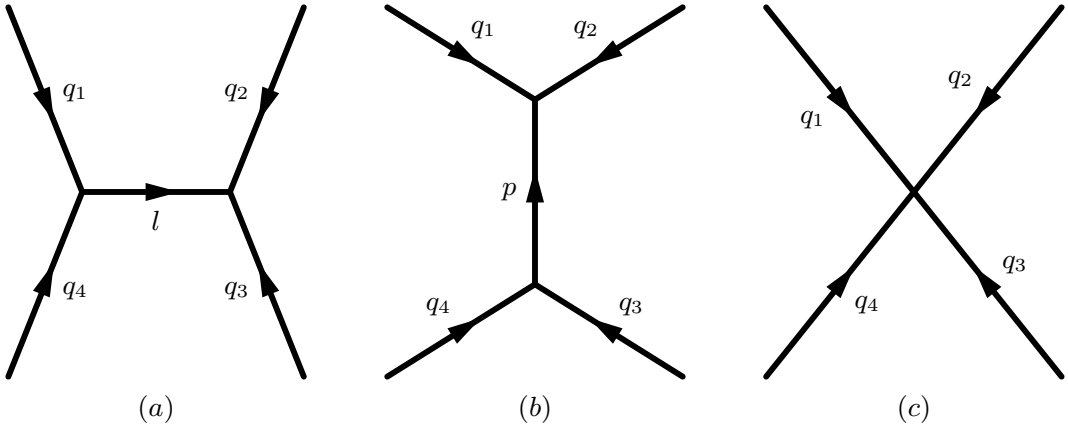

Figure 3.2: Four-point tree diagrams contributing to a two-point one-loop diagram. The external momenta are $q_1 = k_1' + p$, $q_2 = -k_1'$, $q_3 = -l'$, $q_4 = l' - p$. p_μ is a momentum regulator.

Substituting this expression in (3.11), we recover our earlier result (3.7) for the two-point one-loop amplitude. The forward tree amplitude can also be obtained by applying the BCFW recursion relations. In fact, by an appropriate choice of complex momentum shifts, the singularity can be avoided and no need for a regulator arises. Indeed, under the shift,

$$k_1' \mapsto k_1' + w\epsilon_1 \quad , \qquad -k_1' \mapsto -k_1' - w\epsilon_1 \quad , \qquad \epsilon_2' \mapsto \epsilon_2'' \equiv \epsilon_2' - w\frac{\epsilon_1 \cdot \epsilon_2}{k_1^2} k_1' \tag{3.18}$$

the resulting amplitude vanishes as $w \to \infty$, and we obtain a pole at

$$w = w_1 = -\frac{l^2}{2l \cdot \epsilon_1} \ . \tag{3.19}$$

The residue of the pole yields the entire four-point forward tree amplitude,

$$\begin{aligned} A_4^{\text{tree}} \ &= \ \frac{1}{l^2} \sum_{\epsilon_3, \epsilon'} A_3^{\text{tree}}(k_1' + w_1\epsilon_1, \epsilon_1; -l' - w_1\epsilon_1, \epsilon'; l', \epsilon_3) \\ &\quad \times A_3^{\text{tree}}(-k_1' - w_1\epsilon_1, \epsilon_2''; -l' + w_1\epsilon_1, \epsilon_3^*; l' + w_1\epsilon_1, \epsilon'^*) \end{aligned} \tag{3.20}$$

which is a finite expression. After some straightforward algebra, we obtain

$$A_4^{\text{tree}} = \frac{\epsilon_1 \cdot \epsilon_2 \left[\frac{3}{2} w_1 \epsilon_1 \cdot l - \frac{7}{2} z_1 \epsilon_1 \cdot l + \frac{5}{2} k_1^2 - k_1 \cdot l + l^2\right] - \frac{5}{2} \epsilon_1 \cdot l \epsilon_2'' \cdot k_1 + 5 \epsilon_1 \cdot l \epsilon_2'' \cdot l}{l^2} \tag{3.21}$$

Using the explicit expressions (3.5), (3.19), and (4.20) for z_1, w_1, and ϵ_2'', respectively, we recover our earlier result (3.17), which was obtained by a direct calculation using a regulator, up to terms which vanish upon integration over the loop momentum.

Thus, we have shown that an application of the BCFW recursion relations reduces the two-point loop amplitude to three-point tree amplitudes. Even though there are potential singularities from forward amplitudes, these were avoided by a judicious choice of complex momentum shifts.

3.3 Three-point loop amplitude

Next we consider a three-point one-loop color-ordered amplitude

$$A_3^{1-\text{loop}}(k_1, \epsilon_1; k_2, \epsilon_2; k_3, \epsilon_3) = \int \frac{d^{2\omega} l}{(4\pi)^{2\omega}} \mathcal{A}_3^{1-\text{loop}}(k_1, \epsilon_1; k_2, \epsilon_2; k_3, \epsilon_3) \ , \tag{3.22}$$

with $k_1 + k_2 + k_3 = 0$. Two of the momenta, k_1 and k_2, will be on-shell. We shall keep the third momentum k_3 off shell to facilitate explicit calculations. This is necessary also for kinematical reasons, but $k_3^2 = 0$ is allowed if momenta are complex, which is a case that will be useful for the calculation of higher-point amplitudes.

For the polarization vectors, we choose ϵ_1 and ϵ_2 such that $\epsilon_1 \cdot k_i = 0$ and $\epsilon_2 \cdot k_i = 0$, where $i = 1, 2, 3$. This is always possible. Indeed, if $\epsilon_1 \cdot k_2 \neq 0$, then we may shift $\epsilon_1 \mapsto \epsilon_1 - \frac{\epsilon_1 \cdot k_2}{k_1 \cdot k_2} k_1$, and the new polarization vector satisfies $\epsilon_1 \cdot k_i = 0$. Similarly, we arrange $\epsilon_2 \cdot k_i = 0$. For the third polarization vector, since k_3 is off-shell, there are three independent polarizations. Notice that, since $\epsilon_3 \cdot (k_1 + k_2) = 0$, they can be chosen as the set $\{\epsilon_1, \epsilon_2, k_1 - k_2\}$. To apply the BCFW recursion relations, we shift

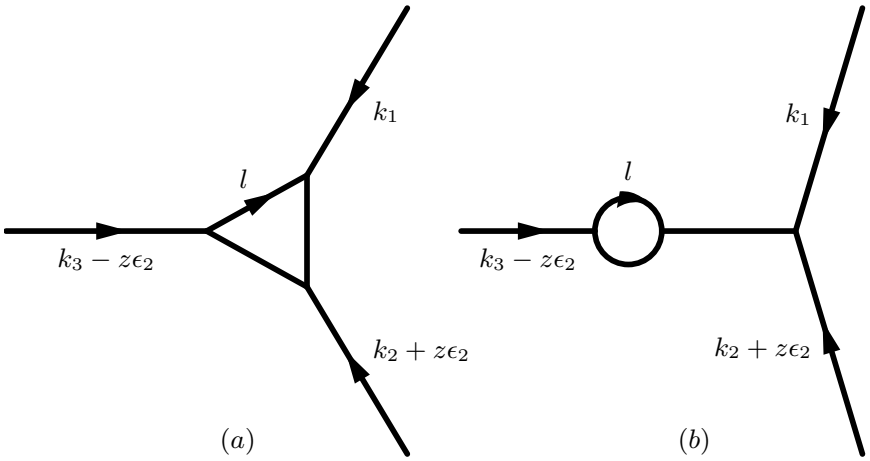

Figure 3.3: Diagrams contributing to a three-point color-ordered one-loop amplitude.

$$k_2 \mapsto k_2 + z\epsilon_2 \ , \quad k_3 \mapsto k_3 - z\epsilon_2 \ , \quad \epsilon_3 \mapsto \epsilon_3 + z\frac{\epsilon_2 \cdot \epsilon_3}{k_3^2} k_3 \ . \tag{3.23}$$

There are two diagrams that contribute to the amplitude (figure 3.3) and we discuss them separately. First we evaluate the triangle diagram *(a)* in figure 3.3 using the background gauge. After the shift (3.23), the large z behavior of the *integrand* is of the form

$$\begin{aligned} \mathcal{A}_3^{1-\text{loop},(a)} = \frac{1}{l^2(l+k_1)^2} \quad & \Big[-4z\epsilon_1 \cdot \epsilon_2 \epsilon_2 \cdot \epsilon_3 + \frac{16\epsilon_1 \cdot l \epsilon_2 \cdot \epsilon_3 k_2 \cdot l}{k_3^2} - \frac{4\epsilon_1 \cdot \epsilon_2 \epsilon_2 \cdot \epsilon_3 k_2 \cdot l}{\epsilon_2 \cdot l} - \\ & \frac{4\epsilon_1 \cdot \epsilon_2 \epsilon_2 \cdot \epsilon_3 l \cdot k_3}{\epsilon_2 \cdot l} \Big] + \frac{2\epsilon_1 \cdot \epsilon_2 \epsilon_2 \cdot \epsilon_3}{\epsilon_2 \cdot l} + 4\epsilon_1 \cdot \epsilon_2 \epsilon_3 \cdot k_1 \Big] + \\ & \mathcal{O}\left(\frac{1}{z}\right) \ . \end{aligned} \tag{3.24}$$

Evidently, it does not vanish, in general, as $z \to \infty$. Upon closer inspection, when $\epsilon_3 = \epsilon_2$, or $\epsilon_3 = k_1 - k_2$, all terms except the last one at leading order ($\mathcal{O}(1)$) in the above expression vanish. The last term vanishes after integration over the loop momentum, because it is proportional to a two-point tensor integral (3.8) with $k_1^2 = 0$. Therefore, in the limit $z \to \infty$, there is no contribution.

If $\epsilon_3 = \epsilon_1$, we need to interchange legs 1 and 2 before shifting the external momenta as in (3.23).

It turns out that the choices $\epsilon_3 = \epsilon_1$ and $\epsilon_3 = \epsilon_2$ yield vanishing amplitudes, so we shall concentrate on the polarization

$$\epsilon_3 = k_1 - k_2 \tag{3.25}$$

for which, as we just showed, there is no contribution to the diagram from the pole at $z \to \infty$.

It follows that the entire contribution to this diagram comes from the pole at

$$z = z_1 \equiv -\frac{(l - k_3)^2}{2\epsilon_2 \cdot l} \ . \tag{3.26}$$

Explicitly, for the integral we obtain

$$\begin{aligned} A_3^{1-\text{loop},(a)}\Big|_{z=0} \quad = \quad & -8\epsilon_1 \cdot \epsilon_2 \epsilon_3 \cdot k_1 k_3 \cdot I(k_1, k_2) + 4\epsilon_1 \cdot \epsilon_2 \epsilon_3 \cdot k_1 I^{\mu}_{\mu}(k_1, k_2) - \\ & 4k_3^2 \epsilon_1 \cdot \epsilon_2 \epsilon_3 \cdot I(k_1, k_2) + 16\epsilon_1^{\mu}\epsilon_2^{\nu}\epsilon_3^{\lambda} I_{\mu\nu\lambda}(k_1, k_2) \end{aligned} \tag{3.27}$$

in terms of three-point tensor integrals,

$$I_{\mu_1\mu_2\ldots} = \int \frac{d^{2\omega}l}{(2\pi)^{2\omega}} \frac{l_{\mu_1} l_{\mu_2} \cdots}{l^2 (l + k_1)^2 (l + k_1 + k_2)^2} \tag{3.28}$$

After standard manipulations, we arrive at

$$A_3^{1-\text{loop},(a)} = \frac{1}{16\pi^2} \epsilon_1 \cdot \epsilon_2 \epsilon_3 \cdot k_1 \left(-\frac{20}{3(2-\omega)} + \frac{40}{3} + \mathcal{O}(2-\omega) \right) \ . \tag{3.29}$$

Next we compute diagram *(b)* in figure 3.3 using the background gauge for the loop and the Gervais-Neveu gauge for the tree part of the diagram. At large z, we obtain

$$\begin{aligned}\mathcal{A}_3^{1-\text{loop},(b)} &= \epsilon_1\cdot\epsilon_2\epsilon_2\cdot\epsilon_3\Big[-\frac{16k_2\cdot l}{{k_3}^4 l^2}\,z-\frac{16k_1\cdot l k_2\cdot l}{k_3^4 l^2\epsilon_2\cdot l}-\frac{16k_2\cdot l k_3\cdot l}{k_3^4 l^2\epsilon_2\cdot l}+\\ &\quad\frac{4k_2\cdot l}{k_3^2 l^2\epsilon_2\cdot l}+\frac{k_2\cdot l}{k_3^4\epsilon_2\cdot l}\Big]+\frac{8\epsilon_1\cdot\epsilon_2\epsilon_3\cdot l}{{k_3}^2 l^2}+\mathcal{O}\left(\frac{1}{z}\right)\,. \end{aligned} \tag{3.30}$$

All $\mathcal{O}(z)$ and $\mathcal{O}(1)$ terms except the last one in the above expression vanish for the choice of polarization (4.42). The last $\mathcal{O}(1)$ term also vanishes after integration over the loop momentum (being proportional to a tadpole tensor integral (3.4)).

Proceeding as with the triangle diagram, we find that the residue of the pole at $z=z_1$ (3.26) is the sole contribution. We obtain

$$\begin{aligned}A_3^{1-\text{loop},(b)} &= \frac{4\epsilon_1\cdot\epsilon_2\epsilon_3^{\mu}}{k_3^2}\Big[-2k_3^2 k_{1\mu}I(k_3)-4k_1{}^{\nu}I_{\mu\nu}(k_3)-\\ &\quad 4k_3{}^{\nu}I_{\mu\nu}(k_3)+2I_{\mu\nu}{}^{\nu}(k_3)+k_3^2 I_{\mu}(k_3)\Big]\end{aligned} \tag{3.31}$$

written in terms of two-point tensor integrals (3.8).

After integrating over the loop momentum, we arrive at

$$A_3^{1-\text{loop},(b)}=\frac{1}{16\pi^2}\epsilon_1\cdot\epsilon_2\epsilon_3\cdot k_1\left(\frac{20}{3(2-\omega)}-12+\mathcal{O}(2-\omega)\right). \tag{3.32}$$

Adding the contributions of the two diagrams, (3.29) and (3.32), we obtain a finite three-point one-loop amplitude,

$$A_3^{1-\text{loop}}=A_3^{1-\text{loop},(a)}+A_3^{1-\text{loop},(b)}=\frac{1}{12\pi^2}\epsilon_1\cdot\epsilon_2\epsilon_3\cdot k_1\,, \tag{3.33}$$

as expected [59].

Recall that this is valid for a choice of polarization vectors ϵ_1 and ϵ_2 obeying $\epsilon_1\cdot k_i=\epsilon_2\cdot k_i=0$ $(i=1,2,3)$. It is easily generalized to arbitrary polarization

vectors,

$$A_3^{1-\text{loop}} = A_3^{1-\text{loop},(a)} + A_3^{1-\text{loop},(b)} = \frac{1}{12\pi^2} A_3^{\text{tree}} \ , \ \ A_3^{\text{tree}} = \epsilon_1\cdot\epsilon_2\epsilon_3\cdot k_1 + \epsilon_2\cdot\epsilon_3\epsilon_1\cdot k_2 + \epsilon_3\cdot\epsilon_1\epsilon_2\cdot k_3 \ . \tag{3.34}$$

This form is also valid in the limit in which all three legs are on shell ($k_i^2 = 0$, $i = 1, 2, 3$), which is kinematically allowed if the momenta are complex, and will be useful in the calculation of higher-order diagrams. On shell k_3 has two polarizations which can be chosen as the set of null vectors $\{k_1 - k_2 \ , \ \epsilon_2\cdot k_1 \epsilon_1 - \epsilon_1\cdot k_2 \epsilon_2 - \epsilon_1\cdot\epsilon_2 \frac{k_1-k_2}{2}\}$. Once again, only polarizations that have non-vanishing components along $\epsilon_3 = k_1 - k_2$ give non-vanishing amplitudes.

Evidently, the residue contributing to the loop amplitude consists of two five-point tree diagrams contributing to the forward amplitude (diagrams *(a)* and *(b)* in figure 3.4),

$$A_5^{\text{tree}}(k_2 + z_1\epsilon_2, \epsilon_2; k_1, \epsilon_1; k_3 - z_1\epsilon_2, \epsilon_3; l - k_3 + z_1\epsilon_2, \epsilon_4; -l + k_3 - z_1\epsilon_2, \epsilon_5) \tag{3.35}$$

with z_1 given by (3.26). All legs are on-shell, but we shall keep the momentum k_3 off shell for convenience, taking the limit $k_3^2 \to 0$ at the end of the day. The contributions of the first two diagrams in figure 3.4, $A_5^{\text{tree},(a)}$ and $A_5^{\text{tree},(b)}$, respectively, match our earlier result after we identify $\epsilon_5 = \epsilon_4^*$ and sum over the polarization vectors ϵ_4. We conclude

$$A_3^{1-\text{loop}} = \int \frac{d^{2\omega} l}{(4\pi)^{2\omega}} \frac{1}{(l-k_3)^2} \sum_{\epsilon_4} \left(A_5^{\text{tree},(a)} + A_5^{\text{tree},(b)} \right) \Big|_{\epsilon_5 = \epsilon_4^*} \ . \tag{3.36}$$

However, the forward tree amplitude is singular. To regulate it, introduce a small momentum p_μ and consider the amplitude with shifted legs $k_3 - z_1\epsilon_2 \mapsto k_3 - z_1\epsilon_2 + p$, $l - k_3 + z_1\epsilon_2 \mapsto l - k_3 + z_1\epsilon_2 - p$ (figure 3.4), in the limit $p_\mu \to 0$. As with the two-point loop amplitude, it can be checked that the singular terms do not contribute

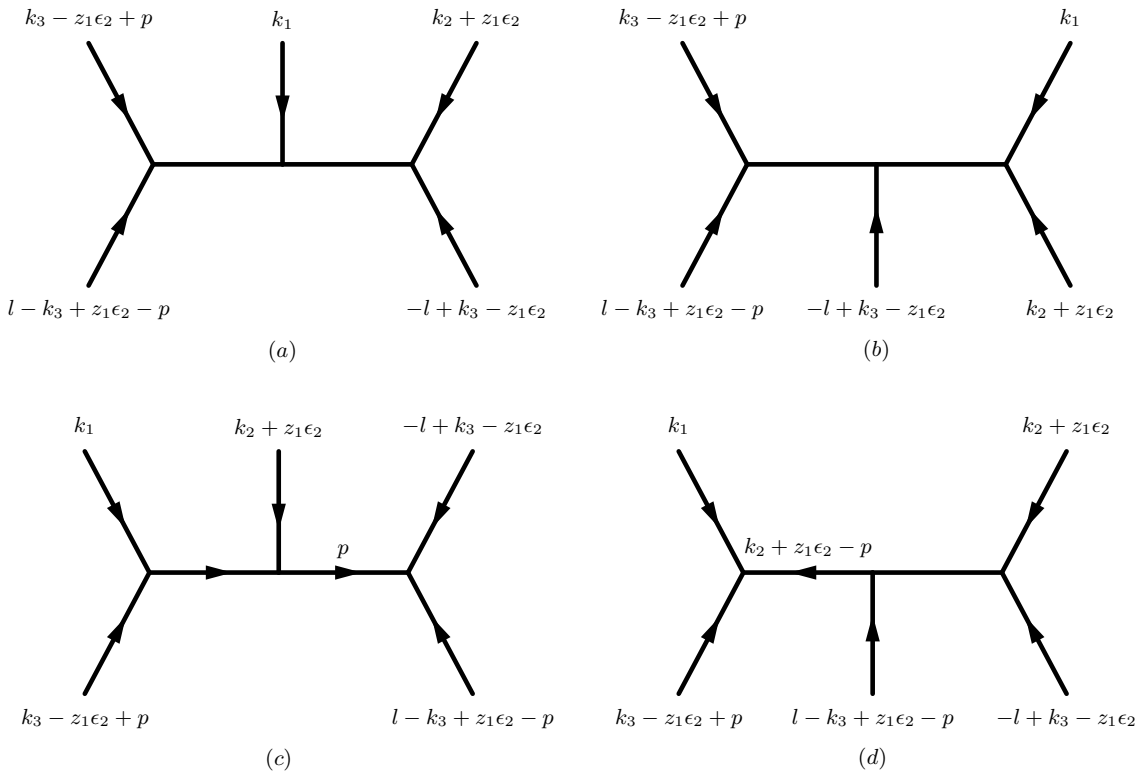

Figure 3.4: Some of the five-point tree diagrams contributing to a three-point color-ordered one-loop amplitude. p_μ is a momentum regulator.

after integration over the loop momentum. We conclude

$$A_3^{1-\text{loop}} = \int \frac{d^{2\omega}l}{(4\pi)^{2\omega}} \frac{1}{(l-k_3)^2} \sum_{\epsilon_4} A_5^{\text{tree}}\Big|_{\epsilon_5=\epsilon_4^*} . \tag{3.37}$$

The calculation of the forward amplitude A_5^{tree} can be done by applying the BCFW recursion relations. By appropriate shifts of momenta, it can thus be reduced to three-point tree amplitudes avoiding the singularities. Indeed, let us shift

$$k_1 \mapsto k_1 + w\epsilon_2 \ , \quad k_2 + z_1\epsilon_2 \mapsto k_2 + z_1\epsilon_2 - w\epsilon_2 \tag{3.38}$$

The contribution from $w \to \infty$ is easily seen to vanish. There is a pole at

$$w = w_1 = -\frac{(l+k_1)^2}{2l\cdot\epsilon_2} \ . \tag{3.39}$$

Its residue gives the entire five-point tree amplitude (3.35),

$$\begin{aligned}
&\frac{\mathrm{Res}_{w\to w_1}}{w_1} = \sum_{\epsilon_4} A_5^{\mathrm{tree}}\Big|_{\epsilon_5=\epsilon_4^*} \\
= \ & \frac{1}{(l+k_1)^2}\sum_{\epsilon_4,\epsilon'} A_3^{\mathrm{tree}}(-l+k_3-z_1\epsilon_2,\epsilon_4;k_2+z_1\epsilon_2-w_1\epsilon_2,\epsilon_2;l+k_1+w_1\epsilon_2,\epsilon)\times \\
& A_4^{\mathrm{tree}}(l-k_3+z_1\epsilon_2,{\epsilon_4}^*;k_3-z_1\epsilon_2,\epsilon_3;k_1+w_1\epsilon_2,\epsilon_1;-l-k_1-w_1\epsilon_2,\epsilon^*).
\end{aligned} \tag{3.40}$$

The four point amplitude in the above expression is a forward amplitude. It can be reduced to a finite expression involving three-point tree amplitudes, as before (see discussion in the case of the two-point loop amplitude leading to eq. (3.20)). After some straightforward algebra, we arrive at the finite expression

$$\sum_{\epsilon_4} A_5^{\mathrm{tree}}\Big|_{\epsilon_5=\epsilon_4^*} = \frac{4\mathcal{N}}{l^2(l+k_1)^2(l-k_3)^2} \tag{3.41}$$

where

$$\begin{aligned}
\mathcal{N} \ = \ & \frac{4\epsilon_1\cdot\epsilon_2\epsilon_3\cdot l(l+k_1)^2k_2\cdot l}{k_3^2} - 2\epsilon_1\cdot\epsilon_2\epsilon_3\cdot k_1(l-k_3)^2 + k_3^2\epsilon_1\cdot\epsilon_2\epsilon_3\cdot(l+k_1) - \\
& 2\epsilon_1\cdot\epsilon_2\epsilon_3\cdot k_1(l+k_1)^2l - 4\epsilon_1\cdot l\epsilon_2\cdot l\epsilon_3\cdot l
\end{aligned} \tag{3.42}$$

which indeed yields the sum of (3.27) and (3.31) (via (3.37)), and therefore the correct (finite) value of the three-point loop amplitude (3.33).

3.4 Four-point loop amplitude

In this section, we consider the four-point color-ordered one-loop amplitude,

$$A_4^{1-\text{loop}}(k_1,\epsilon_1;k_2,\epsilon_2;k_3,\epsilon_3;k_4,\epsilon_4) = \int \frac{d^{2\omega}l}{(4\pi)^{2\omega}} \mathcal{A}_4^{1-\text{loop}}(k_1,\epsilon_1;k_2,\epsilon_2;k_3,\epsilon_3;k_4,\epsilon_4) \tag{3.43}$$

where $k_1+k_2+k_3+k_4=0$ and all momenta are on shell ($k_1^2=k_2^2=k_3^2=k_4^2=0$).

It suffices to consider amplitudes in which

$$\epsilon_1 = \epsilon_2 \ . \tag{3.44}$$

This is because they form a basis: all amplitudes can be expressed as linear combinations of amplitudes with two identical polarization vectors. To see this, first recall that for general momenta k_1 and k_2, the corresponding polarization vectors can be chosen to be common to both. Indeed, if $\epsilon_1 \cdot k_2 \neq 0$, then by shifting $\epsilon_1 \mapsto \epsilon_1 - \frac{\epsilon_1\cdot k_2}{k_1\cdot k_2}k_2$, we satisfy $\epsilon_1 \cdot k_2 = 0$ (in addition to $\epsilon_1 \cdot k_1 = 0$). There are two linearly independent choices for ϵ_1 obeying $\epsilon_1\cdot k_2 = \epsilon_1 \cdot k_1 = 0$. Similarly, we have two linearly independent choices of ϵ_3 such that $\epsilon_3 \cdot k_2 = \epsilon_3 \cdot k_3 = 0$. Then a basis for the polarization vector ϵ_2 can be $\{\epsilon_1, \epsilon_3\}$. Thus, we need only consider amplitudes with $\epsilon_2 = \epsilon_1$ or $\epsilon_2 = \epsilon_3$. Without loss of generality, we adopt (3.44).

To apply the BCFW recursion relations, we shall shift the two adjacent legs,

$$k_1 \mapsto k_1 + z\epsilon_1 \ , \quad k_2 \mapsto k_2 - z\epsilon_1 \ . \tag{3.45}$$

An explicit calculation shows that for polarization vectors obeying (3.44), the *integrand* of the four-point one-loop amplitude (3.43) vanishes in the limit $z \to \infty$,

$$\mathcal{A}_4^{1-\text{loop}}(\epsilon_1, k_1+z\epsilon_1; \epsilon_2, k_2 - z\epsilon_1; \epsilon_3, k_3; \epsilon_4, k_4) = \mathcal{O}\left(\frac{1}{z}\right) \tag{3.46}$$

Therefore, only the poles contribute to the amplitude. To calculate their residues, it is advantageous to consider the basis for the remaining polarization vectors, ϵ_3 and ϵ_4,

$$\epsilon_3 = \left\{ \epsilon_1 - \frac{k_3 \cdot \epsilon_1}{k_3 \cdot k_1} k_1 \ , \ \epsilon_2 - \frac{k_3 \cdot \epsilon_2}{k_3 \cdot k_2} k_2 \right\} \ , \quad \epsilon_4 = \left\{ \epsilon_1 - \frac{k_4 \cdot \epsilon_1}{k_4 \cdot k_1} k_1 \ , \ \epsilon_2 - \frac{k_4 \cdot \epsilon_2}{k_4 \cdot k_2} k_2 \right\} \ . \tag{3.47}$$

3.4.1 Choice (A) of polarization vectors

First, consider the case

$$(\mathbf{A}) \quad : \qquad \epsilon_3 = \epsilon_1 - \frac{k_3 \cdot \epsilon_1}{k_3 \cdot k_1} k_1 \ , \quad \epsilon_4 = \epsilon_1 - \frac{k_4 \cdot \epsilon_1}{k_4 \cdot k_1} k_1 \ . \tag{3.48}$$

Notice that with this choice of polarization vectors, the corresponding four-point tree diagram vanishes.

The entire contribution to the box diagram in figure 3.5 comes from the pole at

$$z = z_1 = -\frac{l^2}{2\epsilon_1 \cdot l} \ . \tag{3.49}$$

Explicitly,

$$A_4^{1-\text{loop}\,,\,(a)}\Big|_{z \to z_1} = 16 \epsilon_1^\mu \epsilon_1^\nu \left[\alpha^{\rho\sigma} I_{\mu\nu\rho\sigma}(k_2, k_3, k_4) + \beta^\rho I_{\mu\nu\rho}(k_2, k_3, k_4) \right] \tag{3.50}$$

written in terms of the four-point tensor integrals,

$$I_{\mu_1 \mu_2 \ldots}(k_2, k_3, k_4) = \int \frac{d^{2\omega} l}{(2\pi)^{2\omega}} \frac{l_{\mu_1} l_{\mu_2} \cdots}{l^2 (l + k_2)^2 (l + k_2 + k_3)^2 (l + k_2 + k_3 + k_4)^2} \tag{3.51}$$

where

$$\begin{aligned}\alpha^{\rho\sigma} &= -\epsilon_1^\rho \epsilon_1^\sigma + \frac{\epsilon_1\cdot k_3 (k_2-k_1)\cdot k_3 \epsilon_1^\rho k_1^\sigma + (\epsilon_1\cdot k_3)^2 k_1^\rho k_1^\sigma}{k_1\cdot k_3 k_2\cdot k_3} \\ \beta^\rho &= \epsilon_1\cdot k_3 \frac{k_1\cdot k_2}{k_1\cdot k_3}\epsilon_4^\rho \ . \end{aligned} \tag{3.52}$$

After we integrate over the loop momentum, we obtain a finite expression,

$$A_4^{1-\text{loop},(a)}\Big|_{z\to z_1} = -\frac{1}{24\pi^2}\frac{(\epsilon_1\cdot k_3)^4 k_1\cdot k_2}{k_1\cdot k_3 (k_2\cdot k_3)^2} \ . \tag{3.53}$$

There is one more diagram that contributes to this amplitude (diagram *(b)* in figure 3.5). The other diagrams vanish for the choice of polarization vectors under consideration (eqs. (3.44) and (3.48)).

Diagram *(b)* in fig. 3.5 has two poles, one given by (4.35), and a new pole at

$$z = z_2 = -\frac{k_2\cdot k_3}{\epsilon_1\cdot k_3} \ . \tag{3.54}$$

The residue of the pole (4.35) gives a contribution to the amplitude,

$$A_4^{1-\text{loop},(b)}\Big|_{z\to z_1} = 16\epsilon_1^\mu \epsilon_1^\nu \left[\alpha^{\rho\sigma} I_{\mu\nu\rho\sigma}(k_2,k_3,k_4') + \beta^\rho I_{\mu\nu\rho}(k_2,k_3,k_4')\right] \tag{3.55}$$

where we introduced the on-shell momentum (it is easy to see that $k_4'^2 = 0$),

$$k_4' = \frac{k_2\cdot k_3}{\epsilon_1\cdot k_3}\epsilon_1 - k_2 - k_3 \tag{3.56}$$

and the coefficients $\alpha^{\rho\sigma}$ and β^ρ are as before (eq. (3.52)). It is easily seen to vanish (by a direct calculation, or, e.g., by replacing $k_1 \mapsto z_2\epsilon_1$ in (3.53)),

$$A_4^{1-\text{loop},(b)}\Big|_{z\to z_1} = 0 \ . \tag{3.57}$$

Therefore (3.53) is the entire contribution of the pole (4.35).

Working as above with the second pole (3.54), after some straightforward algebra we find that the residue of the pole (3.54) gives a finite contribution to the amplitude,

$$A_4^{1-\text{loop},\,(b)}\Big|_{z\to z_2} = \frac{(\epsilon_1\cdot k_3)^4(k_1\cdot k_2)^2}{24\pi^2 k_1\cdot k_3(k_2\cdot k_3)^3}\ . \tag{3.58}$$

Notice that each pole contribution can be written as a single term and the two poles lead to different kinematical expressions.

Combining the contribution of the two poles, (3.53) and (3.58), we obtain the four-point amplitude

$$A_4^{1-\text{loop}} = \frac{(\epsilon_1\cdot k_3)^4 k_1\cdot k_2(k_1-k_3)\cdot k_2}{24\pi^2 k_1\cdot k_3(k_2\cdot k_3)^3}\ , \tag{3.59}$$

which is the same expression (with appropriate identifications) as in [60].

The residue at $z=z_1$ (4.35) can be expressed in terms of a six-point forward tree amplitude. As in the case of a three-point one-loop amplitude, we can introduce a momentum regulator p_μ by shifting the legs $l+z_1\epsilon_1 \mapsto l+z_1\epsilon_1-p$, $k_3\mapsto k_3+p$ (see figure 3.6). An explicit calculation shows that singularities of the forward amplitude do not contribute (in the limit $p_\mu\to 0$) after integration over the loop momentum.

Thus, the contribution to the pole at $z=z_1$ can be written as

$$A_4^{1-\text{loop}}\Big|_{z\to z_1} = \int \frac{d^{2\omega}l}{(4\pi)^{2\omega}}\,\frac{1}{l^2}\sum_{\epsilon_5} A_6^{\text{tree}}\Big|_{\epsilon_6=\epsilon_5^*} \tag{3.60}$$

As with the five-point tree amplitude involved in the calculation of a three-point loop amplitude, the six-point amplitude can be reduced to lower-point amplitudes by a judicious application of the BCFW recursion relations. It is convenient to shift

$$k_1+z_1\epsilon_1\mapsto k_1+z_1\epsilon_1+w\epsilon_4\ \ ,\qquad k_4\mapsto k_4-w\epsilon_4\ . \tag{3.61}$$

There is no shift in the polarization vectors, because $\epsilon_1 \cdot \epsilon_4 = 0$ because of (3.48). One can easily check that the amplitude vanishes in the limit $w \to \infty$. There is a pole at

$$w = w_1 = \frac{(l-k_1)^2}{2\epsilon_4 \cdot l} \ . \tag{3.62}$$

The corresponding residue is given by

$$\begin{aligned} \frac{\text{Res}_{w\to w_1}}{w_1} &= \sum_{\epsilon_5} A_6^{\text{tree}}\Big|_{\epsilon_6=\epsilon_5^*} \\ &= \frac{1}{(l-k_1)^2} \sum_{\epsilon_5,\epsilon'} A_5^{\text{tree}}(l+z_1\epsilon_1, \epsilon_5^*; k_2 - z_1\epsilon_1, \epsilon_1; k_3, \epsilon_3; k_4 - w_1\epsilon_4, \epsilon_4; -l+k_1+w_1\epsilon_4, \epsilon) \\ &\qquad \times A_3^{\text{tree}}(l-k_1-w_1\epsilon_4, \epsilon'; k_1+z_1\epsilon_1+w_1\epsilon_4, \epsilon_4; -l-z_1\epsilon_1, \epsilon_5) \ . \end{aligned} \tag{3.63}$$

The five-point tree amplitude is a forward amplitude containing potential singularities. However, it can be calculated in the same way as the five-point forward amplitude encountered in the calculation of the three-point loop amplitude (see eqs. (3.37) through (3.42)). Thus, by a repeated application of the BCFW recursion relations, it is reduced to on-shell three-point amplitudes. After some algebra, and using (3.60), we obtain agreement with our earlier result (3.53), which was obtained by a direct diagrammatic calculation.

Turning to the other pole that contributes to the amplitude, at $z = z_2$, we obtain the residue

$$\begin{aligned} \mathcal{A}_4^{1-\text{loop}}\Big|_{z\to z_2} = \frac{1}{k_2\cdot k_3} \quad & \sum_{\epsilon'} A_3^{1-\text{loop}}(k_2 - z_2\epsilon_1, \epsilon_1; k_3, \epsilon_3; -k_2-k_3+z_2\epsilon_1, \epsilon') \\ & \times \\ & A_3^{\text{tree}}(k_1+z_2\epsilon_1, \epsilon_1; -k_1-k_4-z_2\epsilon_1, \epsilon'; k_4, \epsilon_4) \ . \end{aligned} \tag{3.64}$$

It is already written in terms of on-shell amplitudes with no singularities. Using our earlier results on three-point amplitudes, and integrating over the loop momentum,

after some algebra, one can show that the contribution of the second pole (3.64) agrees with our earlier result (3.58) obtained by a direct diagrammatic calculation.

Thus, we have shown that the four-point one-loop amplitude with the choice of polarization vectors (3.48) can be expressed in terms of three-point on-shell tree-amplitudes and a three-point one-loop on-shell amplitude (4.46). The latter also reduces to three-point tree-amplitudes, as was shown in the previous section.

3.4.2 Choice (B) of polarization vectors

Next, we consider the case of polarization vectors

$$(\mathbf{B}) \quad : \qquad \epsilon_3 = \epsilon_1 - \frac{k_3 \cdot \epsilon_1}{k_3 \cdot k_1} k_1 \ , \quad \epsilon_4 = \epsilon_2 - \frac{k_4 \cdot \epsilon_2}{k_4 \cdot k_2} k_2 \tag{3.65}$$

Unlike with the previous choice (3.48), the corresponding four-point tree diagram is non-vanishing,

$$A_4^{\text{tree},(\mathbf{B})} = -\frac{(\epsilon_1 \cdot k_3)^4 k_1 \cdot k_2}{(k_1 \cdot k_3)^2 k_2 \cdot k_3} \ . \tag{3.66}$$

One obtains a simple expression because only the t-channel contributes to the color-ordered amplitude.

For the loop amplitude, we obtain eight non-vanishing graphs which contribute for our choice of basis (3.65) shown in figure 3.5. A direct calculation shows that the pole at $z = z_2$ (3.54) gives a vanishing contribution. This is confirmed by an application of the BCFW recursion relations (eq. (3.64)). Therefore, the amplitude is determined solely by the pole at $z = z_1$ (4.35). A calculation of the residue of the pole, using diagrams as before, leads to an expression which is in agreement with the one obtained by a direct diagrammatic calculation. After integrating over the loop

momentum, we obtain a divergent expression,

$$A_4^{1-\text{loop}} = \frac{1}{8\pi^2} A_4^{\text{tree},(\mathbf{B})} \frac{\Gamma^2(\omega-1)\Gamma(3-\omega)}{\Gamma(2\omega-3)} \left(\frac{4\pi\mu^2}{s}\right)^{2-\omega} \times \Big[-\frac{2}{(2-\omega)^2} - \frac{1}{2-\omega}\left(\frac{11}{3} - 2\ln\frac{t}{s}\right) + \frac{11}{6}\ln\frac{\mu^2 t}{s^2} + \frac{\pi^2}{2} - \frac{32}{9} + \mathcal{O}(2-\omega)\Big] , \tag{3.67}$$

where $s = 2k_1 \cdot k_2$, $t = 2k_2 \cdot k_3$. This expression agrees with the ones derived in [60] (see also [61]) with appropriate kinematical identifications, after setting the arbitrary momentum scale $Q^2 = s$.

The contribution to the pole at $z = z_1$ can be written in terms of a six-point forward tree amplitude as in (3.60). The latter can be reduced to lower-point amplitudes by a judicious application of the BCFW recursion relations (avoiding the potential singularities). To this end, instead of the shift (3.61), it is convenient to shift

$$k_3 \mapsto k_3 + wq \quad , \qquad k_4 \mapsto k_4 - wq \quad , \qquad q = \epsilon_1 - \frac{\epsilon_1 \cdot k_3}{k_1 \cdot k_3}(k_1 + k_3) \ . \tag{3.68}$$

There is no shift in the polarization vectors, because $\epsilon_3 \cdot q = \epsilon_4 \cdot q = 0$, where we used (3.44) and (3.65). In fact $\epsilon_i - q$ is along the direction of the corresponding momentum k_i $(i = 3, 4)$. Since the amplitude is on shell, we could replace both polarization vectors ϵ_3 and ϵ_4 by q, to simplify the calculation.

One can easily check that the amplitude vanishes in the limit $w \to \infty$. There is a pole at

$$w = w_1 = -\frac{(l + k_2 + k_3)^2}{2q \cdot (l + k_2)} \tag{3.69}$$

The corresponding residue is given by

$$
\begin{aligned}
&\frac{\text{Res}_{w\to w_1}}{w_1} \\
&= \sum_{\epsilon_5} A_6^{\text{tree}}\Big|_{\epsilon_6=\epsilon_5^*} \\
&= \frac{1}{2(l+k_2)\cdot q}\sum_{\epsilon_5,\epsilon'} A_4^{\text{tree}}(l+z_1\epsilon_1,\epsilon_5^*;k_2-z_1\epsilon_1,\epsilon_1;k_3+wq,q;-l-k_2-k_3-wq,\epsilon'^*) \\
&\quad \times A_4^{\text{tree}}(l+k_2+k_3+wq,\epsilon';k_4-wq,q;k_1+z_1\epsilon_1,\epsilon_1;-l-z_1\epsilon_1,\epsilon_5)\ . \qquad (3.70)
\end{aligned}
$$

The two four-point tree amplitudes are on-shell amplitudes and can be reduced to three-point amplitudes by an application of the BCFW recursion relations. Thus, by a repeated application of the BCFW recursion relations, the six-point amplitude is reduced to on-shell three-point amplitudes. After some algebra, and using (3.60), we obtain agreement with our earlier result (3.67), which was obtained by a direct diagrammatic calculation.

The remaining two choices of polarization vectors can be tackled similarly and will not be discussed explicitly here.

Summarizing, we have shown that four-point one-loop amplitudes can be expressed in terms of three-point on-shell tree-amplitudes.

3.5 Higher-point loop amplitudes

The calculation of the four-point color-ordered one-loop amplidute can be straightforwardly generalized to high-point amplitudes,

$$
A_n^{1-\text{loop}}(\{k_i,\epsilon_i\}) = \int \frac{d^{2\omega}l}{(4\pi)^{2\omega}} \mathcal{A}_n^{1-\text{loop}}(\{k_i,\epsilon_i\}) \qquad (3.71)
$$

As explained in section 3.4, it suffices to consider amplitudes with two identical polarization vectors. Without loss of generality, we shall choose (3.44) for the adjacent legs with momenta k_1, k_2.

To apply the BCFW recursion relations, we shift the momenta k_1, k_2 as in (4.88). Using the Ward identity,

$$A_n^{1-\text{loop}}(k_1 + z\epsilon_1, k_1 + z\epsilon_1; \dots) = 0 \tag{3.72}$$

we deduce

$$\begin{aligned} &A_n^{1-\text{loop}}(k_1 + z\epsilon_1, \epsilon_1; k_2 - z\epsilon_1, \epsilon_1; k_3, \epsilon_3; \dots; k_n, \epsilon_n) = \\ &-\frac{1}{z} A_n^{1-\text{loop}}(k_1 + z\epsilon_1, k_1; k_2 - z\epsilon_1, \epsilon_1; k_3, \epsilon_3; \dots; k_n, \epsilon_n) \ . \end{aligned} \tag{3.73}$$

It is easy to see that the amplitude on the right-hand side of (3.73) has a finite limit as $z \to \infty$. Indeed, e.g., diagram *(a)* in figure 3.7, is a rational function of z. There are two $\mathcal{O}(z)$ vertices that contribute to the numerator, and one $\mathcal{O}(z)$ propagator that contributes to the denominator. The $\mathcal{O}(z)$ contribution is the leading term,

$$\begin{aligned} &\mathcal{A}_n^{1-\text{loop}\ ,\ (a)}\Big|_{\epsilon_1 = k_1} = \\ &\frac{\cdots k_1^{\mu_1} \left[-\eta_{\rho\nu}\epsilon_{1\mu_1} - 2\eta_{\nu\mu_1}\epsilon_{1\rho} + 2\eta_{\mu_1\rho}\epsilon_{1\nu}\right] \eta^{\rho\sigma} \epsilon_1^{\mu_2} \left[-\eta_{\sigma\lambda}\epsilon_{1\mu_2} + 2\eta_{\lambda\mu_2}\epsilon_{1\sigma} - 2\eta_{\mu_2\sigma}\epsilon_{1\lambda}\right] \cdots}{2\epsilon_1 \cdot l} z \\ &+\mathcal{O}(1) \ . \end{aligned} \tag{3.74}$$

Evidently, the numerator of the leading $\mathcal{O}(z)$ term vanishes, showing that the contribution of this diagram is $\mathcal{O}(1)$. Similarly, one can show that the $\mathcal{O}(z)$ terms in all other diagrams, such as *(b)* and *(c)* in figure 3.7 vanish, therefore all diagrams contributing to the amplitude on the right-hand side of (3.73) (with $\epsilon_1 = k_1$) are finite in the limit $z \to \infty$, and the amplitude we are interested in (left-hand side of (3.73)) is

$$\mathcal{A}_n^{1-\text{loop}}(k_1 + z\epsilon_1, \epsilon_1; k_2 - z\epsilon_1, \epsilon_1; k_3, \epsilon_3; \dots; k_n, \epsilon_n) = \mathcal{O}\left(\frac{1}{z}\right) \ . \tag{3.75}$$

Thus, only poles contribute to the integrand. The pole in the one-particle irreducible part of the amplitude has a residue which is a forward tree amplitude with $n+2$ legs. The extra two legs have momenta $\pm(l+z_1\epsilon_1)$ and corresponding polarization vectors ϵ_{n+1} and ϵ_{n+2}, with $\epsilon_{n+2}=\epsilon_{n+1}^*$ and we need to sum over ϵ_{n+1}. Additional poles exist on propagators which lead to a factorized amplitude when cut. Putting these together, we obtain for the loop amplitude

$$\begin{aligned} A_n^{1-\text{loop}} = \quad & \int \frac{d^{2\omega}l}{(2\pi)^{2\omega}} \frac{1}{l^2} \sum_{\epsilon_{n+1}} A_{n+2}^{\text{tree}}\Big|_{\epsilon_{n+2}=\epsilon_{n+1}^*} \\ & + \sum_I \frac{1}{(\sum_{i\in I} k_i)^2} \sum_{\epsilon} A_m^{1-\text{loop}}\left(\{k_i,\epsilon_i\}_{i\in I}; -\sum_{i\in I} k_i, \epsilon'\right) \\ & A_{n-m}^{\text{tree}}\left(-\sum_{j\in J} k_j, \epsilon'^*; \{k_j,\epsilon_j\}_{j\in J}\right) \end{aligned} \tag{3.76}$$

where the second term consists of the contributions of the residues of the poles $z=z_I$, where

$$z_I = \frac{K^2}{2\epsilon_1\cdot K}\ , \quad K=\sum_{i\in I} k_i\ , \tag{3.77}$$

and we sum over all poles, i.e., all possible partitions of the set of external momenta, I and J with m and $n-m$ elements, respectively ($I\cup J = \{k_1+z_I\epsilon_1, k_2 - z_I\epsilon_1, k_3,\ldots,k_n\}$), and $k_1+z_I\epsilon_1\in I$, $k_2-z_I\epsilon_1\in J$.

All amplitudes are on shell, however, the tree amplitude in the first term is a forward amplitude and care must be exercised in calculating it. The method we applied in the case of $n=4$ can be generalized to $n\geq 4$ straightforwardly. Thus, we can reduce the amplitude to three-point amplitudes by a judicious application of the BCFW recursion relations avoiding the singularities. The contribution of the singularities can also be seen to vanish after integration over the loop momentum by a direct calculation, after introducing a momentum regulator.

To define appropriate complex momentum shifts, choose the basis for the polarization vector ϵ_n,

$$\epsilon_n \in \left\{ \epsilon_1 - \frac{\epsilon_1 \cdot k_n}{k_1 \cdot k_n} k_1 \ , \ \epsilon_{n-1} - \frac{\epsilon_{n-1} \cdot k_n}{k_{n-1} \cdot k_n} k_{n-1} \right\} \ . \tag{3.78}$$

For the choice $\epsilon_n = \epsilon_1 - \frac{\epsilon_1 \cdot k_n}{k_1 \cdot k_n} k_1$, shift

$$k_1 + z_1 \epsilon_1 \mapsto k_1 + z_1 \epsilon_1 + w \epsilon_n \quad , \qquad k_n \mapsto k_n - w \epsilon_n \ , \tag{3.79}$$

whereas for the choice $\epsilon_n = \epsilon_{n-1} - \frac{\epsilon_{n-1} \cdot k_n}{k_{n-1} \cdot k_n} k_{n-1}$, shift

$$k_{n-1} \mapsto k_{n-1} + w \epsilon_n \quad , \qquad k_n \mapsto k_n - w \epsilon_n \ . \tag{3.80}$$

Notice that there is no need to shift polarization vectors, because $\epsilon_n \cdot \epsilon_1 = 0$, and $\epsilon_n \cdot \epsilon_{n-1} = 0$, respectively. The contribution from $w \to \infty$ vanishes in both cases and only poles contribute. Thus the $n+2$-point tree amplitude is reduced to lower-point on-shell tree amplitudes. A repetition of this step leads to a reduction to on-shell three-point tree amplitudes.

The final expression (before integrating over the loop momentum) is finite. It should be emphasized that the above reduction process works, and the potential singularity of the forward amplitude is absent, because of the contraction of polarizations of the collinear legs (eq. (3.76)), without which the forward amplitude would be singular.

3.6 Conclusion

We discussed the applicability of the BCFW recursion relations to the *integrand* of loop amplitudes in gauge theories. Working with color-ordered amplitudes, we showed that, with an appropriate choice of basis for the polarization vectors, the contribution from an infinite complex shift can be made to vanish. Thus, only poles contribute

to the loop amplitude. Their residues can be factorized into products of on-shell lower-point loop amplitudes and tree amplitudes. By repeatedly applying the BCFW recursion relations, one thus reduces the loop amplitude to on-shell three-point tree amplitudes.

An obstruction to this reduction procedure is due to one of the poles whose residue is given in terms of a forward amplitude which, in general, contrains singularities. We showed explicitly that the singularities do not contribute to the amplitude, after integrating over the loop momentum. Moreover, by a judicious application of the BCFW recursion relations that we described, potential singularities can be completely avoided. The resulting contribution to the loop amplitude is then written entirely in terms of on-shell three-point tree amplitudes. It would be interesting to see if our results can be generalized to higher-loop gauge theory amplitudes as well as supergravity.

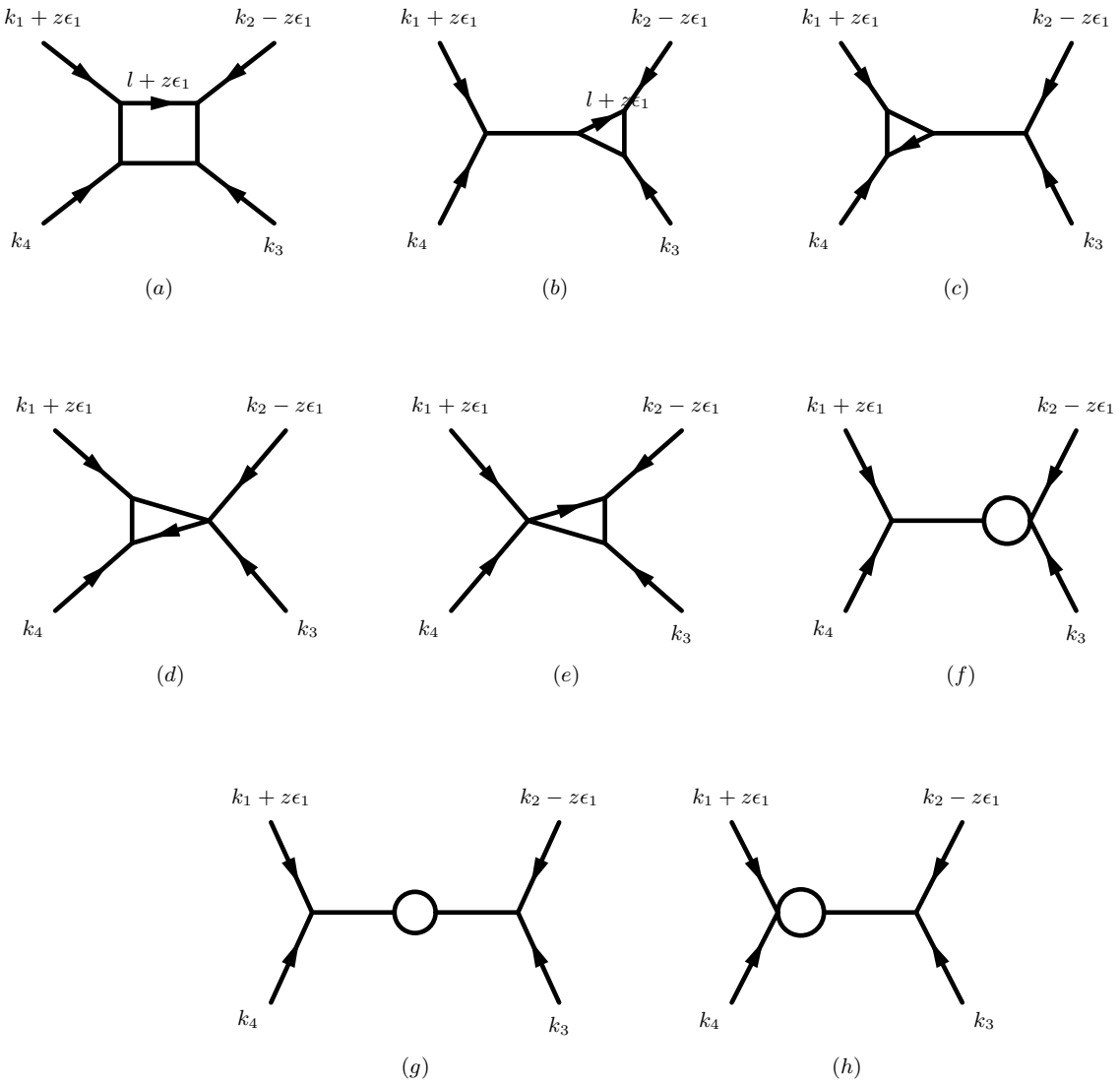

Figure 3.5: Diagrams contributing to a four-point color-ordered one-loop amplitude.

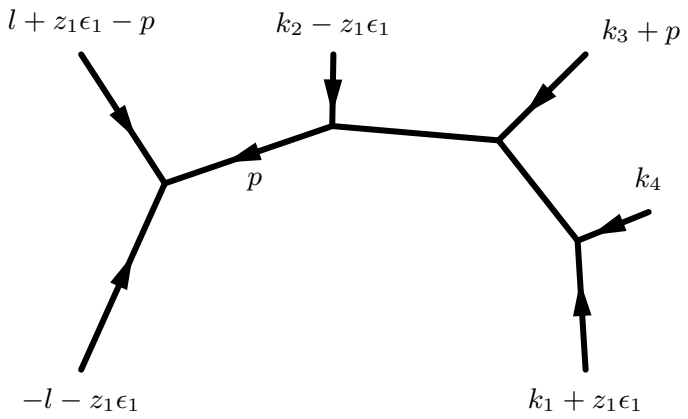

Figure 3.6: A six-point tree diagram that contributes to the four-point color-ordered one-loop amplitude. p_μ is a momentum regulator.

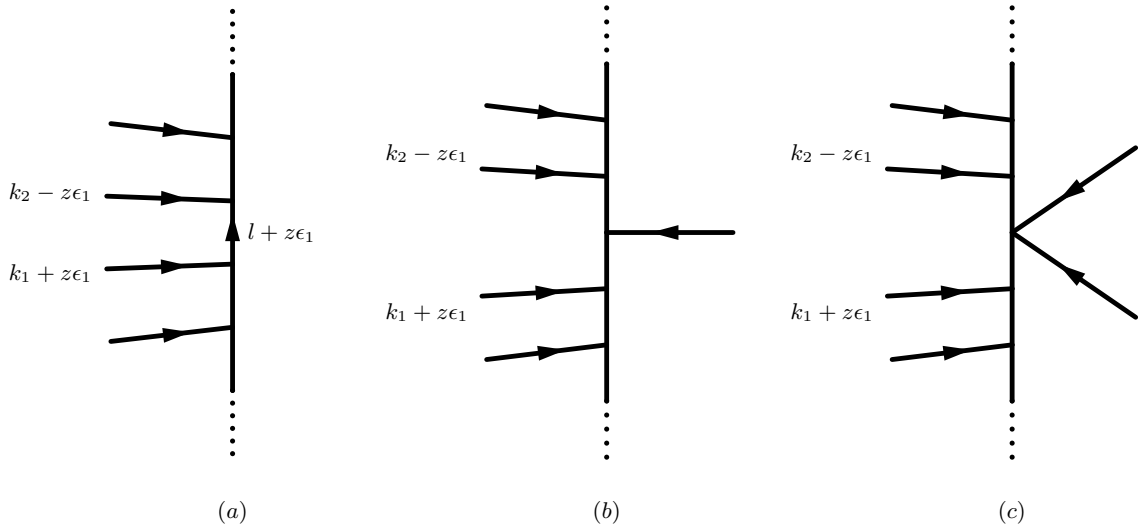

Figure 3.7: Diagrams contributing to higher-point amplitudes.

Chapter 4

Scalar and Vector Amplitudes in Anti-de Sitter Space

4.1 Introduction

The Anti-de Sitter / Conformal Field Theory correspondence (AdS/CFT) has revealed important connections between quantum gravity and gauge theory [26, 27]. Even though AdS/CFT provides a prescription for the holographic computation of correlation functions in a strongly coupled gauge theory with a gravity dual, in practice, computing these correlation functions is quite difficult. The conformal correlators are related to scattering amplitudes in AdS space. The latter are not defined in a standard fashion, as in Minkowski space, because AdS space does not admit asymptotic states which are needed for the standard definition of the S-matrix. Nevertheless, creation and annihilation operators can be defined in AdS space by changing the boundary conditions in the conformal boundary [62]. The resulting scattering amplitudes in AdS space are then related to CFT correlation functions.

AdS scattering amplitudes are derived from Witten diagrams which are difficult to calculate in coordinate space [63, 64, 65, 66, 67]. There have been some interesting developments in the computation of such diagrams in momentum space [68, 70, 69, 71].

Working in momentum space entails taking a Fourier transform of the amplitude, which is well-suited for flat Minkowski space, but does not appear to be advantageous in AdS space. Another approach using the Mellin representation of conformal correlation functions was proposed in [72, 73, 62]. In more recent work [75, 74], it was shown that CFT correlation functions factorize on poles in a Mellin representation, which suggests that Witten diagrams can be computed via a set of Feynman rules, as is the case with correlation functions of field theories on Minkowski space in the momentum (Fourier) representation.

In the case of scalar fields, by taking the Mellin transform, one trades coordinates for Mandelstam invariants of the scattering amplitude. This does not extend straightforwardly to vector or general tensor fields because of the index structure. After taking a Mellin transform, one is still left with expressions which involve coordinates, as well as Mandestam invariants. The index structure complicates calculations which involve integrals over coordinates in AdS space. Our aim is to extend the results of [75] and provide a general procedure for the calculation of Witten diagrams involving fields of arbitrary spin. We shall show that diagrams of vector fields can be written in terms of the same Mellin functions as scalar field diagrams. Our method is an iterative procedure that calculates a diagram of a certain order by sewing together lower-order diagrams. The index structure is dealt with by taking advantage of the conformal properties of the correlation functions. This work was published in [80].

The outline of our discussion is the following. In section 4.2, we review the basic ingredients in the embedding formalism which seems to be the most natural framework for the Mellin representation. In sections 4.3, 4.4, and 4.5, we calculate explicitly three-, four-, and five-point amplitudes, respectively, for scalar fields with a cubic interaction as well as vector fields. In section 4.6, we discuss the calculation of a general N-point diagram from lower-order constituents. Finally, in section 4.7, we summarize our conclusions. Appendix C.1 contains all necessary integrals over AdS space together with their derivation.

4.2 Basics

In this section, we review the basic ingredients to be used in our discussion. We adopt the notation used in [75], where further discussion can be found.

It is natural to use the embedding space formalism, which goes back to Dirac [76](also see [78]), as it provides a convenient framework for the computation of Witten diagrams. The embedding is a $(d+2)$-dimensional flat Minkowski spsace $(\mathbb{M}_{d+2})$ with metric given by

$$ds^2 = dX_A dX^A = -(dX^0)^2 + (dX^1)^2 + \cdots + (dX^d)^2 + (dX^{d+1})^2 \ . \tag{4.1}$$

The Euclidean AdS_{d+1} space is defined as the hyperboloid $X^2 = -R^2$, where $X^0 > 0$, $X^A \in \mathbb{M}^{d+2}$. Henceforth, we set $R = 1$. In this formalism, it is convenient to think of the conformal boundary of AdS as the space of null rays P^A (with $P^2 = 0$, and $P \sim \lambda P$). Then a correlation function of the dual CFT of weight Δ scales as $\mathcal{F}_\Delta(\lambda P) = \lambda^{-\Delta}\mathcal{F}_\Delta(P)$. We will be interested in n-point correlation functions of the form $\mathcal{F}(P_1, P_2, \ldots, P_n)$, and frequently use the notation

$$P_{ij} = -2P_i \cdot P_j \ . \tag{4.2}$$

We will use X^A, Y^A, etc., for points in the bulk, and P^A, Q^A, etc., for points on the boundary of AdS space. We have briefly discussed the propagators in AdS in the introduction (2.4.1). The bulk to boundary propagator for a scalar field is given by

$$E(X, P) = \frac{\Gamma(\Delta)}{2\pi^{d/2}\Gamma(1 + \Delta - d/2)}(-2P \cdot X)^{-\Delta} \ . \tag{4.3}$$

The bulk to bulk propagator for a scalar field can be written as an integral over the boundary point Q [62],

$$G(X,Y) = \int_{-i\infty}^{+i\infty} \frac{dc}{2\pi i} f_{\delta,0}(c)\Gamma(d/2+c)\Gamma(d/2-c) \int_{\partial AdS} dQ(-2X\cdot Q)^{-d/2-c}(-2Y\cdot Q)^{-d/2+c} \,, \tag{4.4}$$

where

$$f_{\delta,0}(c) = \frac{c\sin\pi c}{2\pi^{d+1}[(\delta-d/2)^2-c^2]} \,. \tag{4.5}$$

These expressions for the propagators are crucial for the factorization of amplitudes into lower-point diagrams. We are interested in calculating the N-point scalar amplitude

$$A^{(N,s)} = \langle \mathcal{O}_{\Delta_1}(P_1)\mathcal{O}_{\Delta_2}(P_2)\cdots\mathcal{O}_{\Delta_N}(P_N)\rangle \,, \tag{4.6}$$

where $\mathcal{O}_\Delta$ is a conformal operator of scaling dimension Δ.

Similarly, the bulk to boundary propagator for a vector field can be written as [75],

$$E_{MA}(X,P) = D_{MA}(\Delta,P)E(X,P) = \frac{\Gamma(\Delta)}{2\pi^{d/2}\Gamma(1+\Delta-d/2)} J_{MA}(-2P\cdot X)^{-\Delta} \tag{4.7}$$

where,

$$D_{MA}(\Delta,P) = \frac{\Delta-1}{\Delta}\eta_{MA} + \frac{1}{\Delta}\frac{\partial}{\partial P^M}P_A \tag{4.8}$$

and $J_{MA} = \eta_{MA} - \frac{P_A X_M}{P\cdot X}$ has the property, $P^M J_{MA} = J_{MA}X^A = 0$. D_{MA} is an extremely convenient operator as it organizes and simplifies the index structure of vector amplitudes, allowing us to relate them to amplitudes of scalar fields. In this regard, a useful identity is

$$D_{MA}(\Delta,P)\frac{\partial}{\partial P_A}\mathcal{F}_{\Delta-1}(P) = 0 \,, \tag{4.9}$$

where $\mathcal{F}_{\Delta-1}$ is a function of weight $\Delta-1$, i.e., $\mathcal{F}_{\Delta-1}(P) = \lambda^{-(\Delta-1)}\mathcal{F}_{\Delta-1}(P)$, and therefore $P\cdot\frac{\partial}{\partial P}\mathcal{F}_{\Delta-1} = -(\Delta-1)\mathcal{F}_{\Delta-1}$.

The bulk to bulk propagator for a vector field can be written as an integral over the boundary point Q, as in the scalar case,

$$\begin{aligned} G_{AB}(X,Y) &= \int_{-i\infty}^{+i\infty} \frac{dc}{2\pi i} f_{\delta,1}(c)\Gamma(d/2+c)\Gamma(d/2-c) \\ &\quad \times \int_{\partial AdS} dQ \eta^{MN} D_{MA}(d/2+c,Q) D_{NB}(d/2-c,Q) \\ &\quad (-2X\cdot Q)^{-d/2-c}(-2Y\cdot Q)^{-d/2+c} \ , \end{aligned} \tag{4.10}$$

where,

$$f_{\delta,1}(c) = f_{\delta,0}(c) \frac{\frac{d^2}{4}-c^2}{(\delta-\frac{d}{2})^2-c^2} \ . \tag{4.11}$$

We are interested in calculating the N-point vector amplitude

$$A^{(N,v)M_1\ldots M_N,a_1\ldots a_N} = \langle \mathcal{J}^{M_1,a_1}(P_1)\mathcal{J}^{M_2,a_2}(P_2)\cdots\mathcal{J}^{M_N,a_N}(P_N)\rangle \ , \tag{4.12}$$

where a_i $(i=1,\ldots,N)$ are gauge group indices. It should be pointed out that all current operators have dimension $\Delta = d-1$. However, we need to calculate off-shell amplitudes as well, because we are interested in sewing diagrams together in order to form higher-point amplitudes. The two legs to be sewn must be off shell, and have dimensions $\frac{d}{2}\pm c$, on account of (4.10). Therefore, we will be generally working with arbitrary dimensions of the external legs of a N-point vector amplitude.

The Mellin transform of the above N-point amplitudes will be given in terms of Mandelstam invariants δ_{ij} $(i,j=1,\ldots,N)$. They are defined with the properties

$$\delta_{ii} = 0 \quad , \quad \delta_{ij} = \delta_{ji} \quad , \quad \sum_{j=1}^{N} \delta_{ij} = \Delta_i \ . \tag{4.13}$$

4.3 Three-point Amplitudes

Having introduced all necessary ingredients, we now proceed to the explicit calculation of amplitudes, starting with the simplest amplitude.

4.3.1 Scalar amplitudes

The three-point amplitude for scalar fields of scaling dimensions Δ_i interacting via a cubic interaction of coupling constant g is (Fig. 4.1)

$$A^{(3,s)}(\Delta_1, P_1; \Delta_2, P_2; \Delta_3, P_3) = \frac{g}{\prod_i 2\pi^h \Gamma(\Delta_i + 1 - d/2)} \mathcal{A}_3(\Delta_1, P_1; \Delta_2, P_2; \Delta_3, P_3) \tag{4.14}$$

where

$$\mathcal{A}_3(\{\Delta_i, P_i\}) \equiv \int_{AdS} dX \prod_{i=1}^{3} \Gamma(\Delta_i)(-2P_i \cdot X)^{-\Delta_i} \ . \tag{4.15}$$

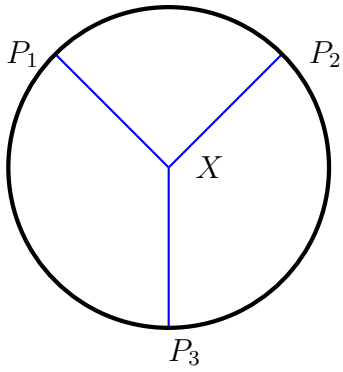

Figure 4.1: The three-point scalar amplitude (4.14)

The integral over the bulk vector X^A is of the form (C.12). Using (C.16), we obtain

$$\mathcal{A}_3(\Delta_1, P_1; \Delta_2, P_2; \Delta_3, P_3) = \frac{\pi^{d/2}}{2} \mathcal{M}_3 \Gamma(\delta_{12})\Gamma(\delta_{23})\Gamma(\delta_{13})(P_{12})^{-\delta_{12}}(P_{23})^{-\delta_{23}}(P_{13})^{-\delta_{13}} \tag{4.16}$$

where

$$\mathcal{M}_3 = \Gamma\left(\frac{\Delta_1 + \Delta_2 + \Delta_3 - d}{2}\right) \tag{4.17}$$

is the Mellin transform of the scalar three-point amplitude. There are no remaining integrals, because the constraints (C.11) completely fix the integration variables,

$$\delta_{12} = \frac{\Delta_1 + \Delta_2 - \Delta_3}{2} \ , \quad \delta_{23} = \frac{\Delta_2 + \Delta_3 - \Delta_1}{2} \ , \quad \delta_{31} = \frac{\Delta_1 + \Delta_3 - \Delta_2}{2} \tag{4.18}$$

which are the Mandelstam invariants (4.44) for a three-point amplitude.

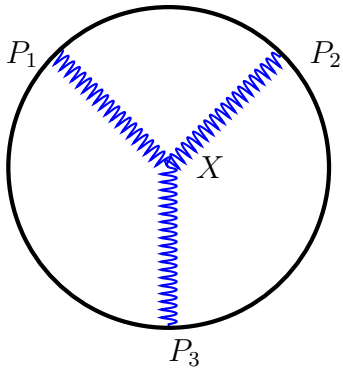

Figure 4.2: The three-point vector amplitude (4.20).

The three-point scalar amplitude is

$$A^{(3,s)}(\Delta_1, P_1; \Delta_2, P_2; \Delta_3, P_3) = \frac{g\pi^{d/2}}{2\prod_i 2\pi^{d/2}\Gamma(\Delta_i + 1 - d/2)} \mathcal{M}_3 \prod_{i<j} \Gamma(\delta_{ij}) P_{ij}^{-\delta_{ij}} \ . \tag{4.19}$$

4.3.2 Vector amplitudes

Similarly, a three-point vector amplitude is given by (fig. 4.2)

$$A^{(3,v)M_1M_2M_3,a_1a_2a_3}(\Delta_1, P_1; \Delta_2, P_2; \Delta_3, P_3) = f^{a_1a_2a_3} \prod_{i=1}^{3} D^{M_iA_i}(\Delta_i, P_i) \mathcal{A}_{A_1A_2A_3} \tag{4.20}$$

where,

$$\mathcal{A}_{A_1A_2A_3} = \int_{AdS} dX I_{A_1A_2A_3} \prod_{i=1}^{3} (-2P_i \cdot X)^{-\Delta_i} \ , \tag{4.21}$$

and the index structure is similar to a gauge theory three point vertex in flat space,

$$I_{A_1A_2A_3} = \eta_{A_1A_2} \left(K_{1A_3} - K_{2A_3}\right) + \cdots + \cdots \ , \tag{4.22}$$

with

$$K_A = (-2P \cdot X)^{\Delta} \frac{\partial}{\partial X^A} (-2P \cdot X)^{-\Delta} = -\Delta \frac{P_A}{P \cdot X} \tag{4.23}$$

We can express the three point with one leg off-shell that we can use in four and higher point diagrams in the following way,

$$\begin{aligned}\mathcal{A}_{A_1A_2A_3} &= -\int_{AdS} dX \left[\eta_{A_1A_2}\Delta_1 \frac{P_{1A_3}}{P_1\cdot X} + \eta_{A_2A_3}\left(\Delta_2\frac{P_{2A_1}}{P_2\cdot X} - \Delta_3\frac{P_{3A_1}}{P_3\cdot X}\right) - (1\leftrightarrow 2)\right] \\ &\quad \prod_{i=1}^{3}\Gamma(\Delta_i)(-2P_i\cdot X)^{-\Delta_i}\ . \end{aligned} \tag{4.24}$$

As in the scalar case, the integral over the bulk vector X^A is of the form (C.12). Using (C.16), we obtain

$$\begin{aligned}\mathcal{A}_{A_1A_2A_3} &= \eta_{A_1A_2}P_{1A_3}\mathcal{A}_3(\Delta_1+1,P_1;\Delta_2,P_2;\Delta_3,P_3) \\ &\quad +\eta_{A_2A_3}\Big[P_{2A_1}\mathcal{A}_3(\Delta_1,P_1;\Delta_2+1,P_2;\Delta_3,P_3) - \\ &\quad P_{3A_1}\mathcal{A}_3(\Delta_1,P_1;\Delta_2,P_2;\Delta_3+1,P_3)\Big] - (1\leftrightarrow 2)\end{aligned} \tag{4.25}$$

Thus, the vector amplitude is written in terms of scalar amplitudes.

As in the scalar case (Eq. (4.16)), we may write this in terms of a Mellin amplitude,

$$\mathcal{A}_{A_1A_2A_3} = \frac{\pi^{d/2}}{2}\mathcal{M}_{A_1A_2A_3}\prod_{i<j}\Gamma\left(\delta_{ij}+\frac{1}{2}\right)P_{ij}^{-\delta_{ij}+\frac{1}{2}} \tag{4.26}$$

where

$$\mathcal{M}_{A_1A_2A_3} = \Gamma\left(\frac{\Delta_1+\Delta_2+\Delta_3-d+1}{2}\right)[\mathcal{I}(1,2,3)+\mathcal{I}(2,3,1)+\mathcal{I}(3,1,2)] \tag{4.27}$$

and

$$\mathcal{I}(1,2,3) = \frac{\eta_{A_1A_2}}{P_{12}}\left(\frac{1}{\delta_{23}-\frac{1}{2}}\frac{P_{1A_3}}{P_{13}} - \frac{1}{\delta_{13}-\frac{1}{2}}\frac{P_{2A_3}}{P_{23}}\right) \tag{4.28}$$

The above expressions are simplified if all legs are on shell. Setting $\Delta_1 = \Delta_2 = \Delta_3 = d-1$, we obtain

$$\mathcal{A}^{(\text{on shell})}_{A_1A_2A_3} = \pi^{d/2}\Gamma\left(d-2\right)\left[\eta_{A_1A_2}\left(P_{23}P_{1A_3} - P_{13}P_{2A_3}\right) + \cdots + \cdots\right]\prod_{j<j}\Gamma(d/2)P_{ij}^{-d/2} \ . \tag{4.29}$$

In order to use this amplitude in a higher-point diagram, it is convenient to eliminate terms that contain the coordinate that corresponds to the leg which is to be sewn (off-shell) with a free index (i.e., not in a dot product). Without loss of generality we choose the last leg, a practice that we will follow throughout.

Thus, we wish to eliminate terms containing P_3^A. To this end, we will use the identity (4.9). Choosing $\Delta = \Delta_3$, $P^A = P_1^{A_1}$, and $\mathcal{F}_{\Delta_1-1}(P_1) = \prod_{i<j}(P_{ij})^{-\delta_{ij}+\frac{1}{2}}$, we obtain

$$\left[\left(\delta_{12}-\frac{1}{2}\right)\frac{P_2^{A_1}}{P_{12}} + \left(\delta_{13}-\frac{1}{2}\right)\frac{P_3^{A_1}}{P_{13}}\right]\prod_{i<j}(P_{ij})^{-\delta_{ij}+\frac{1}{2}} = 0 \tag{4.30}$$

Therefore,

$$\mathcal{I}(2,3,1) = \frac{2\eta_{A_2A_3}P_{2A_1}}{(\delta_{13}-\frac{1}{2})P_{12}P_{23}} \tag{4.31}$$

up to terms which vanish upon acting with $D^{M_1A_1}$, and similarly for $\mathcal{I}(3,1,2)$.

There are more terms in the amplitude involving P_3^A, due to the action of $D^{M_3A_3}$ on the off-shell leg, which also need to be eliminated. We have

$$P_{3A_3}\mathcal{I}(1,2,3) + \cdots + \cdots = \frac{1}{(\delta_{13}-\frac{1}{2})P_{12}}\left(-\eta^{A_1A_2} + \frac{2P_2^{A_1}P_3^{A_2}}{P_{23}}\right) - (1 \leftrightarrow 2) \tag{4.32}$$

Using the identity (4.9) again, the second term on the right-hand side of (4.32) is easily seen to be symmetric, and therefore vanishes. We arrive at an expression which is independent of P_3,

$$P_{3A_3}\mathcal{I}(1,2,3) + \cdots + \cdots = \frac{\Delta_1-\Delta_2}{(\delta_{23}-\frac{1}{2})(\delta_{13}-\frac{1}{2})}\frac{\eta^{A_1A_2}}{P_{12}} \ . \tag{4.33}$$

Notice that in the case of $\Delta_1 = \Delta_2$ (on-shell legs), this vanishes, so the action of $D^{M_3 A_3}$ is simple in this case.

Differentiating with respect to P_3, we obtain an additional factor,

$$\frac{\partial}{\partial P_3^{M_3}} \prod_{i<j} (P_{ij})^{-\delta_{ij}+\frac{1}{2}} = \left[(2\delta_{13}-1)\frac{P_1^{M_3}}{P_{13}} + (2\delta_{23}-1)\frac{P_2^{M_3}}{P_{23}} \right] \prod_{i<j} (P_{ij})^{-\delta_{ij}+\frac{1}{2}} \ . \tag{4.34}$$

It follows that

$$\begin{aligned} D_{M_3 A_3} \mathcal{A}^{A_1 A_2 A_3} \ &= \ \frac{\pi^{d/2}}{2} \Gamma\left(\frac{\Delta_1 + \Delta_2 + \Delta_3 - d + 1}{2} \right) \left[(\mathcal{D}_3 \mathcal{I})(1,2) - (\mathcal{D}_3 \mathcal{I})(2,1) \right] \\ & \prod_{i<j} \Gamma\left(\delta_{ij} + \frac{1}{2} \right) (P_{ij})^{-\delta_{ij}+\frac{1}{2}} \end{aligned} \tag{4.35}$$

where

$$(\mathcal{D}_3 \mathcal{I})(1,2) = \frac{(\Delta_3 + \Delta_1 - \Delta_2 - 1)\eta^{A_1 A_2} P_{1 M_3} - 2(\Delta_3 - 1)\delta^{A_1}_{M_3} P_1^{A_2}}{\Delta_3 (\delta_{23} - \frac{1}{2}) P_{12} P_{13}} \ . \tag{4.36}$$

In this form, the three-point vector amplitude can be used in higher-point amplitudes in much the same way as its scalar counterpart (4.16).

4.4 Four-point Amplitudes

In this section, we calculate scalar and vector four-point amplitudes by sewing together two three-point amplitudes calculated in section 4.3. Using the results in appendix C.1, the integrals over AdS space are performed with little effort. In the vector case, there is an additional type of diagram contributing due to the existence of a four-point vertex. A quartic interaction can also be added in the scalar case. The calculation proceeds as in the vector case.

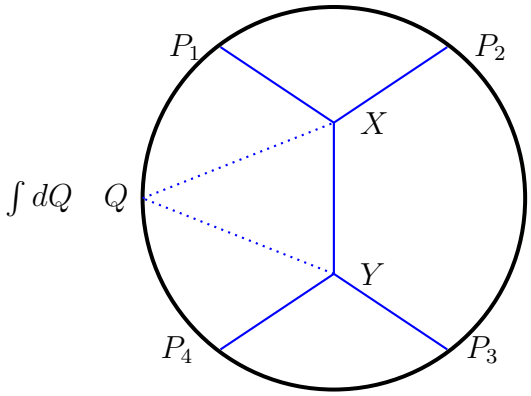

Figure 4.3: The four-point scalar amplitude (4.37).

4.4.1 Scalar amplitudes

The four-point scalar amplitude reads (Fig. 4.3)

$$A^{(4,s)}(\Delta_1,P_1;\Delta_2,P_2;\Delta_3,P_3;\Delta_4,P_4) = \frac{g^2}{\prod_i 2\pi^{d/2}\Gamma(\Delta_i+1-\frac{d}{2})}\int\frac{dc}{2\pi i}f_{\delta,0}(c) \mathcal{A}_4(\Delta_1,P_1;\Delta_2,P_2;\Delta_3,P_3;\Delta_4,P_4|c) \quad (4.37)$$

where

$$\mathcal{A}_4(\Delta_1,P_1;\Delta_2,P_2;\Delta_3,P_3;\Delta_4,P_4|c) = \int_{\partial AdS} dQ\mathcal{A}_3(\Delta_1,P_1;\Delta_2,P_2;d/2+c,Q) \mathcal{A}_3(\Delta_3,P_3;\Delta_4,P_4;d/2-c,Q) \quad (4.38)$$

and $\mathcal{A}_3$ is given by (4.16). To integrate over Q, we need to calculate

$$\int_{\partial AdS} dQ\prod_{i=1}^4\Gamma(\lambda_i)(-2Q\cdot P_i)^{-\lambda_i}\ , \quad (4.39)$$

where

$$\lambda_1=\frac{\Delta_1-\Delta_2+d/2+c}{2}\ , \qquad \lambda_2=\frac{\Delta_2-\Delta_1+d/2+c}{2}\ , \quad \lambda_3=\frac{\Delta_3-\Delta_4+d/2-c}{2}\ , \quad \lambda_4=\frac{\Delta_4-\Delta_3+d/2-c}{2} \quad (4.40)$$

Notice that $\lambda_1 + \cdots + \lambda_4 = d$. Using the result (C.10) in the Appendix, we obtain

$$\int_{\partial AdS} dQ \prod_{i=1}^{4} \Gamma(\lambda_i)(-2Q \cdot P_i)^{-\lambda_i} = \frac{\pi^{d/2}}{2} \int \prod_{i<j} d\tilde{\delta}_{ij} \Gamma(\tilde{\delta}_{ij}) P_{ij}^{-\tilde{\delta}_{ij}} \tag{4.41}$$

where the integration variables are constrained by

$$\sum_{j \neq i} \tilde{\delta}_{ij} = \lambda_i \ . \tag{4.42}$$

The integration variables are related to the Mandelstam invariants by

$$\delta_{12} = \frac{\Delta_1 + \Delta_2 - d/2 - c}{2} + \tilde{\delta}_{12} \quad , \quad \delta_{34} = \frac{\Delta_3 + \Delta_4 - d/2 + c}{2} + \tilde{\delta}_{34} \ , \tag{4.43}$$

and $\delta_{ij} = \tilde{\delta}_{ij}$, otherwise. The constraints (4.42) in terms of the standard Mandelstam variables read

$$\sum_{j \neq i} \delta_{ij} = \Delta_i \tag{4.44}$$

as expected (Eq. (4.44)).

The four-point function (4.38) becomes

$$\mathcal{A}_4(\{\Delta_i, P_i\}|c) = \frac{\pi^{d/2}}{2} \int \prod_{i<j} d\delta_{ij} \Gamma(\delta_{ij}) \mathcal{M}_4(\delta_{ij}|c) P_{ij}^{-\delta_{ij}} \tag{4.45}$$

where

$$\mathcal{M}_4 = \frac{\prod_{\sigma=\pm} \Gamma(\frac{\Delta_1+\Delta_2-d/2+\sigma c}{2}) \Gamma(\frac{\Delta_3+\Delta_4-d/2+\sigma c}{2}) \Gamma(\delta_{12} - \frac{\Delta_1+\Delta_2-d/2+\sigma c}{2})}{\Gamma(\delta_{12})\Gamma(\delta_{34})} \tag{4.46}$$

Notice that the Mellin transform (4.46) is a function of a single Mandelstam invariant, δ_{12}, because δ_{34} and δ_{12} are related through $\delta_{12} - \delta_{34} = \frac{\Delta_1+\Delta_2-\Delta_3-\Delta_4}{2}$.

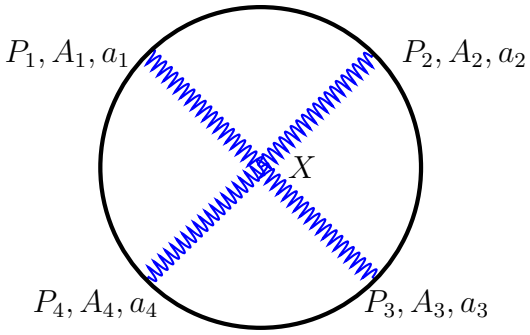

Figure 4.4: The four-point vector amplitude contact diagram (4.47).

4.4.2 Vector amplitudes

In the vector case, there are two types of diagrams, and we consider them separately. First we discuss the four-point diagram due to the four-point gauge interaction (Fig. 4.4). The amplitude is

$$A^{(4,v,(a))M_1M_2M_3M_4,a_1a_2a_3a_4} = \int_{AdS} dX\, I^{a_1a_2a_3a_4}_{A_1A_2A_3A_4} \prod_{i=1}^{4} E^{M_iA_i}(X,P_i)\ , \tag{4.47}$$

where

$$I^{a_1a_2a_3a_4}_{A_1A_2A_3A_4} = \left(f^{a_1a_4b}f^{a_2a_3b} + f^{a_1a_3b}f^{a_2a_4b}\right)\eta_{A_1A_2}\eta_{A_3A_4} + \cdots + \cdots \tag{4.48}$$

is independent of the points P_i $(i = 1, 2, 3, 4)$ and X.

The integral over the bulk vector X is of the form (C.12). Using the result (C.16), we obtain

$$A^{(4,v,(a))M_1M_2M_3M_4,a_1a_2a_3a_4} = \frac{\pi^{d/2}}{2\prod_i 2\pi^{d/2}\Gamma(1+\Delta_i-\frac{d}{2})} \prod_{i=1}^{4} D^{M_iA_i}(\Delta_i,P_i)\mathcal{A}^{a_1a_2a_3a_4}_{A_1A_2A_3A_4} \tag{4.49}$$

where

$$\mathcal{A}^{a_1a_2a_3a_4}_{A_1A_2A_3A_4} = \int \mathcal{M}^{a_1a_2a_3a_4}_{A_1A_2A_3A_4}(\delta_{ij}) \prod_{i<j} \Gamma(\delta_{ij}) P_{ij}^{-\delta_{ij}} d\delta_{ij} \tag{4.50}$$

where,

$$\mathcal{M}^{a_1a_2a_3a_4}_{A_1A_2A_3A_4} = \Gamma\left(\frac{\sum_i \Delta_i - d}{2}\right) I^{a_1a_2a_3a_4}_{A_1A_2A_3A_4}. \tag{4.51}$$

On shell ($\Delta_i = d-1$, $i = 1,2,3,4$), this amplitude reads

$$\mathcal{A}^{a_1a_2a_3a_4}_{A_1A_2A_3A_4} = \Gamma\left(\frac{3d-4}{2}\right) I^{a_1a_2a_3a_4}_{A_1A_2A_3A_4} \int \prod_{i<j} \Gamma(\delta_{ij}) P_{ij}^{-\delta_{ij}} d\delta_{ij} \ . \tag{4.52}$$

To use it in a higher-point diagram, we need to act with $D^{M_4A_4}$ and eliminate P_4 with a free index. By using the identity (4.9) with $\Delta = \Delta_3$, $P^A = P_3^{A_3}$, and $\mathcal{F}_{\Delta_3-1}(P_3) = P_{34}\prod_{i<j} P_{ij}^{-\delta_{ij}}$, we obtain

$$\left[\delta_{13}\frac{P_{34}}{P_{13}}P_1^{A_3} + \delta_{23}\frac{P_{34}}{P_{23}}P_2^{A_3} + (\delta_{34}-1)P_4^{A_3}\right]\prod_{i<j} P_{ij}^{-\delta_{ij}} = 0 \ , \tag{4.53}$$

up to terms which vanish upon acting with $D_{M_3A_3}$. We deduce

$$P_4^{A_4}\eta_{A_3A_4} = -\frac{1}{\delta_{34}-1}\left[\delta_{13}\frac{P_{1A_3}}{P_{13}} + \delta_{23}\frac{P_{2A_3}}{P_{23}}\right] P_{34} \ . \tag{4.54}$$

Differentiation with respect to P_{4M_4} has the effect of multiplication by a factor given by

$$\frac{\partial}{\partial P_{4M_4}} P_{34}\prod_{i=1}^{3} P_{i4}^{-\delta_{i4}} = 2\left[\delta_{14}\frac{P_1^{M_4}}{P_{14}} + \delta_{24}\frac{P_2^{M_4}}{P_{24}} + (\delta_{34}-1)\frac{P_3^{M_4}}{P_{34}}\right] P_{34}\prod_{i=1}^{3} P_{i4}^{-\delta_{i4}} \tag{4.55}$$

It follows that in the amplitude (4.49),

$$\begin{aligned} D^{M_4A_4}\eta_{A_3A_4} \ = \ & \frac{\Delta_4-1}{\Delta_4}\delta^{M_4}_{A_3} - \frac{2}{\Delta_4}\left(\delta_{13}\frac{P_{1A_3}}{P_{13}} + \delta_{23}\frac{P_{2A_3}}{P_{23}}\right) \\ & \left(\frac{\delta_{14}}{\delta_{34}-1}\frac{P_{34}}{P_{14}}P_1^{M_4} + \frac{\delta_{24}}{\delta_{34}-1}\frac{P_{34}}{P_{24}}P_2^{M_4} + P_3^{M_4}\right) \ . \end{aligned} \tag{4.56}$$

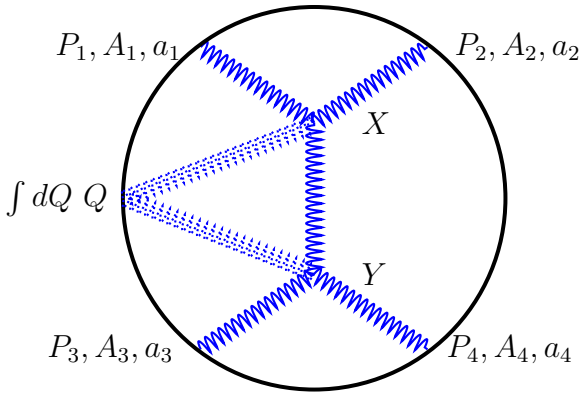

Figure 4.5: The four-point vector amplitude with gluon exchange(4.57).

This expression allows us to use this amplitude in the calculation of a higher-point amplitude in which the leg corresponding to P_4 is internal.

Next, we calculate the four-point vector amplitude depicted in Fig. 4.5. We have

$$\begin{aligned} A^{(4,v,(b))M_1M_2M_3M_4,a_1a_2a_3a_4} &= g^2 f^{a_1a_2b} f^{a_3a_4b} \int \frac{dc}{2\pi i} f_{\delta,1}(c) \\ &\quad \prod_{i=1}^{4} D^{M_iA_i}(\Delta_i, P_i) \mathcal{A}_{A_1A_2A_3A_4}(\{\Delta_i, P_i\}|c) \end{aligned} \tag{4.57}$$

where

$$\begin{aligned} \mathcal{A}_{A_1A_2A_3A_4}(\{\Delta_i, P_i\}|c) &= \int_{\partial AdS} dQ \eta_{NN'} D^{NC}(d/2+c, Q) \\ &\quad \mathcal{A}_{A_1A_2C}(\Delta_1, P_1; \Delta_2, P_2; d/2+c, Q) \\ &\quad \times D^{N'C'}(d/2-c, Q) \\ &\quad \mathcal{A}_{A_3A_4C'}(\Delta_3, P_3; \Delta_4, P_4; d/2-c, Q) \end{aligned} \tag{4.58}$$

Using (4.35), we can express this in terms of the scalar functions (4.38). The integral over Q corresponding to the product of (4.35) and its counterpart in the second

amplitude (with $1 \to 3$ and $2 \to 4$) is

$$\int_{\partial AdS} dQ \prod_{i=1}^{4} \Gamma(\lambda_i)(-2P_i \cdot Q)^{-\lambda_i} = \frac{\pi^{d/2}}{2} \int \prod_{i<j} d\tilde{\delta}_{ij} \Gamma(\tilde{\delta}_{ij}) P_{ij}^{-\tilde{\delta}_{ij}} \tag{4.59}$$

where

$$\begin{aligned} \lambda_1 &= \frac{\Delta_1 - \Delta_2 + \frac{d}{2} + c + 1}{2} \ , \quad \lambda_2 = \frac{\Delta_2 - \Delta_1 + \frac{d}{2} + c - 1}{2} \ , \\ \lambda_3 &= \frac{\Delta_3 - \Delta_4 + \frac{d}{2} - c + 1}{2} \ , \quad \lambda_4 = \frac{\Delta_4 - \Delta_3 + \frac{d}{2} - c - 1}{2} \ . \end{aligned} \tag{4.60}$$

The Mandelstam invariants are

$$\delta_{12} = \tilde{\delta}_{12} + \frac{\Delta_1 + \Delta_2 - \frac{d}{2} - c + 1}{2} \ , \quad \delta_{34} = \tilde{\delta}_{34} + \frac{\Delta_3 - \Delta_4 - \frac{d}{2} + c + 1}{2} \ , \quad \delta_{13} = \tilde{\delta}_{13} - 1 \ , \tag{4.61}$$

and $\delta_{ij} = \tilde{\delta}_{ij}$, otherwise.

Thus, the four-point vector amplitude (4.58) can be put in the form (4.45), as in the scalar case,

$$\mathcal{A}_{A_1A_2A_3A_4}(\{\Delta_i, P_i\}|c) = \frac{\pi^{d/2}}{2} \int \mathcal{M}_{A_1A_2A_3A_4}(\delta_{ij}|c) \prod_{i<j} \Gamma(\delta_{ij}) P_{ij}^{-\delta_{ij}} d\delta_{ij} \tag{4.62}$$

where

$$\begin{aligned} \mathcal{M}_{A_1A_2A_3A_4}(\delta_{ij}|c) = \frac{(\frac{d}{2}-1)^2 - c^2}{\frac{d^2}{4} - c^2} \quad & \Big[\delta_{13}\mathcal{I}(1,2,3,4) - \delta_{14}\mathcal{I}(1,2,4,3) \\ & -\delta_{23}\mathcal{I}(2,1,3,4) + \delta_{24}\mathcal{I}(2,1,4,3)\Big] \times \\ & \mathcal{M}_4 \ , \end{aligned} \tag{4.63}$$

$\mathcal{M}_4$ is as in the scalar case (Eq. (4.46)), but with the replacements $\Delta_1 \to \Delta_1+1, \Delta_3 \to \Delta_3+1$, and

$$\begin{aligned}\mathcal{I}(1,2,3,4) &= -\frac{(\frac{d}{2}+c-\Delta_1+\Delta_2-1)(\frac{d}{2}-c-\Delta_3+\Delta_4-1)}{2[(\frac{d}{2}-1)^2-c^2]}\eta_{A_1A_2}\eta_{A_3A_4} \\ &\quad -2\frac{\frac{d}{2}+c-\Delta_1+\Delta_2-1}{\frac{d}{2}+c-1}\eta_{A_1A_2}\frac{P_{1A_3}P_{3A_4}}{P_{13}} - 2\frac{\frac{d}{2}-c-\Delta_3+\Delta_4-1}{\frac{d}{2}-c-1} \\ &\quad \eta^{A_3A_4}\frac{P_{1A_2}P_{3A_1}}{P_{13}} + 4\eta_{A_1A_3}\frac{P_{1A_2}P_{3A_4}}{P_{13}} \end{aligned} \tag{4.64}$$

The above expressions simplify for on-shell amplitudes. Setting $\Delta_i = d-1$ $(i = 1,2,3,4)$, we obtain

$$\begin{aligned}\mathcal{M}_{A_1A_2A_3A_4}(\delta_{ij}|c) &= \frac{(\frac{d}{2}-1)^2-c^2}{\frac{d^2}{4}-c^2}\Big[-\eta_{A_1A_2}\eta_{A_3A_4} - 2\eta_{A_1A_2}\left(\frac{P_{1A_3}P_{3A_4}}{P_{13}}+\frac{P_{2A_4}P_{4A_3}}{P_{24}}\right) \\ &\quad -2\eta_{A_3A_4}\left(\frac{P_{1A_2}P_{3A_1}}{P_{13}}+\frac{P_{2A_1}P_{4A_2}}{P_{24}}\right) + 4\eta_{A_1A_3}\frac{P_{1A_2}P_{3A_4}}{P_{13}} + \\ &\quad 4\eta_{A_2A_4}\frac{P_{2A_1}P_{4A_3}}{P_{24}}\Big]\delta_{13}\mathcal{M}_4 - (3 \longleftrightarrow 4)\ , \end{aligned} \tag{4.65}$$

where

$$\mathcal{M}_4 = \frac{\prod_{\sigma=\pm}\Gamma^2(\frac{\frac{3d}{2}-1+\sigma c}{2})\Gamma(\delta_{12}-\frac{\frac{3d}{2}-1+\sigma c}{2})}{\Gamma^2(\delta_{12})}\ . \tag{4.66}$$

To use this function in higher-point amplitudes, it is convenient to eliminate all terms with $P_4^{A_i}$ $(i=1,2,3)$.

By using the identity (4.9) with $\Delta = \Delta_1$, $P^A = P_1^{A_2}$, and $\mathcal{F}_{\Delta_1}(P_1) = P_1^{A_2}\prod_{i<j}P_{ij}^{-\delta_{ij}}$, we obtain

$$\left[\frac{1}{2}\eta^{A_1A_2}+\sum_{k\neq 1}\delta_{1k}\frac{P_k^{A_1}P_1^{A_2}}{P_{1k}}\right]\prod_{i<j}P_{ij}^{-\delta_{ij}} = 0\ . \tag{4.67}$$

We deduce from (4.53) and (4.67),

$$\begin{aligned}\mathcal{I}(1,2,4,3) &= -\frac{(\frac{d}{2}+c-\Delta_1+\Delta_2-1)(\frac{d}{2}-c+\Delta_3-\Delta_4-1)}{2[(\frac{d}{2}-1)^2-c^2]}\eta_{A_1A_2}\eta_{A_3A_4}\\ &\quad -\frac{2}{\delta_{34}-1}\left(2\eta_{A_1A_4}P_{1A_2}-\frac{\frac{d}{2}+c-\Delta_1+\Delta_2-1}{\frac{d}{2}+c-1}\eta_{A_1A_2}P_{1A_4}\right)\\ &\quad \left(\delta_{13}\frac{P_{1A_3}}{P_{13}}+\delta_{23}\frac{P_{2A_3}}{P_{23}}\right)\frac{P_{34}}{P_{14}}+\frac{2}{\delta_{14}}\frac{\frac{d}{2}-c-\Delta_3+\Delta_4-1}{\frac{d}{2}-c-1}\\ &\quad \eta^{A_3A_4}\left(\frac{1}{2}\eta^{A_1A_2}+\delta_{12}\frac{P_{2A_1}P_{1A_2}}{P_{12}}+\delta_{13}\frac{P_{3A_1}P_{1A_2}}{P_{13}}\right)\end{aligned} \tag{4.68}$$

and similarly for $\mathcal{I}(2,1,4,3)$. $\mathcal{I}(1,2,3,4)$ and $\mathcal{I}(2,1,3,4)$ are unaltered.

Next we act with $D^{M_4A_4}$. We have

$$\begin{aligned}P_4^{A_4}\mathcal{I}(1,2,3,4) &= -\frac{(\frac{d}{2}+c-\Delta_1+\Delta_2-1)\frac{d}{2}-c-\Delta_3+\Delta_4-1)}{2[(\frac{d}{2}-1)^2-c^2]}\eta_{A_1A_2}P_{4A_3}\\ &\quad +\frac{\frac{d}{2}+c-\Delta_1+\Delta_2-1}{\frac{d}{2}+c-1}\eta_{A_1A_2}P_{1A_3}\frac{P_{34}}{P_{13}}-2\frac{\frac{d}{2}-c-\Delta_3+\Delta_4-1}{\frac{d}{2}-c-1}\\ &\quad \frac{P_{4A_3}P_{1A_2}P_{3A_1}}{P_{13}}+4\eta_{A_1A_3}P_{1A_2}\frac{P_{34}}{P_{13}}\end{aligned} \tag{4.69}$$

and

$$\begin{aligned}P_4^{A_4}\mathcal{I}(1,2,4,3) &= -\frac{(\frac{d}{2}+c-\Delta_1+\Delta_2-1)(\frac{d}{2}-c+\Delta_3-\Delta_4-1)}{2[(\frac{d}{2}-1)^2-c^2]}\eta_{A_1A_2}P_{4A_3}\\ &\quad -\frac{1}{\delta_{34}-1}\left(4P_{4A_1}P_{1A_2}+\frac{\frac{d}{2}+c-\Delta_1+\Delta_2-1}{\frac{d}{2}+c-1}\eta_{A_1A_2}P_{14}\right)\\ &\quad \left(\delta_{13}\frac{P_{1A_3}}{P_{13}}+\delta_{23}\frac{P_{2A_3}}{P_{23}}\right)\frac{P_{34}}{P_{14}}+\frac{2}{\delta_{14}}\frac{\frac{d}{2}-c-\Delta_3+\Delta_4-1}{\frac{d}{2}-c-1}P_{4A_3}\\ &\quad \left(\eta_{A_1A_2}+\delta_{12}\frac{P_{2A_1}P_{1A_2}}{P_{12}}+\delta_{13}\frac{P_{3A_1}P_{1A_2}}{P_{13}}\right)\end{aligned} \tag{4.70}$$

and similarly for $P_4^{A_4}\mathcal{I}(2,1,3,4)$ and $P_4^{A_4}\mathcal{I}(2,1,4,3)$.

P_4 with a free index is eliminated from (4.69) using (4.53) and

$$\left[\frac{1}{2}\eta^{A_1A_3}+(\delta_{13}+1)\frac{P_3^{A_1}P_1^{A_3}}{P_{13}}+\delta_{23}\frac{P_3^{A_1}P_2^{A_3}}{P_{23}}+(\delta_{34}-1)\frac{P_3^{A_1}P_4^{A_3}}{P_{34}}\right]\frac{P_{34}}{P_{13}}\prod_{i<j}P_{ij}^{-\delta_{ij}}=0\ . \tag{4.71}$$

We obtain

$$\begin{aligned}\frac{P_{13}}{P_{34}}P_4^{A_4}\mathcal{I}(1,2,3,4) \;=\;& \frac{(\frac{d}{2}+c-\Delta_1+\Delta_2-1)(\frac{d}{2}-c-\Delta_3+\Delta_4-1)}{2(\delta_{34}-1)[(\frac{d}{2}-1)^2-c^2]}\eta_{A_1A_2}\\ &\left(\delta_{13}P_{1A_3}+\delta_{23}\frac{P_{13}}{P_{23}}P_{2A_3}\right)+\frac{\frac{d}{2}+c-\Delta_1+\Delta_2-1}{\frac{d}{2}+c-1}\eta_{A_1A_2}P_{1A_3}\\ &+4\eta_{A_1A_3}P_{1A_2}+\frac{2}{\delta_{34}-1}\frac{\frac{d}{2}-c-\Delta_3+\Delta_4-1}{\frac{d}{2}-c-1}P_{1A_2}\\ &\left(\frac{1}{2}\eta_{A_1A_3}+(\delta_{13}+1)\frac{P_{3A_1}P_{1A_3}}{P_{13}}+\delta_{23}\frac{P_{3A_1}P_{2A_3}}{P_{23}}\right)\ .\end{aligned} \tag{4.72}$$

Notice that P_4 only enters through an overall factor of P_{34}.

Similarly, P_4 is eliminated from (4.70) using (4.53), (4.67), (4.71), and

$$\begin{aligned}&\left[\frac{1}{2}\eta^{A_1A_2}P_1^{A_3}+\frac{1}{2}\eta^{A_1A_3}P_1^{A_2}+\left(\delta_{12}\frac{P_2^{A_1}}{P_{12}}+(\delta_{13}+1)\frac{P_3^{A_1}}{P_{13}}+\delta_{14}\frac{P_4^{A_1}}{P_{14}}\right)P_1^{A_2}P_1^{A_3}\right]\\ &\frac{1}{P_{13}}\prod_{i<j}P_{ij}^{-\delta_{ij}}=0\ .\end{aligned} \tag{4.73}$$

We obtain

$$
\begin{aligned}
&\frac{P_{13}}{P_{34}}P_4^{A_4}\mathcal{I}(1,2,4,3) = \\
&\frac{(\frac{d}{2}+c-\Delta_1+\Delta_2-1)(\frac{d}{2}-c+\Delta_3-\Delta_4-1)}{2(\delta_{34}-1)[(\frac{d}{2}-1)^2-c^2]}\eta_{A_1A_2}\left(\delta_{13}P_{1A_3}+\delta_{23}\frac{P_{13}}{P_{23}}P_{2A_3}\right)\\
&+\frac{4\delta_{13}}{\delta_{14}(\delta_{34}-1)}\Big[\frac{1}{2}\eta_{A_1A_2}P_{1A_3}+\frac{1}{2}\eta_{A_1A_3}P_{1A_2}+\left(\delta_{12}\frac{P_{2A_1}}{P_{12}}+(\delta_{13}+1)\frac{P_{3A_1}}{P_{13}}\right)\\
&P_{1A_2}P_{1A_3}\Big]\\
&+\frac{4\delta_{23}}{\delta_{14}(\delta_{34}-1)}\frac{P_{2A_3}}{P_{23}}P_{13}\left(\frac{1}{2}\eta_{A_1A_2}+\delta_{12}\frac{P_{2A_1}P_{1A_2}}{P_{12}}+\delta_{13}\frac{P_{3A_1}P_{1A_2}}{P_{13}}\right)\\
&-\frac{1}{\delta_{34}-1}\frac{\frac{d}{2}+c-\Delta_1+\Delta_2-1}{\frac{d}{2}+c-1}\eta_{A_1A_2}\left(\delta_{13}P_{1A_3}+\delta_{23}\frac{P_{13}}{P_{23}}P_{2A_3}\right)\\
&-\frac{2}{\delta_{14}(\delta_{34}-1)}\frac{\frac{d}{2}-c-\Delta_3+\Delta_4-1}{\frac{d}{2}-c-1}\left(\eta_{A_1A_2}+\delta_{12}\frac{P_{2A_1}P_{1A_2}}{P_{12}}\right)\\
&\left(\delta_{13}P_{1A_3}+\delta_{23}\frac{P_{13}}{P_{23}}P_{2A_3}\right)\\
&-\frac{2\delta_{13}}{\delta_{14}(\delta_{34}-1)}\frac{\frac{d}{2}-c-\Delta_3+\Delta_4-1}{\frac{d}{2}-c-1}P_{1A_2}\\
&\left(\frac{1}{2}\eta_{A_1A_3}+(\delta_{13}+1)\frac{P_{3A_1}P_{1A_3}}{P_{13}}+\delta_{23}\frac{P_{3A_1}P_{2A_3}}{P_{23}}\right)
\end{aligned}
\tag{4.74}
$$

Again, P_4 only enters through an overall factor of P_{34}. It follows that the part of the amplitude involving P_4 is $P_{34}\prod_{i=1}^3 P_{i4}^{-\delta_{i4}}$. Therefore, differentiation with respect to P_{4M_4} has the effect of multiplication by an overall factor,

$$
\frac{\partial}{\partial P_{4M_4}}P_{34}\prod_{i=1}^3 P_{i4}^{-\delta_{i4}} = 2\left[\delta_{14}\frac{P_1^{M_4}}{P_{14}}+\delta_{24}\frac{P_2^{M_4}}{P_{24}}+(\delta_{34}-1)\frac{P_3^{M_4}}{P_{34}}\right]P_{34}\prod_{i=1}^3 P_{i4}^{-\delta_{i4}} \tag{4.75}
$$

The amplitude with $D^{M_4A_4}$ acted upon is given by

$$
D^{M_4A_4}\mathcal{A}_{A_1A_2A_3A_4}(\{\Delta_i,P_i\}|c) = \frac{\pi^{d/2}}{2}\int(\mathcal{D}_4\mathcal{M})^{M_4}_{A_1A_2A_3}(\delta_{ij}|c)\prod_{i<j}P_{ij}^{-\delta_{ij}}\Gamma(\delta_{ij})d\delta_{ij} \tag{4.76}
$$

where

$$(\mathcal{D}_4\mathcal{M})^{M_4}_{A_1A_2A_3} = \Big[\frac{\Delta_4-1}{\Delta_4}\eta^{M_4A_4} + \frac{2}{\Delta_4}\left(\delta_{14}P_1^{M_4}\frac{P_{34}}{P_{14}} + \delta_{24}P_2^{M_4}\frac{P_{34}}{P_{24}} + (\delta_{34}-1)P_3^{M_4}\right) \frac{P_{4A_4}}{P_{34}}\Big]\mathcal{M}_{A_1A_2A_3A_4}(\delta_{ij}|c)\ . \tag{4.77}$$

In the above expression, the only dependence on P_4 is through the ratios $\frac{P_{34}}{P_{14}}$ and $\frac{P_{34}}{P_{24}}$. This expression will be used in the calculation of five- and higher-point vector amplitudes.

4.5 Five-point Amplitudes

In this section, we calculate scalar and vector five-point amplitudes by sewing together three- and four-point amplitudes. The integrals over AdS space that are involved are similar to the ones encountered in the case of four-point amplitudes in section 4.4 and can be performed using the results of appendix C.1 without additional effort. The Mellin amplitudes are found as integrals over the Mandelstam invariants of the constituent four-point amplitudes. These integrals can all be performed, resulting in expressions involving generalized Hypergeometric functions. Thus, our approach provides an alternative to integration over Schwinger parameters [75].

4.5.1 Scalar amplitudes

The five-point scalar amplitude (Fig. 4.6) reads

$$A^{(5,s)}(\Delta_1,P_1;\ldots;\Delta_5,P_5) = \frac{g^3}{\prod_i 2\pi^{d/2}\Gamma(\Delta_i+1-d/2)} \int \frac{dcdc'}{(2\pi i)^2} f_{\delta_1,0}(c) f_{\delta_2,0}(c') \mathcal{A}_5(\{\Delta_i,P_1\}|c,c') \tag{4.78}$$

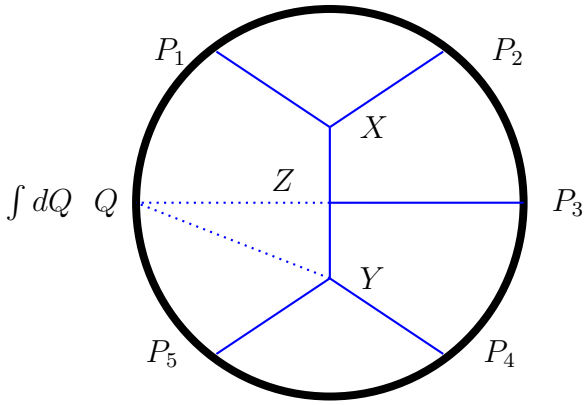

Figure 4.6: The five-point scalar amplitude (4.107).

where

$$\mathcal{A}_5(\{\Delta_i, P_i\}|c, c') = \int_{\partial AdS} dQ \qquad \mathcal{A}_4(\Delta_1, P_1; \Delta_2, P_2; \Delta_3, P_3; d/2 + c', Q|c)$$
$$\mathcal{A}_3(\Delta_4, P_4; \Delta_5, P_5; d/2 - c', Q) \tag{4.79}$$

The integral over Q involves

$$\int_{\partial AdS} dQ \prod_{i=1}^{5} \Gamma(\lambda_i)(-2Q \cdot P_i)^{-\lambda_i} \tag{4.80}$$

where

$$\lambda_1 = \delta'_{14} \ , \quad \lambda_2 = \delta'_{24} \ , \quad \lambda_3 = \delta'_{34} \ , \quad \lambda_4 = \frac{\Delta_4 - \Delta_5 + \frac{d}{2} - c'}{2} \ , \quad \lambda_5 = \frac{\Delta_5 - \Delta_4 + \frac{d}{2} - c'}{2} \tag{4.81}$$

and δ'_{ij} are the Mandelstam invariants for the four-point function constrained by

$$\begin{aligned} \delta'_{12} + \delta'_{13} + \delta'_{14} &= \Delta_1 \\ \delta'_{12} + \delta'_{23} + \delta'_{24} &= \Delta_2 \\ \delta'_{13} + \delta'_{23} + \delta'_{34} &= \Delta_3 \\ \delta'_{14} + \delta'_{24} + \delta'_{34} &= h + c' \end{aligned} \tag{4.82}$$

Working as before, we obtain

$$\int_{\partial AdS} dQ \prod_{i=1}^{5} \Gamma(\lambda_i)(-2Q\cdot P_i)^{-\lambda_i} = \frac{\pi^{d/2}}{2}\int \prod_{i<j} d\tilde{\delta}_{ij}\Gamma(\tilde{\delta}_{ij})P_{ij}^{-\tilde{\delta}_{ij}} \tag{4.83}$$

where the integration variables are constrained by

$$\sum_{j\neq i}\tilde{\delta}_{ij} = \lambda_i \ . \tag{4.84}$$

The part of the amplitude involving the vectors P_i is

$$P_{12}^{-\delta'_{12}}P_{13}^{-\delta'_{13}}P_{23}^{-\delta'_{23}}P_{45}^{-\frac{\Delta_4+\Delta_5-d/2+c'}{2}}\prod_{i<j}P_{ij}^{-\tilde{\delta}_{ij}} = \prod_{i<j}P_{ij}^{-\delta_{ij}} \tag{4.85}$$

where δ_{ij} are the Mandelstam invariants defined by

$$\delta_{12} = \tilde{\delta}_{12}+\delta'_{12}\ , \quad \delta_{23} = \tilde{\delta}_{23}+\delta'_{23}\ , \quad \delta_{13} = \tilde{\delta}_{13}+\delta'_{13}\ , \quad \delta_{45} = \tilde{\delta}_{45}+\frac{\Delta_4+\Delta_5-d/2+c'}{2}\ , \tag{4.86}$$

and $\delta_{ij} = \tilde{\delta}_{ij}$, otherwise. It is easily seen that they obey the standard constraints (4.44).

The five-point function simplifies to

$$\mathcal{A}_5(\{\Delta_i,P_i\}|c,c') = \frac{\pi^{d/2}}{2}\int\prod_{i<j}d\delta_{ij}\Gamma(\delta_{ij})\mathcal{M}_5(\delta_{ij}|c,c')P_{ij}^{-\delta_{ij}} \tag{4.87}$$

where

$$\begin{aligned}\mathcal{M}_5(\delta_{ij}|c,c') \ &= \ \int\prod_{i<j}d\delta'_{ij}\frac{\Gamma(\delta_{12}-\delta'_{12})\Gamma(\delta'_{12})\Gamma(\delta_{23}-\delta'_{23})\Gamma(\delta'_{23})\Gamma(\delta_{13}-\delta'_{13})\Gamma(\delta'_{13})}{\Gamma(\delta_{12})\Gamma(\delta_{23})\Gamma(\delta_{13})}\\ &\quad\times\frac{\Gamma(\delta_{45}-\frac{\Delta_4+\Delta_5-d/2+c'}{2})\Gamma(\frac{\Delta_4+\Delta_5-d/2+c'}{2})}{\Gamma(\delta_{45})}\mathcal{M}_4(\delta'_{12}|c)\mathcal{M}_3\end{aligned} \tag{4.88}$$

and

$$\mathcal{M}_3 = \Gamma\left(\frac{\Delta_4+\Delta_5-\frac{d}{2}-c'}{2}\right) \tag{4.89}$$

$$\mathcal{M}_4(\delta'_{12}|c) = \frac{\prod_{\sigma=\pm}\Gamma(\frac{\Delta_1+\Delta_2-d/2+\sigma c}{2})\Gamma(\frac{\Delta_3+c'+\sigma c}{2})\Gamma(\delta'_{12}-\frac{\Delta_1+\Delta_2-d/2+\sigma c}{2})}{\Gamma(\delta'_{12})\Gamma(\delta'_{34})} \tag{4.90}$$

with $\delta'_{34} = \delta'_{12} - \frac{\Delta_1+\Delta_2-\Delta_3-d/2-c'}{2}$, $\delta'_{23} = \frac{\Delta_1+\Delta_2+\Delta_3-d/2-c'}{2} - \delta'_{12} - \delta'_{13}$.

The two integrals in (4.88) are performed as follows. From Barnes first lemma, we have

$$\int \frac{d\delta'_{13}}{2\pi i}\frac{\Gamma(\delta'_{23})\Gamma(\delta_{23}-\delta'_{23})\Gamma(\delta'_{13})\Gamma(\delta_{13}-\delta'_{13})}{\Gamma(\delta_{13})\Gamma(\delta_{23})} = \frac{\Gamma(\delta_{13}+\delta_{23}-\frac{\Delta_1+\Delta_2+\Delta_3-d/2-c'}{2}+\delta'_{12})\Gamma(\frac{\Delta_1+\Delta_2+\Delta_3-d/2-c'}{2}-\delta'_{12})}{\Gamma(\delta_{13}+\delta_{23})} . \tag{4.91}$$

Next, we need

$$\begin{aligned}\mathcal{F} &= \int \frac{d\delta'_{12}}{2\pi i}\frac{\Gamma(\delta'_{12}+\delta_{13}+\delta_{23}-\frac{\Delta_1+\Delta_2+\Delta_3-d/2-c'}{2})}{\Gamma(\delta_{13}+\delta_{23})} \\ &\quad \frac{\Gamma(\frac{\Delta_1+\Delta_2+\Delta_3-d/2-c'}{2}-\delta'_{12})\Gamma(\delta_{12}-\delta'_{12})}{\Gamma(\delta'_{12}-\frac{\Delta_1+\Delta_2-\Delta_3-d/2-c'}{2})} \\ &\quad \times \prod_{\sigma=\pm}\Gamma\left(\delta'_{12}-\frac{\Delta_1+\Delta_2-\frac{d}{2}+\sigma c}{2}\right) .\end{aligned} \tag{4.92}$$

This is calculated with the aid of the identity

$$\int \frac{ds}{2\pi i}\frac{\Gamma(a+s)\Gamma(b+s)\Gamma(f-c+s)\Gamma(e-a-b-s)\Gamma(-s)}{\Gamma(f+s)} = \frac{\Gamma(a)\Gamma(b)\Gamma(e-a)\Gamma(e-b)\Gamma(f-c)}{\Gamma(e)\Gamma(f)}{}_3F_2\left[\begin{array}{c} a,b,c \\ e,f \end{array}\right] . \tag{4.93}$$

where ${}_3F_2\left[\begin{array}{c} a,b,c \\ e,f \end{array}\right] = {}_3F_2(a,b,c;e,f;1)$. We obtain

$$\begin{aligned}\mathcal{F} &= \frac{\Gamma(\delta_{45}-\frac{\Delta_4+\Delta_5-d/2-c'}{2})\Gamma(\frac{\Delta_3+c-c'}{2})\prod_{\sigma=\pm}\Gamma(\delta_{12}-\frac{\Delta_1+\Delta_2-\frac{d}{2}+\sigma c}{2})}{\Gamma(\delta_{45}-\frac{\Delta_4+\Delta_5-\Delta_3-d/2-c}{2})\Gamma(\delta_{12}-\frac{\Delta_1+\Delta_2-\Delta_3-d/2-c'}{2})} \\ &\quad \times {}_3F_2\left[\begin{array}{c} \delta_{45}-\frac{\Delta_4+\Delta_5-d/2-c'}{2}, \delta_{12}-\frac{\Delta_1+\Delta_2-\frac{d}{2}-c}{2}, \frac{\Delta_3+c'+c}{2} \\ \delta_{45}-\frac{\Delta_4+\Delta_5-\Delta_3-d/2-c}{2}, \delta_{12}-\frac{\Delta_1+\Delta_2-\Delta_3-d/2-c'}{2} \end{array}\right] . \end{aligned} \tag{4.94}$$

where we used $\delta_{12}+\delta_{13}+\delta_{23}-\frac{\Delta_1+\Delta_2}{2} = \delta_{45}-\frac{\Delta_4+\Delta_5}{2}$. Therefore,

$$\begin{aligned}\mathcal{M}_5(\delta_{ij}|c,c') &= \frac{\Gamma(\frac{\Delta_3+c-c'}{2})\prod_{\sigma=\pm}\Gamma(\delta_{12}-\frac{\Delta_1+\Delta_2-d/2+\sigma c}{2})\Gamma(\delta_{45}-\frac{\Delta_4+\Delta_5-\frac{d}{2}+\sigma c'}{2})}{\Gamma(\delta_{12})\Gamma(\delta_{12}-\frac{\Delta_1+\Delta_2-\Delta_3-d/2-c'}{2})\Gamma(\delta_{45})\Gamma(\delta_{45}-\frac{\Delta_4+\Delta_5-\Delta_3-d/2-c}{2})} \\ &\quad \times \prod_{\sigma=\pm}\Gamma\left(\frac{\Delta_3+\sigma c+c'}{2}\right)\Gamma\left(\frac{\Delta_1+\Delta_2-\frac{d}{2}+\sigma c}{2}\right) \\ &\quad \Gamma\left(\frac{\Delta_4+\Delta_5-\frac{d}{2}+\sigma c'}{2}\right) \\ &\quad \times {}_3F_2\left[\begin{array}{c} \delta_{45}-\frac{\Delta_4+\Delta_5-d/2-c'}{2}, \delta_{12}-\frac{\Delta_1+\Delta_2-\frac{d}{2}-c}{2}, \frac{\Delta_3+c'+c}{2} \\ \delta_{45}-\frac{\Delta_4+\Delta_5-\Delta_3-d/2-c}{2}, \delta_{12}-\frac{\Delta_1+\Delta_2-\Delta_3-d/2-c'}{2} \end{array}\right] . \end{aligned} \tag{4.95}$$

4.5.2 Vector amplitudes

In order to avoid an unnecessarily long calculation, we restrict attention to the case of on-shell amplitudes by setting $\Delta_i = d-1$ $(i=1,\ldots,5)$. There are two different diagrams which we need to consider separately.

The diagram depicted in figure 4.7 has amplitude

$$A^{(5,v,(a))M_1\ldots M_5,a_1\ldots a_5} = g^3\int\frac{dc}{2\pi i}f_{\delta,1}(c)\prod_{i=1}^{5}D^{M_iA_i}(\Delta_i,P_i)\mathcal{A}^{a_1a_2a_3a_4a_5}_{A_1A_2A_3A_4A_5}(\{\Delta_i,P_i\}|c) \tag{4.96}$$

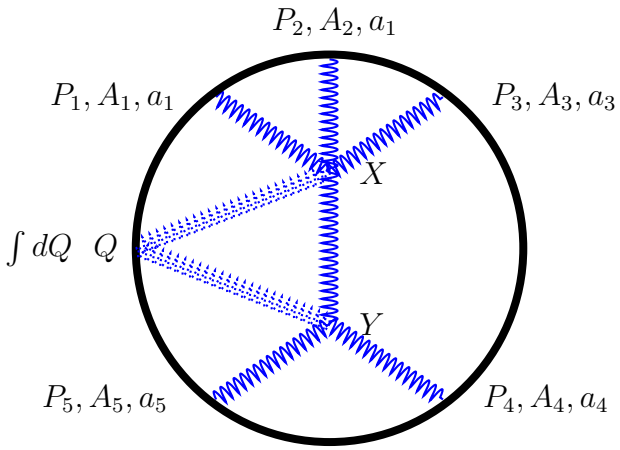

Figure 4.7: An example of the five-point vector amplitude (4.96).

where

$$\begin{aligned}\mathcal{A}^{a_1a_2a_3a_4a_5}_{A_1A_2A_3A_4A_5}(\{\Delta_i,P_i\}|c) &= \int_{\partial AdS} dQ\eta_{NN'}D^{NC}(h+c,Q)\\ &\quad \mathcal{A}^{a_1a_2a_3b}_{A_1A_2A_3C}(\Delta_1,P_1;\Delta_2,P_2;\Delta_3,P_3;d/2+c,Q)\\ &\quad \times D^{N'C'}(d/2-c,Q)f^{a_4a_5b}\\ &\quad \mathcal{A}_{A_4A_5C'}(\Delta_4,P_4;\Delta_5,P_5;d/2-c,Q)\ . \end{aligned} \tag{4.97}$$

The three-point amplitude in (4.97) simplifies to

$$\begin{aligned}D^{N'C'}(d/2-c,Q)\mathcal{A}_{A_4A_5C'} &= \frac{2}{\frac{d}{2}-c}\Gamma\left(\frac{\frac{3d}{2}-c-1}{2}\right)\Gamma\left(\frac{\frac{3d}{2}+c-1}{2}\right)\Gamma^2\left(\frac{\frac{d}{2}-c+1}{2}\right)\\ &\quad \times\left[\eta_{A_4A_5}P_4^{N'}-2\delta^{N'}_{A_4}P_{4A_5}\right]P_{45}^{-\frac{\frac{3d}{2}+c+1}{2}}(-2P_4\cdot Q)^{-\frac{\frac{d}{2}-c+1}{2}}\\ &\quad (-2P_5\cdot Q)^{-\frac{\frac{d}{2}-c-1}{2}}\ .-(4\longleftrightarrow 5)\end{aligned} \tag{4.98}$$

The four-point amplitude in (4.97) simplifies to

$$\begin{aligned} D^{NC}(d/2+c,Q)\mathcal{A}^{a_1a_2a_3b}_{A_1A_2A_3C} &= \left(f^{a_1bb'}f^{a_2a_3b'}+f^{a_1a_3b'}f^{a_2bb'}\right) \\ &\quad \int (\mathcal{D}_4\mathcal{M})^N_{A_1A_2A_3}(\delta'_{ij}|c)\prod_{i<j}P_{ij}^{-\delta'_{ij}}\Gamma(\delta'_{ij})d\delta'_{ij}+ \\ &\quad \cdots+\cdots \end{aligned} \tag{4.99}$$

where

$$\begin{aligned} (\mathcal{D}_4\mathcal{M})^N_{A_1A_2A_3} &= \Gamma\left(\frac{\frac{5d}{2}-3+c}{2}\right)\eta_{A_1A_2}\Big[\frac{\frac{d}{2}+c-1}{\frac{d}{2}+c}\delta^N_{A_3} \\ &\quad -\frac{2}{\frac{d}{2}+c}\left(\delta'_{13}\frac{P_{1A_3}}{P_{13}}+\delta'_{23}\frac{P_{2A_3}}{P_{23}}\right) \\ &\quad \left(\frac{\delta'_{14}}{\delta'_{34}-1}\frac{P_3\cdot Q}{P_1\cdot Q}P_1^N+\frac{\delta'_{24}}{\delta'_{34}-1}\frac{P_3\cdot Q}{P_2\cdot Q}P_2^N+P_3^N\right)\Big]\ . \end{aligned} \tag{4.100}$$

The integral over Q involves

$$\int_{\partial AdS}dQ\prod_{i=1}^{5}\Gamma(\lambda_i)(-2Q\cdot P_i)^{-\lambda_i}=\frac{\pi^{d/2}}{2}\int\prod_{i<j}\frac{d\tilde{\delta}_{ij}}{2\pi i}\Gamma(\tilde{\delta}_{ij})P_{ij}^{-\tilde{\delta}_{ij}} \tag{4.101}$$

where

$$\lambda_1=\delta'_{14}+n_1\ ,\quad \lambda_2=\delta'_{24}+n_2\ ,\quad \lambda_3=\delta'_{34}+n_3\ ,\quad \lambda_4=\frac{\frac{d}{2}-c+1}{2}\ ,\quad \lambda_5=\frac{\frac{d}{2}-c-1}{2} \tag{4.102}$$

and δ'_{ij} are the Mandelstam invariants for the four-point function, as in the scalar case. The various terms have $n_i\in\{-1,0,+1\}$, with $\sum_i n_i=0$ $(i=1,2,3)$. The integration variables are constrained by

$$\sum_{j\neq i}\tilde{\delta}_{ij}=\lambda_i\ . \tag{4.103}$$

In terms of the Mandelstam invariants,

$$\tilde{\delta}_{12} = \delta_{12} - \delta'_{12} \ , \quad \tilde{\delta}_{23} = \delta_{23} - \delta'_{23} \ , \qquad \tilde{\delta}_{13} = \delta_{13} - \delta'_{13} \ , \quad \tilde{\delta}_{45} = \delta_{45} - \frac{\frac{3d}{2} + c - 3}{2} \ ,$$
$$\tilde{\delta}_{i4} = \delta_{i4} + n_i \quad (i = 1, 2, 3) \ , \tag{4.104}$$

and $\tilde{\delta}_{ij} = \delta_{ij}$, otherwise.

We arrive at

$$\begin{aligned} \mathcal{A}_{A_1A_2A_3A_4A_5} &= \frac{\pi^{d/2}}{2} \int \prod_{i<j} \frac{d\tilde{\delta}_{ij}}{2\pi i} \Gamma(\tilde{\delta}_{ij}) P_{ij}^{-\tilde{\delta}_{ij}} \\ &\quad \times \Big[\left(f^{a_1b'b} f^{a_2a_3b} + f^{a_1a_3b} f^{a_2b'b} \right) f^{b'a_4a_5} \mathcal{M}_{A_1 \ldots A_5} + \\ &\quad \text{permutations of } (123) - (4 \longleftrightarrow 5) \Big] \end{aligned} \tag{4.105}$$

where

$$\begin{aligned} &\mathcal{M}_{A_1 \ldots A_5} = \\ &\frac{\frac{d}{2} - c - 1}{\frac{d}{2} - c} \Gamma\left(\frac{\frac{3d}{2} - c - 1}{2} \right) \Gamma\left(\frac{\frac{3d}{2} + c - 1}{2} \right) \Gamma\left(\frac{\frac{5d}{2} - 3 + c}{2} \right) \\ &\eta_{A_1A_2} \left[\eta_{A_4A_5} P_{4N} - 2\eta_{A_4N} P_{4A_5} \right] \\ &\times \int \prod_{i<j} d\delta'_{ij} \frac{\Gamma(\delta_{12} - \delta'_{12}) \Gamma(\delta'_{12}) \Gamma(\delta_{23} - \delta'_{23}) \Gamma(\delta'_{23}) \Gamma(\delta_{13} - \delta'_{13}) \Gamma(\delta'_{13}) \Gamma(\delta_{45} - \frac{\frac{3d}{2} + c - 3}{2})}{\Gamma(\delta_{12}) \Gamma(\delta_{23}) \Gamma(\delta_{13}) \Gamma(\delta_{45})} \\ &\times \left[\frac{\frac{d}{2} + c - 1}{\frac{d}{2} + c} \delta^N_{A_3} - \frac{2}{\frac{d}{2} + c} \left(\delta'_{13} \frac{P_{1A_3}}{P_{13}} + \delta'_{23} \frac{P_{2A_3}}{P_{23}} \right) \left(\frac{\delta_{14}}{\delta_{34} - 1} P_1^N + \frac{\delta_{24}}{\delta_{34} - 1} P_2^N + P_3^N \right) \right] \end{aligned} \tag{4.106}$$

The integrals over the four-point Mandelstam invariants δ'_{ij} can be performed as in the scalar case.

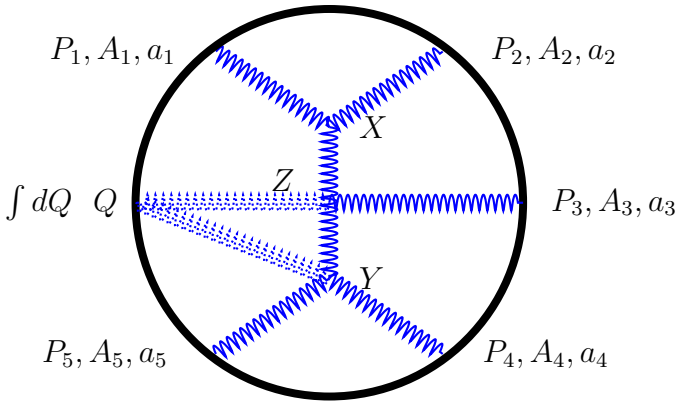

Figure 4.8: Another example of five-point vector amplitude (4.107).

Next, we turn to the diagram depicted in figure 4.8. It is given by (suppressing standard group theory indices)

$$\begin{aligned} A^{(5,v,(b))M_1M_2M_3M_4M_5} &= g^3 \int \frac{dcdc'}{(2\pi i)^2} f_{\delta,1}(c) f_{\delta,1}(c') \prod_{i=1}^{5} D^{M_iA_i}(\Delta_i, P_i) \\ &\quad \mathcal{A}_{A_1A_2A_3A_4A_5}(\{\Delta_i, P_i\}|c, c') \end{aligned} \tag{4.107}$$

where

$$\begin{aligned} \mathcal{A}_{A_1A_2A_3A_4A_5}(\{\Delta_i, P_i\}|c, c') &= \int_{\partial AdS} dQ \eta_{NN'} D^{NC}(d/2 + c, Q) \\ &\quad \mathcal{A}_{A_1A_2A_3C}(\Delta_1, P_1; \Delta_2, P_2; \Delta_3, P_3; d/2 + c, Q|c') \\ &\quad \times D^{N'C'}(h - c', Q) \\ &\quad \mathcal{A}_{A_4A_5C'}(\Delta_4, P_4; \Delta_5, P_5; d/2 - c, Q) \end{aligned} \tag{4.108}$$

The three-point amplitude in (4.108) is given by (4.98). The four-point amplitude simplifies to

$$D^{NC}(d/2 + c, Q)\mathcal{A}_{A_1A_2A_3C} = \int (\mathcal{D}_4\mathcal{M})^N_{A_1A_2A_3}(\delta'_{ij}|c') \prod_{i<j} P_{ij}^{-\delta'_{ij}} \Gamma(\delta'_{ij}) d\delta'_{ij} \tag{4.109}$$

where

$$(\mathcal{D}_4\mathcal{M})^N_{A_1A_2A_3} = \frac{\frac{d}{2}+c-1}{\frac{d}{2}+c}\eta^{NC}\mathcal{M}_{A_1A_2A_3C} - \frac{1}{\frac{d}{2}+c}\left(\delta'_{14}P_1^N\frac{P_3\cdot Q}{P_1\cdot Q} + \delta'_{24}P_2^N\frac{P_3\cdot Q}{P_2\cdot Q} + (\delta'_{34}-1)P_3^N\right)\frac{Q^C}{P_3\cdot Q}\mathcal{M}_{A_1A_2A_3C} \tag{4.110}$$

$$\begin{aligned}\mathcal{M}_{A_1A_2A_3C} &= \frac{(\frac{d}{2}-1)^2-c'^2}{\frac{d^2}{4}-c'^2}\left[\mathcal{I}(1,2,3,4)\delta'_{13}+\mathcal{I}(1,2,4,3)\delta'_{14}-(1\longleftrightarrow 2)\right] \\ &\quad\times\frac{\prod_{\sigma=\pm}\Gamma(\frac{\frac{3d}{2}+\sigma c'-1}{2})\Gamma(\frac{d+c+\sigma c'}{2})\Gamma(\delta'_{12}-\frac{\frac{3d}{2}+\sigma c'-1}{2})}{\Gamma(\delta'_{12})\Gamma(\delta'_{12}+1-\frac{\frac{d}{2}+h-c+1}{2})}\end{aligned} \tag{4.111}$$

$$\mathcal{I}(1,2,3,4) = -\frac{c-c'}{d-2(c'+1)}\eta_{A_1A_2}\eta_{A_3C} - 2\eta_{A_1A_2}\frac{P_{1A_3}P_{3C}}{P_{13}} + 4\eta_{A_1A_3}\frac{P_{1A_2}P_{3C}}{P_{13}} - 2\frac{c-c'}{\frac{d}{2}-c'-1}\eta_{A_3C}\frac{P_{1A_2}P_{3A_1}}{P_{13}} \tag{4.112}$$

$$\mathcal{I}(1,2,4,3) = \frac{c+c'-d+2}{d-2(c'+1)}\eta_{A_1A_2}\eta_{A_3C} - \frac{2}{\delta'_{34}-1}\left(2\eta_{A_1A_4}P_{1A_2}-\eta_{A_1A_2}P_{1C}\right)\left(\delta'_{13}\frac{P_{1A_3}}{P_{13}}+\delta'_{23}\frac{P_{2A_3}}{P_{23}}\right)\frac{P_3\cdot Q}{P_1\cdot Q} - \frac{2}{\delta'_{14}}\frac{c+c'}{\frac{d}{2}-c'-1}\eta_{A_3C}\left(\frac{1}{2}\eta_{A_1A_2}+\delta'_{12}\frac{P_{2A_1}P_{1A_2}}{P_{12}}+\delta'_{13}\frac{P_{3A_1}P_{1A_2}}{P_{13}}\right) \tag{4.113}$$

$$
\begin{aligned}
&\frac{P_{13}}{-2P_3\cdot Q}Q^C\mathcal{I}(1,2,3,4)\\
&=\frac{c-c'}{(\delta'_{34}-1)(d-2(c'+1))}\eta_{A_1A_2}\left(\delta'_{13}P_{1A_3}+\delta'_{23}\frac{P_{13}}{P_{23}}P_{2A_3}\right)+\eta_{A_1A_2}P_{1A_3}+4\eta_{A_1A_3}P_{1A_2}\\
&+\frac{2}{\delta'_{34}-1}\frac{c-c'}{\frac{d}{2}-c'-1}P_{1A_2}\left(\frac{1}{2}\eta_{A_1A_3}+(\delta'_{13}+1)\frac{P_{3A_1}P_{1A_3}}{P_{13}}+\delta'_{23}\frac{P_{3A_1}P_{2A_3}}{P_{23}}\right)
\end{aligned}
\tag{4.114}
$$

and

$$
\begin{aligned}
&\frac{P_{13}}{-2P_3\cdot Q}Q^C\mathcal{I}(1,2,4,3)=\\
&-\frac{c+c'-d+2}{(\delta'_{34}-1)(d-2(c'+1))}\eta_{A_1A_2}\left(\delta'_{13}P_{1A_3}+\delta'_{23}\frac{P_{13}}{P_{23}}P_{2A_3}\right)\\
&-\frac{1}{\delta'_{34}-1}\eta_{A_1A_2}\left(\delta'_{13}P_{1A_3}+\delta'_{23}\frac{P_{13}}{P_{23}}P_{2A_3}\right)\\
&+\frac{4\delta'_{13}}{\delta'_{14}(\delta'_{34}-1)}\left[\frac{1}{2}\eta_{A_1A_2}P_{1A_3}+\frac{1}{2}\eta_{A_1A_3}P_{1A_2}+\left(\delta'_{12}\frac{P_{2A_1}}{P_{12}}+(\delta'_{13}+1)\frac{P_{3A_1}}{P_{13}}\right)P_{1A_2}P_{1A_3}\right]\\
&+\frac{4\delta'_{23}}{\delta'_{14}(\delta'_{34}-1)}\frac{P_{2A_3}}{P_{23}}P_{13}\left(\frac{1}{2}\eta_{A_1A_2}+\delta'_{12}\frac{P_{2A_1}P_{1A_2}}{P_{12}}+\delta'_{13}\frac{P_{3A_1}P_{1A_2}}{P_{13}}\right)\\
&-\frac{2}{\delta'_{14}(\delta'_{34}-1)}\frac{c-c'}{\frac{d}{2}-c'-1}\left(\eta_{A_1A_2}+\delta_{12}\frac{P_{2A_1}P_{1A_2}}{P_{12}}\right)\left(\delta'_{13}P_{1A_3}+\delta'_{23}\frac{P_{13}}{P_{23}}P_{2A_3}\right)\\
&-\frac{2\delta'_{13}}{\delta'_{14}(\delta'_{34}-1)}\frac{c-c'}{\frac{d}{2}-c'-1}P_{1A_2}\left(\frac{1}{2}\eta_{A_1A_3}+(\delta'_{13}+1)\frac{P_{3A_1}P_{1A_3}}{P_{13}}+\delta'_{23}\frac{P_{3A_1}P_{2A_3}}{P_{23}}\right)
\end{aligned}
\tag{4.115}
$$

The integral over Q is of the same form as before (Eq. (4.101) with exponents given by (4.102)). However, this case is slightly more complicated because $n_i \in \{0, \pm 1, \pm 2\}$, $\sum_i n_i = 0$ $(i = 1, 2, 3)$. The integration variables are constrained by (4.103), and are given in terms of the Mandelstam invariants by (4.104).

4.6 Higher-point amplitudes

In this section, we suppress group theory indices, as they are not involved in the calculations except as constant factors. Thus, but amplitude we mean a sub-amplitude with a given group theory structure.

Higher point amplitudes can be calculated recursively by sewing together diagrams. Consider two scalar diagrams with N_1 and N_2 external legs, respectively. Suppose they have been calculated and put in the form

$$A_{N_1 s}(\Delta_1, P_1; \ldots; \Delta_{N_1}, P_{N_1}) = \frac{g^{N_1-2}}{\prod_i 2\pi^{d/2}\Gamma(\Delta_i + 1 - \frac{d}{2})} \int [dc'] \mathcal{A}_{N_1}(\{\Delta_i, P_i\}|[c']) \tag{4.116}$$

with

$$\mathcal{A}_{N_1}(\{\Delta_i, P_i\}|[c']) = \frac{\pi^{d/2}}{2} \int \mathcal{M}_{N_1}(\delta'_{ij}|[c']) \prod_{i<j} \Gamma(\delta'_{ij}) P_{ij}^{-\delta'_{ij}} d\delta'_{ij} \ , \quad \sum_{i\neq j} \delta'_{ij} = \Delta_i \tag{4.117}$$

and similarly

$$A_{N_2 s}(\Delta'_1, P'_1; \ldots; \Delta'_{N_2}, P'_{N_2}) = \frac{g^{N_2-2}}{\prod_i 2\pi^{d/2}\Gamma(\Delta'_i + 1 - \frac{d}{2})} \int [dc''] \mathcal{A}_{N_2}(\{\Delta'_i, P'_i\}|[c'']) \tag{4.118}$$

with

$$\mathcal{A}_{N_2}(\{\Delta'_i, P'_i\}|[c'']) = \frac{\pi^{d/2}}{2} \int \mathcal{M}_{N_2}(\delta''_{ij}|[c'']) \prod_{i<j} \Gamma(\delta''_{ij}) (P'_{ij})^{-\delta''_{ij}} d\delta''_{ij} \ , \quad \sum_{i\neq j} \delta''_{ij} = \Delta'_i \ . \tag{4.119}$$

After sewing together the last two legs in the respective diagrams, we create a N-point diagram with $N = N_1 + N_2 - 2$. Its amplitude is given by

$$\begin{aligned} A_{Ns}(\Delta_1, P_1; \ldots; \Delta_N, P_N) \ &= \ \frac{g^{N-2}}{\prod_i 2\pi^{d/2}\Gamma(\Delta_i + 1 - \frac{d}{2})} \int [dc'][dc''] \frac{dc}{2\pi i} f_{\delta,0}(c) \\ &\quad \mathcal{A}_N(\{\Delta_i, P_i\}|[c'], [c''], c) \end{aligned} \tag{4.120}$$

with

$$\begin{aligned}\mathcal{A}_N &= \int_{\partial AdS} dQ \mathcal{A}_{N_1}(\Delta_1, P_1; \ldots; \Delta_{N_1-1}, P_{N_1-1}; d/2+c, Q|[c']) \\ &\quad \mathcal{A}_{N_2}(\Delta_{N_1}, P_{N_1}; \ldots; \Delta_N, P_N; d/2-c, Q|[c'']) \ . \end{aligned} \tag{4.121}$$

The integral over Q involves

$$\int_{\partial AdS} dQ \prod_{i=1}^{N} \Gamma(\lambda_i)(-2Q\cdot P_i)^{-\lambda_i} = \frac{\pi^{d/2}}{2} \int \prod_{i<j} d\tilde{\delta}_{ij} \Gamma(\tilde{\delta}_{ij}) P_{ij}^{-\tilde{\delta}_{ij}} \tag{4.122}$$

with $\sum_{j\neq i} \tilde{\delta}_{ij} = \lambda_i$, and

$$\lambda_i = \delta'_{iN_1} \quad (i = 1, \ldots, N_1 - 1) \ , \quad \lambda_{N_1+i} = \delta''_{iN_2} \quad (i = 1, \ldots, N_2 - 1) \ . \tag{4.123}$$

Then the part of the amplitude involving the vectors P_i is

$$\left(\prod_{i<j}^{N_1-1} P_{ij}^{-\delta'_{ij}} \right) \left(\prod_{i<j}^{N_2-1} P_{N_1+i-1\, N_1+j-1}^{-\delta''_{ij}} \right) \left(\prod_{i<j}^{N} P_{ij}^{-\tilde{\delta}_{ij}} \right) = \prod_{i<j} P_{ij}^{-\delta_{ij}} \tag{4.124}$$

where δ_{ij} are the Mandelstam invariants for the N-point amplitude given by

$$\begin{aligned} &\delta_{ij} = \tilde{\delta}_{ij} + \delta'_{ij} \quad (i,j = 1, \ldots, N_1 - 1) \ , \\ &\delta_{N_1+i-1\, N_1+j-1} = \tilde{\delta}_{N_1+i-1\, N_1+j-1} + \delta''_{ij} \quad (i,j = 1, \ldots, N_2 - 1) \ , \end{aligned} \tag{4.125}$$

and $\delta_{ij} = \tilde{\delta}_{ij}$, otherwise. They obey the constraints $\sum_{i\neq j} \delta_{ij} = \Delta_i$, as can easily be checked.

It follows that the N-point amplitude can be cast in the form

$$\mathcal{A}_N = \frac{\pi^{d/2}}{2} \int \mathcal{M}_N \prod_{i<j} \Gamma(\delta_{ij}) P_{ij}^{-\delta_{ij}} d\delta_{ij} \tag{4.126}$$

where

$$\mathcal{M}_N = \frac{\pi^{d/2}}{2}\int d\delta'_{ij}\int d\delta''_{ij}\prod_{i<j}^{N_1-1}\frac{\Gamma(\delta_{ij}-\delta'_{ij})\Gamma(\delta'_{ij})}{\Gamma(\delta_{ij})} \prod_{i<j}^{N_2-1}\frac{\Gamma(\delta_{N_1+i-1\,N_1+j-1}-\delta''_{ij})\Gamma(\delta''_{ij})}{\Gamma(\delta_{N_1+i-1\,N_1+j-1})}\mathcal{M}_{N_1}\mathcal{M}_{N_2} \tag{4.127}$$

The above procedure can be applied to the the case of vector amplitudes which can thus be written in the form (4.126). In the vector case, a N_1-point diagram is given by

$$A_{N_1 v}^{M_1\cdots M_{N_1}}(\Delta_1,P_1;\ldots;\Delta_{N_1},P_{N_1}) = \int [dc']\prod_{i=1}^{N_1} D^{M_iA_i}(\Delta_i,P_i)\mathcal{A}_{A_1\cdots A_{N_1}}(\{\Delta_i,P_i\}|[c']) \tag{4.128}$$

with

$$\mathcal{A}_{A_1\cdots A_{N_1}}(\{\Delta_i,P_i\}|[c']) = \frac{\pi^{d/2}}{2}\int \mathcal{M}_{A_1\cdots A_{N_1}}(\delta'_{ij}|[c'])\prod_{i<j}\Gamma(\delta'_{ij})P_{ij}^{-\delta'_{ij}}d\delta'_{ij}\ . \tag{4.129}$$

Similarly, a N_2-point diagram is given by

$$A_{N_2 v}^{M_1\cdots M_{N_2}}(\Delta'_1,P'_1;\ldots;\Delta'_{N_1},P'_{N_1}) = \int [dc'']\prod_{i=1}^{N_2} D^{M_iA_i}(\Delta'_i,P'_i)\mathcal{A}_{A_1\cdots A_{N_1}}(\{\Delta'_i,P'_i\}|[c']) \tag{4.130}$$

with

$$\mathcal{A}_{A_1\cdots A_{N_1}}(\{\Delta'_i,P'_i\}|[c'']) = \frac{\pi^{d/2}}{2}\int \mathcal{M}_{A_1\cdots A_{N_1}}(\delta''_{ij}|[c''])\prod_{i<j}\Gamma(\delta''_{ij})(P'_{ij})^{-\delta''_{ij}}d\delta''_{ij}\ . \tag{4.131}$$

By sewing together these two diagrams, we obtain a N-point vector diagram of amplitude

$$A_{Nv}^{M_1\cdots M_N}(\Delta_1,P_1;\ldots;\Delta_N,P_N) = \int [dc'][dc'']\frac{dc}{2\pi i}f_{\delta,1}(c)\prod_{i=1}^{N} D^{M_iA_i}(\Delta_i,P_i) \mathcal{A}_{A_1\cdots A_N}(\{\Delta_i,P_i\}|[c'],[c''],c) \tag{4.132}$$

with

$$\begin{aligned}\mathcal{A}_{A_1\cdots A_N} &= \int_{\partial AdS} dQ\eta_{MM'}D^{MC}(d/2+c,Q)\\ &\quad \mathcal{A}_{A_1\cdots A_{N_1-1}C}(\Delta_1,P_1;\ldots;\Delta_{N_1-1},P_{N_1-1};d/2+c,Q|[c'])\times D^{M'C'}(d/2-c,Q)\\ &\quad \mathcal{A}_{A_1\cdots A_{N_2-1}C'}(\Delta_{N_1},P_{N_1};\ldots;\Delta_N,P_N;d/2-c,Q|[c''])\ . \end{aligned} \tag{4.133}$$

The integration over Q can be performed in the same way as in the scalar case provided Q only appears in dot products (as in $P_i\cdot Q$, and no terms with Q with a free index exist). This can be ensured by the repeated application of the identity (4.9), as we have already demonstrated. This leads to expressions for the two factors in (4.133), $D^{MC}\mathcal{A}_{A_1\cdots A_{N_1-1}C}$ and $D^{M'C'}\mathcal{A}_{A_1\cdots A_{N_2-1}C'}$, respectively, containing no Q with a free index.

After integrating over Q, we arrive at an expression for the amplitude of the form

$$\mathcal{A}_{A_1\cdots A_N}=\frac{\pi^{d/2}}{2}\int \mathcal{M}_{A_1\cdots A_N}\prod_{i<j}\Gamma(\delta_{ij})P_{ij}^{-\delta_{ij}}d\delta_{ij} \tag{4.134}$$

where $\mathcal{M}_{A_1\cdots A_N}$ is given in terms of the same functions as in the scalar case.

To complete the iteration, we need to apply the identity (4.9) again, as many times as needed, on $D^{M_iA_i}\mathcal{A}_{A_1\cdots A_N}$, in order to eliminate all occurrences of Q with a free index. The resulting expressions can then be used for the calculation of higher-point amplitudes.

4.7 Conclusion

We discussed an iterative method of calculation of Witten diagrams in AdS space based on the formalism developed in [75]. We applied our method to scalar and vector fields and showed that they can both be written in terms of Mellin amplitudes which can be computed explicitly. We showed how this is done in detail for three-, four-, and five-point diagrams. We demonstrated that the index structure in the

vector case did not present additional difficulties in the calculation of integrals over AdS space, by taking advantage of the conformal structure of the amplitudes.

Our method can be straightforwardly generalized to higher-spin fields (calculation of correlators of stress-energy tensors, etc). As it provides a systematic way of calculating diagrams, which appears to be uniformly applicable to fields of any spin, it would be interesting to use our method toward the development of general Feynman rules for the calculation of Witten diagrams. Work in this direction is in progress.

Chapter 5

Discussion and Outlook

In chapter 3 we studied scattering amplitudes in flat space. The loop integrand is a rational function of both the internal momenta and the external kinematical variables. Just as the BCFW recursion relation allows us to compute a rational function from its poles under a complex shift, our goal was to treat loop integrands as tree amplitudes, which could then be calculated efficiently with the on-shell recursion relation. We encountered three subtle obstacles. First, the unintegrated internal momenta in integrands of loop amplitudes are merely dummy variables, and shifting them by arbitrary momenta yields the same answer after integration. It was therefore important for us to choose unambiguous internal momenta appropriate for our analysis. Second, after a single cut of internal momentum, loop amplitudes expressed as tree amplitudes often present a singularity known as a forward limit. We can see this in a Feynman diagram: if adjacent legs are attached to the same external line, conservation of momentum produces a $1/p^2$ singularity when $p \mapsto 0$. We needed to ensure that singularities resulting from the forward limit did not affect our analysis. Third, we intended to use the BCFW on-shell recursion relation to express loop integrands as products of lower-point amplitudes. To do so, we needed to ensure vanishing large z behavior by avoiding poles at infinity. The solutions to these problems were as subtle as the problems themselves. We resolved the ambiguity

of loop momenta by cutting the integrand with two adjacent shifts. We then checked the large z behavior to ensure the integrand had no poles from infinity. To obtain a good large z behavior, we chose an appropriate basis for polarization vectors. We found that divergences from the *forward limit* can be eliminated after integration over the loop momenta. * We can now treat loop integrands as factorized lower-point integrands using the on-shell recursion relation. We found explicit recursion relations for two-, three-, and four-point one-loop gauge theory amplitudes. As most of our analysis should work for higher-loop amplitudes as well, in the future we would like to calculate specific examples. This analysis can also be used to compute leading and next-to-leading order corrections to QCD backgrounds in high-energy colliders.

There has been considerable work in the calculation of tree-level scattering amplitudes for gravitons, in which we see structures that are not transparent at the level of the Lagrangian. [39, 40, 41, 42]. It is an intriguing aspect of on-shell recursion relations that they eliminate the need for infinitely many interaction terms. We would like to use recursive techniques to study graviton loop amplitudes. The first step in this exploration will be to calculate one-loop graviton amplitudes. Many of the methods developed in the present work are transferable to such an exploration.

Our construction of one-loop Yang-Mills amplitudes as a sum over elementary building blocks will, beside its use with graviton amplitudes, help build more complicated on-shell processes for theories with less-than-maximal supersymmetry. Over the years, physicists have made remarkable progress in expressing amplitudes in terms of geometric structures such as twistors, the positive Grassmanian, and the amplituhedron [14, 17, 84], but most of this progress has been in specialized theories containing maximum possible supersymmetry. It would be extremely interesting to investigate whether we could express pure Yang-Mills theory and QCD amplitudes in terms of such nifty geometric structures.

* In general, loop amplitudes can be written in terms of rational functions of kinematical terms and scalar integrals such as box integrals, triangle integrals, and bubble integrals. The bubble-integral basis does not contribute to the amplitudes, and the forward limit corresponding to these bubble diagrams vanishes after integration over loop momenta.

In chapter 4, we presented a new tool for studying scattering amplitudes in AdS space. We were inspired by the dramatic progress in S-Matrix theory in flat space, which was made possible by the study of hidden symmetries, recursion relations, and well-chosen representations such as twistors. We began our investigation in a similar spirit by studying Mellin representation of AdS amplitudes in embedding space. This new formalism teaches us about both quantum gravity in asymptotically Anti-de Sitter spaces and conformal field theories with gravity duals. We found it a very useful framework for AdS amplitudes, which are correlation functions in conformal field theory. We also discovered that the Mellin representation is structurally identical to the momentum representation used to calculate flat-space S-matrix elements.

Mellin space is a very exciting representation with which to do calculations, and it seems the value of this space will be explored in different contexts in the coming the years. Already there has been renewed interest in studying supergravity amplitudes in terms of Mellin representations [82]. Furthermore, some study of Mellin space and Grassmanian has been done in [83], which suggests Mellin space has broader application in physics than the calculation of AdS amplitudes.

We are eager in future work to explore the fascinating similarities between Mellin space for Anti-de Sitter space and momentum space in flat- space scattering amplitudes. We have already seen structures remarkably similar to Mandelstam invariants in flat-space scattering amplitudes. It is natural to ask whether we could use this formalism to compute scattering amplitudes in AdS space for higher-spin particles. Some work in calculating AdS amplitudes for gravitons has been done in [68, 70], wherein computation is done in momentum space. But we would like to use the analytical tools developed in this work to investigate graviton scattering in AdS, which are correlators of stress tensors in CFT. Recently there has been significant progress in higher-spin massless theories (see [90] and the references therein). These higher-spin theories could be plausibly written in terms of Mellin space.

Futhermore, Penedones has conjectured that in the high-energy limit, where the δ_{ij} parameters become large, the Mellin amplitudes reduce to flat-space amplitudes

of massless particles [62]. In this sense, AdS space can be thought of as naturally providing an IR cut-off for flat-space amplitudes. Penedones's work is still in progress, but our results seem to agree with it. The obvious next step is to see if curvature of AdS space can be thought of as a regulator. We also hope to address the problem of bulk locality [86, 87, 88, 89]. Is the interaction that occurs inside the Anti-de Sitter space local? This is an interesting and important question. We believe that Mellin representation will illuminate these matters.

Bibliography

[1] S. J. Parke, T. R. Taylor, "An Amplitude for n Gluon Scattering," Phys. Rev. Lett. **56**, 2459 (1986). 2, 24

[2] B. S. DeWitt, "Quantum Theory of Gravity. 2. The Manifestly Covariant Theory," Phys. Rev. **162**, 1195 (1967). 2

[3] F. A. Berends and W. T. Giele, "Recursive Calculations for Processes with n Gluons," Nucl. Phys. B **306**, 759 (1988). 2

[4] Z. Bern, L. J. Dixon, D. C. Dunbar and D. A. Kosower, Nucl. Phys. B **425**, 217 (1994) [hep-ph/9403226]. 2, 25

[5] Z. Bern, J. J. M. Carrasco and H. Johansson, "New Relations for Gauge-Theory Amplitudes," Phys. Rev. D **78**, 085011 (2008) [arXiv:0805.3993 [hep-ph]]. 3

[6] G. P. Korchemsky and E. Sokatchev, "Symmetries and analytic properties of scattering amplitudes in N=4 SYM theory," Nucl. Phys. B **832**, 1 (2010) [arXiv:0906.1737 [hep-th]]. 3

[7] J. M. Henn, "Duality between Wilson loops and gluon amplitudes," Fortsch. Phys. **57**, 729 (2009) [arXiv:0903.0522 [hep-th]]. 3

[8] T. Adamo, M. Bullimore, L. Mason and D. Skinner, "Scattering Amplitudes and Wilson Loops in Twistor Space," J. Phys. A **44**, 454008 (2011) [arXiv:1104.2890 [hep-th]]. 3

[9] E. Witten, Commun. Math. Phys. **252**, 189 (2004) [arXiv:hep-th/0312171].

[10] N. Arkani-Hamed, F. Cachazo, C. Cheung and J. Kaplan, "A Duality For The S Matrix," JHEP **1003**, 020 (2010) [arXiv:0907.5418 [hep-th]]. 3, 24
4

[11] N. Arkani-Hamed, F. Cachazo and J. Kaplan, "What is the Simplest Quantum Field Theory?," JHEP **1009**, 016 (2010) [arXiv:0808.1446 [hep-th]]. 4

[12] N. Arkani-Hamed, J. L. Bourjaily, F. Cachazo, S. Caron-Huot and J. Trnka, "The All-Loop Integrand For Scattering Amplitudes in Planar N=4 SYM," JHEP **1101**, 041 (2011) [arXiv:1008.2958 [hep-th]]. 4

[13] N. Arkani-Hamed, J. L. Bourjaily, F. Cachazo and J. Trnka, "Local Integrals for Planar Scattering Amplitudes," JHEP **1206**, 125 (2012) [arXiv:1012.6032 [hep-th]]. 4

[14] N. Arkani-Hamed, J. L. Bourjaily, F. Cachazo, A. B. Goncharov, A. Postnikov and J. Trnka, "Scattering Amplitudes and the Positive Grassmannian," arXiv:1212.5605 [hep-th]. 4, 89

[15] N. Arkani-Hamed, J. Bourjaily, F. Cachazo and J. Trnka, "Unification of Residues and Grassmannian Dualities," JHEP **1101**, 049 (2011) [arXiv:0912.4912 [hep-th]]. 4

[16] N. Arkani-Hamed, J. L. Bourjaily, F. Cachazo, A. Hodges and J. Trnka, "A Note on Polytopes for Scattering Amplitudes," JHEP **1204**, 081 (2012) [arXiv:1012.6030 [hep-th]]. 4

[17] N. Arkani-Hamed and J. Trnka, "The Amplituhedron," arXiv:1312.2007 [hep-th]. 4, 89

[18] N. Arkani-Hamed and J. Trnka, "Into the Amplituhedron," arXiv:1312.7878 [hep-th]. 89

[19] E. Kiritsis, String Theory in a Nutshell, Princeton University Press, 2007. 22

[20] M. Srednicki, Cambridge, UK: Univ. Pr. (2007) 641 p 14

[21] M. E. Peskin and D. V. Schroeder, "An Introduction to quantum field theory," Reading, USA: Addison-Wesley (1995) 842 p 7

[22] M. E. Peskin, "Simplifying Multi-Jet QCD Computation," [arXiv:hep-ph/1101.2414]. 25

[23] L. J. Dixon, "Scattering amplitudes: the most perfect microscopic structures in the universe," J. Phys. A **A44**, 454001 (2011). [arXiv:hep-th/1105.0771]. 25

[24] L. J. Dixon, In *Boulder 1995, QCD and beyond* 539-582 [hep-ph/9601359]. 14

[25] F. Cachazo, P. Svrcek, E. Witten, "MHV vertices and tree amplitudes in gauge theory," JHEP **0409**, 006 (2004). [hep-th/0403047]. 25

[26] J. M. Maldacena, "The Large N limit of superconformal field theories and supergravity," Adv. Theor. Math. Phys. **2**, 231 (1998) [hep-th/9711200]. 17, 52

[27] E. Witten, "Anti-de Sitter space and holography," Adv. Theor. Math. Phys. **2**, 253 (1998) [hep-th/9802150]. 52

[28] J. Polchinski, "Introduction to Gauge/Gravity Duality," arXiv:1010.6134 [hep-th]. 17, 18, 21

[29] O. Aharony, S. S. Gubser, J. M. Maldacena, H. Ooguri and Y. Oz, "Large N field theories, string theory and gravity," Phys. Rept. **323**, 183 (2000) [hep-th/9905111]. 18

[30] S. S. Gubser and A. Karch, Ann. Rev. Nucl. Part. Sci. **59**, 145 (2009) [arXiv:0901.0935 [hep-th]]. 21

[31] S. Sachdev, Lect. Notes Phys. **828**, 273 (2011) [arXiv:1002.2947 [hep-th]]. 21

[32] E. D'Hoker and D. Z. Freedman, "Supersymmetric gauge theories and the AdS / CFT correspondence," hep-th/0201253. 18

[33] J. D. Bekenstein, "Black holes and the second law," Lett. Nuovo Cim. **4**, 737 (1972). 18

[34] S. W. Hawking, "Particle Creation by Black Holes," Commun. Math. Phys. **43**, 199 (1975) [Erratum-ibid. **46**, 206 (1976)]. 18

[35] G. 't Hooft, "Dimensional reduction in quantum gravity," Salamfest 1993:0284-296 [gr-qc/9310026]. [35, 36] 4, 95

[36] L. Susskind, "The World as a hologram," J. Math. Phys. **36**, 6377 (1995) [hep-th/9409089]. 4, 95

[37] S. Weinberg and E. Witten, Phys. Lett. B **96**, 59 (1980). 18

[38] R. Britto, F. Cachazo, B. Feng and E. Witten, "Direct proof of tree-level recursion relation in Yang-Mills theory," Phys. Rev. Lett. **94**, 181602 (2005) [arXiv:hep-th/0501052].

[39] N. Arkani-Hamed, J. Kaplan, "On Tree Amplitudes in Gauge Theory and Gravity," JHEP **0804**, 076 (2008). [arXiv:hep-th/0801.2385]. 16, 25, 89

[40] J. Bedford, A. Brandhuber, B. J. Spence, G. Travaglini, "A Recursion relation for gravity amplitudes," Nucl. Phys. **B721**, 98-110 (2005). [hep-th/0502146]. 25, 89

[41] F. Cachazo, P. Svrcek, "Tree level recursion relations in general relativity," [hep-th/0502160]. 25, 89

[42] P. Benincasa, C. Boucher-Veronneau, F. Cachazo, "Taming Tree Amplitudes In General Relativity," JHEP **0711**, 057 (2007). [hep-th/0702032]. 25, 89

[43] N. E. J. Bjerrum-Bohr, D. C. Dunbar, H. Ita, W. B. Perkins, K. Risager, "MHV-vertices for gravity amplitudes," JHEP **0601**, 009 (2006). [hep-th/0509016]. 25

[44] C. Cheung, D. O'Connell and B. Wecht, "BCFW Recursion Relations and String Theory," JHEP **1009**, 052 (2010) [arXiv:1002.4674 [hep-th]]. 25

[45] R. H. Boels, D. Marmiroli and N. A. Obers, JHEP **1010**, 034 (2010) [arXiv:1002.5029 [hep-th]]. 25

[46] A. Fotopoulos, N. Prezas, "Pomerons and BCFW recursion relations for strings on D-branes," Nucl. Phys. **B845**, 340-380 (2011). [arXiv:hep-th/1009.3903]. 25

[47] S. Raju, "BCFW for Witten Diagrams," arXiv:1011.0780 [hep-th]. 25, 52, 90

[48] Z. Bern, L. J. Dixon, D. C. Dunbar, D. A. Kosower, "One loop n point gauge theory amplitudes, unitarity and collinear limits," Nucl. Phys. **B425**, 217-260 (1994). [arXiv:hep-ph/9403226]. 2, 25

[49] Z. Bern, L. J. Dixon, D. C. Dunbar, D. A. Kosower, "Fusing gauge theory tree amplitudes into loop amplitudes," Nucl. Phys. **B435**, 59-101 (1995). [arXiv:hep-ph/9409265]. 25

[50] Z. Bern, L. J. Dixon and D. A. Kosower, "Progress in one-loop QCD computations," Ann. Rev. Nucl. Part. Sci. **46**, 109 (1996) [arXiv:hep-ph/9602280]. 25

[51] Z. Bern, L. J. Dixon and D. A. Kosower, "On-shell recurrence relations for one-loop QCD amplitudes," Phys. Rev. D **71**, 105013 (2005) [arXiv:hep-th/0501240]. 25

[52] Z. Bern, L. J. Dixon and D. A. Kosower, "Bootstrapping multi-parton loop amplitudes in QCD," Phys. Rev. D **73**, 065013 (2006) [arXiv:hep-ph/0507005]. 25

[53] C. F. Berger *et al.*, "An Automated Implementation of On-Shell Methods for One-Loop Amplitudes," Phys. Rev. D **78**, 036003 (2008) [arXiv:0803.4180 [hep-ph]]. 25

[54] D. C. Dunbar, J. H. Ettle and W. B. Perkins, "Augmented Recursion For One-loop Amplitudes," Nucl. Phys. Proc. Suppl. **205-206**, 74 (2010) [arXiv:1011.0559 [hep-th]]. 25

[55] R. H. Boels, "On BCFW shifts of integrands and integrals," JHEP **1011**, 113 (2010) [arXiv:1008.3101 [hep-th]]. 25

[56] S. Kharel and G. Siopsis, "Gauge theory one-loop amplitudes and the BCFW recursion relations," Phys. Rev. D **86**, 025004 (2012) [arXiv:1111.5278 [hep-th]]. 26

[57] N. Arkani-Hamed, J. L. Bourjaily, F. Cachazo, S. Caron-Huot and J. Trnka, "The All-Loop Integrand For Scattering Amplitudes in Planar N=4 SYM," JHEP **1101**, 041 (2011) [arXiv:1008.2958 [hep-th]]. 25

[58] L. F. Abbott, M. T. Grisaru and R. K. Schaefer, "The Background Field Method and the S Matrix," Nucl. Phys. B **229**, 372 (1983). 16, 26

[59] Z. Bern and G. Chalmers, "Factorization in one loop gauge theory," Nucl. Phys. B **447**, 465 (1995) [arXiv:hep-ph/9503236]. 34

[60] Z. Bern and D. A. Kosower, "The Computation of loop amplitudes in gauge theories," Nucl. Phys. B **379**, 451 (1992). 41, 44

[61] R. K. Ellis and J. C. Sexton, "QCD Radiative Corrections to Parton-Parton Scattering," Nucl. Phys. B **269**, 445 (1986). 44

[62] J. Penedones, "Writing CFT correlation functions as AdS scattering amplitudes," JHEP **1103**, 025 (2011) [arXiv:1011.1485 [hep-th]]. 52, 53, 55, 91

[63] D. Z. Freedman, S. D. Mathur, A. Matusis and L. Rastelli, "Comments on 4 point functions in the CFT / AdS correspondence," Phys. Lett. B **452**, 61 (1999) [hep-th/9808006]. 52

[64] H. Liu and A. A. Tseytlin, "On four point functions in the CFT / AdS correspondence," Phys. Rev. D **59**, 086002 (1999) [hep-th/9807097]. 52

[65] D. Z. Freedman, S. D. Mathur, A. Matusis and L. Rastelli, "Correlation functions in the CFT(d) / AdS(d+1) correspondence," Nucl. Phys. B **546**, 96 (1999) [hep-th/9804058]. 52

[66] E. D'Hoker, D. Z. Freedman and L. Rastelli, "AdS / CFT four point functions: How to succeed at z integrals without really trying," Nucl. Phys. B **562**, 395 (1999) [hep-th/9905049]. 52

[67] E. D'Hoker, D. Z. Freedman, S. D. Mathur, A. Matusis and L. Rastelli, "Graviton exchange and complete four point functions in the AdS / CFT correspondence," Nucl. Phys. B **562**, 353 (1999) [hep-th/9903196]. 52

[68] S. Raju, "BCFW for Witten Diagrams," Phys. Rev. Lett. **106**, 091601 (2011) [arXiv:1011.0780 [hep-th]]. 25, 52, 90

[69] S. Raju, "Four Point Functions of the Stress Tensor and Conserved Currents in AdS4/CFT3," Phy. Rev. D **85**, 126008 (2012) [arXiv:1201.6452 [hep-th]]. 52

[70] S. Raju, "New Recursion Relations and a Flat Space Limit for AdS/CFT Correlators," Phy. Rev. D **85**, 126009 (2012) [arXiv:1201.6449 [hep-th]]. 52, 90

[71] S. Raju, "Recursion Relations for AdS/CFT Correlators," Phys. Rev. D **83**, 126002 (2011) [arXiv:1102.4724 [hep-th]]. 52

[72] G. Mack, "D-independent representation of Conformal Field Theories in D dimensions via transformation to auxiliary Dual Resonance Models. Scalar amplitudes," arXiv:0907.2407 [hep-th]. 53

[73] G. Mack, "D-dimensional Conformal Field Theories with anomalous dimensions as Dual Resonance Models," Bulg. J. Phys. **36**, 214 (2009) [arXiv:0909.1024 [hep-th]]. 53

[74] A. L. Fitzpatrick, J. Kaplan, J. Penedones, S. Raju and B. C. van Rees, "A Natural Language for AdS/CFT Correlators," JHEP **1111**, 095 (2011) [arXiv:1107.1499 [hep-th]]. 53

[75] M. F. Paulos, "Towards Feynman rules for Mellin amplitudes," JHEP **1110**, 074 (2011) [arXiv:1107.1504 [hep-th]]. 53, 54, 55, 72, 86

[76] P. A. M. Dirac, "Wave equations in conformal space," Annals Math. **37**, 429 (1936). 54

[77] L. Cornalba, M. S. Costa and J. Penedones, "Deep Inelastic Scattering in Conformal QCD," JHEP **1003**, 133 (2010) [arXiv:0911.0043 [hep-th]].

[78] S. Weinberg, "Six-dimensional Methods for Four-dimensional Conformal Field Theories," Phys. Rev. D **82**, 045031 (2010) [arXiv:1006.3480 [hep-th]]. 54

[79] M. S. Costa, J. Penedones, D. Poland and S. Rychkov, "Spinning Conformal Blocks," JHEP **1111**, 154 (2011) [arXiv:1109.6321 [hep-th]].

[80] S. Kharel and G. Siopsis, "Tree-level Correlators of scalar and vector fields in AdS/CFT," JHEP **1311**, 159 (2013) [arXiv:1308.2515 [hep-th]]. 53

[81] R. Britto, F. Cachazo, B. Feng and E. Witten, "Direct proof of tree-level recursion relation in Yang-Mills theory," Phys. Rev. Lett. **94**, 181602 (2005) [hep-th/0501052].

[82] S. Stieberger and T. R. Taylor, "Superstring Amplitudes as a Mellin Transform of Supergravity," Nucl. Phys. B **873**, 65 (2013) [arXiv:1303.1532 [hep-th]]. 90

[83] S. Stieberger and T. R. Taylor, "Superstring/Supergravity Mellin Correspondence in Grassmannian Formulation," Phys. Lett. B **725**, 180 (2013) [arXiv:1306.1844 [hep-th]]. 90

[84] N. Arkani-Hamed and J. Trnka, "Into the Amplituhedron," arXiv:1312.7878 [hep-th]. 89

[85] N. Arkani-Hamed and J. Trnka, "The Amplituhedron," arXiv:1312.2007 [hep-th].

[86] S. B. Giddings, "Flat space scattering and bulk locality in the AdS /CFT correspondence," Phys. Rev. D **61**, 106008 (2000) [hep-th/9907129]. 91

[87] S. B. Giddings, "The gravitational S-matrix: Erice lectures," arXiv:1105.2036 [hep-th].

[88] S. El-Showk and K. Papadodimas, "Emergent Spacetime and Holographic CFTs," JHEP **1210**, 106 (2012) [arXiv:1101.4163 [hep-th]]. 91

[89] I. Heemskerk, J. Penedones, J. Polchinski and J. Sully, "Holography from Conformal Field Theory," JHEP **0910**, 079 (2009) [arXiv:0907.0151 [hep-th]]. 91

[90] S. Giombi and X. Yin, "Higher Spin Gauge Theory and Holography: The Three-Point Functions," JHEP **1009**, 115 (2010) [arXiv:0912.3462 [hep-th]]. 91
90

Appendix

Appendix A

Computational tools

A.1 Spinor Helicity Formalism

Momentum can be written as a four-vector, i.e.,

$$p_{\alpha\dot{\alpha}} = p_\mu(\sigma^\mu)_{\alpha\dot{\alpha}} = (p^0 I - p^i\sigma^i)_{\alpha\dot{\alpha}} = \begin{pmatrix} p_0 - p_3 & -(p^1 - ip^2) \\ -(p^1 + ip^2) & p^0 + ip^3 \end{pmatrix} \tag{A.1}$$

Hence, one can write down momentum in a 2×2 matrix. Then, one can write down a determinant of the matrix in the following way:

$$det(p_\mu p^\mu) = 0 \tag{A.2}$$

In terms of the linear algebra, the matrix is rank 1 and hence can be written as a two- component spinor.

$$p_{\alpha\dot{\alpha}} = \lambda_\alpha \tilde{\lambda}_{\dot{\alpha}} \tag{A.3}$$

Without any loss of generality let's consider the following. Say $p^0 = E > 0$ and p is pointing in the third direction. Then,

$$p_{\alpha\dot{\alpha}} = \begin{pmatrix} E-p & 0 \\ 0 & E+p \end{pmatrix} \tag{A.4}$$

Then one can write,

$$p = 2E \begin{pmatrix} 0 & 0 \\ 0 & 1 \end{pmatrix} \tag{A.5}$$

Then, one can write,

$$p = 2E \begin{pmatrix} 0 & 0 \\ 0 & 1 \end{pmatrix} = 2E \begin{pmatrix} 0 \\ 1 \end{pmatrix} \begin{pmatrix} 0 & 1 \end{pmatrix} \tag{A.6}$$

One can write the spinor as:

$$\lambda = \tilde{\lambda} = \sqrt{2E} \begin{pmatrix} 0 \\ 1 \end{pmatrix} \tag{A.7}$$

One can think of the Pauli spinors as a square root of the four-vector. Two spinors of the same chirality can be contracted with the epsilon tensors. We use different shapes of brackets for the two chiralities, and define antisymmetric spinor products as:

$$\langle \lambda \mu \rangle = \epsilon^{ab} \lambda_a \mu_b \tag{A.8}$$

and similarly,

$$[\lambda \mu] = \epsilon^{\dot{a}\dot{b}} \lambda_{\dot{a}} \mu_{\dot{b}} \tag{A.9}$$

Similarly, one can write down:

$$p.q = \frac{1}{2} \langle \lambda \mu \rangle \left[\tilde{\mu} \tilde{\lambda} \right] \tag{A.10}$$

$$\langle ij \rangle [ij] = s_{ij} \tag{A.11}$$

where s_{ij} is the well known Mandelstam invariant. In the same way, we can express, polarization vectors in terms of spinors. For instance, one can write down

$$\epsilon^{-}_{a\dot{a}} = -\sqrt{2}\frac{\lambda_a \tilde{\mu}_{\dot{a}}}{\left[\tilde{\lambda}\tilde{\mu}\right]} \tag{A.12}$$

Similarly one can write down,

$$\epsilon^{+}_{a\dot{a}} = -\sqrt{2}\frac{\mu_a \tilde{\lambda}_{\dot{a}}}{[\mu\lambda]} \tag{A.13}$$

Appendix B

Anti-de Sitter Space

Anti-de Sitter space is a space of Lorenzian signature, i.e. $(-,+,+,+,+)$ and has a constant negative curvature (as opposed to de-Sitter space which has constant positive curvature). One can write down the de Sitter space embedded in a $d+1$ dimensions in the following way

$$\begin{aligned} ds^2 &= -dz^2 + \sum_{i=1}^{d-1} dx_i^2 + dx_{d+1}^2 \\ & \quad -z^2 + \sum_{i=1}^{d-1} x_i^2 + x_d^2 = R^2 \end{aligned} \tag{B.1}$$

The space is invariant under $SO(1,d)$

$$\begin{aligned} ds^2 &= -dz^2 + \sum_{i=1}^{d-1} dx_i^2 - dx_{d+1}^2 \\ & \quad -z^2 + \sum_{i=1}^{d-1} x_i^2 - x_d^2 = R^2 \end{aligned} \tag{B.2}$$

It is invariant under the group $SO(2,d-1)$ that rotates the coordinates by $x'^{\mu} = \Lambda^{\mu}_{\nu} x^{\nu}$. Sometimes the metric can be conveniently written using the so called Poincare

coordinates:

$$ds^2 = \frac{R^2}{z^2}\left(-dt^2 + \sum_{i=1}^{d-2} + dz^2\right) \tag{B.3}$$

where $-\infty < t,\ x_i < +\infty$ and $0 < z < \infty$. In the Poincare coordinates, the AdS space looks like a three-dimensional Minkowski space up to a conformal factor. In Poincare coordinates one does not cover all of space. In the finite coordinates τ, θ one finds that one can analytically continue to the whole space. The space that covers the whole space is the global coordinates whose metric can be written in the following way:

$$ds_d^2 = R^2(-\cosh^2\rho\ d\tau^2 + d\rho^2 + \sinh^2\rho\ d\Omega_{d-2}^2) \tag{B.4}$$

Appendix C

Various Integrals

C.1 AdS integral

Here we derive integrals over AdS space (bulk or boundary) that are used in our discussion.

Integrals on the boundary are often of the form

$$I = \int_{\partial AdS} dQ \prod_i \Gamma(\lambda_i)(-2P_i \cdot Q)^{-\lambda_i} \tag{C.1}$$

where Q, P_i are all points on the boundary and the exponents λ_i are constrained

$$\sum_i \lambda_i = d \tag{C.2}$$

To perform the integral over the vector Q^A, use the Mellin transform,

$$\Gamma(\lambda_i)(-2P_i \cdot Q)^{-\lambda_i} = \int_0^\infty \frac{dv_i}{v_i} v_i^{\lambda_i} e^{2v_i P_i \cdot Q} \tag{C.3}$$

to write the integral I in the form

$$I = \int_0^\infty \prod_i \frac{dv_i}{v_i} v_i^{\lambda_i} \int_{\partial AdS} dQ e^{2T \cdot Q} \quad , \quad T^A = \sum_i v_i P_i^A \tag{C.4}$$

Going to the rest frame of T_A in which $T_A = (T_0, 0, \ldots, 0)$ with $T_0 \geq 0$, and parametrizing the null vector Q^A by

$$Q^A = \left(\frac{x^2+1}{2}, \frac{x^2-1}{2}, x^\mu \right) \tag{C.5}$$

we obtain

$$\int_{\partial AdS} dQ e^{2T\cdot Q} = \frac{\pi^{d/2}}{T_0^{d/2}} e^{-T_0} \tag{C.6}$$

After rescaling $v_i \to v_i T_0$, we obtain

$$I = \pi^{d/2} \int_0^\infty \prod_i \frac{dv_i}{v_i} v_i^{\lambda_i} e^{T^2} \quad , \quad T^2 = -\sum_{i<j} v_i v_j P_{ij} \ , \tag{C.7}$$

where we used $T^2 = -T_0^2$.

This expression can be simplified further by using the inverse Mellin transform

$$e^{-y} = \int_{c-i\infty}^{c+i\infty} \frac{ds}{2\pi i} \Gamma(s) y^{-s} \quad (c > 0) \tag{C.8}$$

We obtain

$$I = \pi^{d/2} \int_0^\infty \prod_i \frac{dv_i}{v_i} v_i^{\lambda_i} \int_{c-i\infty}^{c+i\infty} \prod_{i<j} \frac{ds_{ij}}{2\pi i} \Gamma(s_{ij}) (v_i v_j P_{ij})^{-s_{ij}} \ . \tag{C.9}$$

Each integral over v_i yields a δ-function. We deduce

$$I = \frac{\pi^{d/2}}{2} \int \prod_{i<j} \frac{ds_{ij}}{2\pi i} \Gamma(s_{ij}) P_{ij}^{-s_{ij}} \ , \tag{C.10}$$

where the integration variables are constrained by

$$\sum_j s_{ij} = \lambda_i \tag{C.11}$$

and we have defined $s_{ji} = s_{ij}$, $s_{ii} = 0$.

Integrals in the bulk are of a similar form,

$$J = \int_{AdS} dX \prod_i \Gamma(\Delta_i)(-2P_i \cdot X)^{-\lambda_i} = \int_0^\infty \prod_i \frac{dv_i}{v_i} v_i^{\lambda_i} \int_{AdS} dX e^{2T\cdot X} \tag{C.12}$$

where this time the exponents λ_i are not constrained.

Parametrizing the bulk point X^A by

$$X = \frac{1}{x_0}\left(\frac{x_0^2 + x^2 + 1}{2}, \frac{x_0^2 + x^2 - 1}{2}, x^\mu\right) \tag{C.13}$$

we obtain

$$\int_{AdS} dX e^{2T\cdot X} = \pi^{d/2} \int_0^\infty \frac{dx_0}{x_0} x_0^{-d/2} e^{-x_0 + T^2/x_0} \tag{C.14}$$

After rescaling $v_i \to v_i\sqrt{x_0}$, the integral over x_0 can be performed, and we obtain

$$J = \pi^{d/2}\Gamma\left(\frac{\sum_i \lambda_i - d}{2}\right) \int_0^\infty \prod_i \frac{dv_i}{v_i} v_i^{\lambda_i} e^{T^2} \ . \tag{C.15}$$

The remaining integrals are simplified, as before,

$$J = \frac{\pi^{d/2}}{2}\Gamma\left(\frac{\sum_i \lambda_i - d}{2}\right) \int \prod_{i<j} \frac{ds_{ij}}{2\pi i}\Gamma(s_{ij}) P_{ij}^{-s_{ij}} \ , \tag{C.16}$$

where the integration variables are constrained by (C.11).

Appendix D

Conformal Field Theory

D.1 Conformal Algebra

The conformal group in d dimensions preserves the space-time metric, $g^{\mu\nu}$ up to a scale factor. Here $\mu, \nu \in 1 \cdots d$. For $d > 2$ the generators corresponds to Lorentz rotations ($M^{\mu\nu}$), translations (P^{μ}), dilations D and so called special conformal transformations (K_{ν}).

$$\begin{aligned} P^{\mu} &: x^{\mu} + \alpha^{\mu} \\ D &: x^{\mu} \mapsto (1+\epsilon)\, x^{\mu} \qquad \text{(D.1)} \\ K_{\nu} &: x^{\mu} + \epsilon_{\nu}(g^{\mu\nu}x^2 - 2x^{\mu}x^{\nu}). \qquad \text{(D.2)} \end{aligned}$$

One can check that they obey the following relation:

$$\begin{aligned} [D, K_{\mu}] &= iK_{\mu} \\ [D, P_{\mu}] &= iP_{\mu} \\ [P_{\mu}, K_{\nu}] &= 2iM_{\mu\nu} - 2ig_{\mu\nu}D \qquad \text{(D.3)} \end{aligned}$$

D.2 Local Field Operators in Conformal Field Theory

In quantum field theories, local field operators $\mathcal{O}(x^\mu)$ is classified by local field operators. Using Euclidean signature and radial quantization, the $SO(d)$ group is the irreducible representation of the field and $SO(2)$ is the scaling dimensions of the field,

$$\mathcal{O}(\lambda x^\mu) = \lambda^{-\Delta}\mathcal{O}_\Delta(x^\mu) \tag{D.4}$$

This statement is the same as saying:

$$[D, \mathcal{O}_\Delta(0)] = -i\Delta\mathcal{O}_\Delta(0) \tag{D.5}$$

Primary operators are annihilated by special conformal generators, K^μ,

$$\begin{aligned}
[P_\mu, \mathcal{O}_\Delta(x)] &= i\partial_\mu\mathcal{O}_\Delta(x) \\
[M_{\mu\nu}, \mathcal{O}_\Delta(x)] &= \left[i(x_\mu\partial_\nu - x_\nu\partial_\mu) + \Sigma^R_{\mu\nu}\right]\mathcal{O}_\Delta(x) \\
[D, \mathcal{O}_\Delta(x)] &= i(x^\mu\partial_\mu - \Delta)\mathcal{O}_\Delta(x) \\
[K_\mu, \mathcal{O}_\Delta(x)] &= i[(x^\mu\partial_\mu - 2x_\mu x^\nu\partial_\nu - 2x_\mu\Delta) - 2x^\nu\Sigma^R_{\mu\nu}]\mathcal{O}_\Delta(x)
\end{aligned} \tag{D.6}$$

Here Δ is the conformal dimension of the primary operator, $\Sigma^R_{\mu\nu}$ are the representation matrices of the irreducible spin R of the primary which acts on its spin indices.

D.3 Conformal Correlator

The scalar primary operators for conformal correlator for primary, 2-, 3-, and 4-

$$\langle\mathcal{O}_{\Delta_1}(x_1)\mathcal{O}_{\Delta_2}(x_2)\rangle = \delta_{1,2}\sum_{i\le j}^{2} x_{ij}^{-\Delta} \tag{D.7}$$

Similarly,

$$\langle \mathcal{O}_{\Delta_1}(x_1)\mathcal{O}_{\Delta_2}(x_2)\mathcal{O}_{\Delta_3}(x_3)\rangle = c_{1,2,3}\sum_{i\leq j}^{2} x_{ij}^{\Delta-2\Delta_i-2\Delta_j} \tag{D.8}$$

$$\langle \mathcal{O}_{\Delta_1}(x_1)\mathcal{O}_{\Delta_2}(x_2)\mathcal{O}_{\Delta_3}(x_3)\mathcal{O}_{\Delta_4}(x_4)\rangle = c_{1,2,3,4}(u,v)\sum_{i\leq j}^{2} x_{ij}^{1/3\Delta-\Delta_i-\Delta_j} \tag{D.9}$$

In the above u and v are conformal invariant cross-ratios:

$$u = \frac{x_{12}x_{34}}{x_{13}x_{24}}, v = \frac{x_{14}x_{23}}{x_{13}x_{24}} \tag{D.10}$$

Then,

$$\mathcal{O}_{\Delta_i}(x)\mathcal{O}_{\Delta_j}(0) = \sum_k c_{ijk}|x|^{-\Delta_i-\Delta_j+\Delta_k}(\mathcal{O}_{\Delta_k}(0) + \text{descendants}) \tag{D.11}$$

where the sum on the right side is over all descendants. Then,

$$\langle \mathcal{O}_{\Delta_1}\mathcal{O}_{\Delta_2}(x_2)\cdots\rangle = \frac{\partial^n Z[\phi_{\Delta_i}]}{\partial_{\Delta_1}(x_1)\partial_{\Delta_2}(x_2)\cdots}\Big|_{\phi_{\Delta_i}} = 0 \tag{D.12}$$

Then,

$$\int d^dx\phi_\Delta(x)\mathcal{O}_\Delta(x) = \int d^d(\lambda x)\phi_\Delta(\lambda x)\mathcal{O}_\Delta(\lambda x) = \lambda^{d-\Delta}\int d^dx\phi_\Delta(\lambda x)\mathcal{O}_\Delta(x) \tag{D.13}$$

so Z is invariant under the following scaling transformations

$$\phi_\Delta(x) \mapsto \lambda^{d-\Delta}\phi_\Delta(\lambda x) \tag{D.14}$$

In general $Z[\phi_\Delta]$ in an invariant combination of these fields.

Vita

Savan Kharel was born in Kathmandu, Nepal, to the parents of Dadhi Ram Kharel and Kamala Kharel. He grew up in Kathmandu and completed his undergraduate studies in Physics at “Indiana University South Bend". He started his graduate education in August 2008 and worked with Professor George Siopsis on various projects in high-energy theoretical physics and string theory.